Enclosure 3

Extension of FULL SPECTRUM™ LOCA (FSLOCA™) Evaluation Methodology to 2-loop Westinghouse Pressurized Water Reactors (PWRs) with Information to Satisfy Limitations and Conditions Specific to 2-loop Plant Types

(Non-Proprietary)

(310 pages attached)

August 2021

Westinghouse Electric Company
1000 Westinghouse Drive
Cranberry Township, PA 16066

LIST OF TABLES

LIST OF FIGURES

1 INTRODUCTION

1.1 BACKGROUND

In 1996, Westinghouse's best-estimate Evaluation Model (EM) for Large Break Loss-of-Coolant Accident (LBLOCA), WCAP-12945-P-A (Bajorek et al., 1998), was approved by the United States Nuclear Regulatory Commission (US NRC) for application to the Westinghouse designed 3- and 4-loop pressurized water reactors (PWRs) with emergency core cooling system (ECCS) injection into the cold legs. Three years later, Westinghouse's best estimate LBLOCA EM for its 2-loop PWR design equipped with upper plenum injection (UPI) was approved in 1999, as described in WCAP-14449-P-A, Revision 1 (Dederer et al., 1999). The latter was extended from the former with most parts of the methodology in common, except for additional uncertainty parameters in the treatment of the analysis uncertainty based on the validation tests unique to the UPI thermal hydraulic phenomena. The two approved methods were referred to as the Code Qualification Document (CQD) and UPI CQD methodologies, respectively, for the 3-/4-loop and 2-loop UPI PWRs.

Following the approval of the CQD and UPI CQD methods, Westinghouse's best-estimate LBLOCA methods continued to be improved. In 2005, the more advanced non-parametric order statistic approach was introduced into both the CQD and UPI CQD methods to replace their response surface uncertainty approach. With this major update, the new method was collectively referred as the Automated Statistical Treatment of Uncertainty Method (ASTRUM) (Nissley et al., 2005), applicable to the Westinghouse designed 2-, 3- and 4-loop plants, as well as the Combustion Engineering designs.

While the licensing basis methods for LBLOCA had evolved throughout the years in Westinghouse, the Small Break LOCA (SBLOCA) EMs complying with the highly conservative rules in Appendix K to the Title 10, Part 50 of the Code of Federal Regulations (10 CFR 50) remained largely unchanged until the **FULL SPECTRUM™** LOCA (**FSLOCA™**) methodology (Kobelak et al., 2016) was approved. The FSLOCA methodology is Westinghouse's latest approved best estimate LOCA methodology (or EM) for cold leg breaks spanning the full range of possible break sizes. However, it is currently licensed only for the Westinghouse designed 3- and 4-loop plants with ECCS injection into the cold legs.

It is desirable to apply the FSLOCA EM to the Westinghouse designed 2-loop plants with UPI as well, due to numerous enhancements in computer code models and simulation approaches. It is particularly so for the SBLOCA, as it represents significant advancement in the computational tool and modeling accuracy compared with the existing Appendix K methods.

This report documents the development for extension of the approved FSLOCA methodology to apply to the 2-loop plants equipped with UPI.

1.2 EXTENSION OF THE WESTINGHOUSE FSLOCA METHODOLOGY TO UPI PLANTS

Many dominant phenomena during a postulated LOCA are common to all Westinghouse PWR plants, including the 3- and 4-loop cold leg injection and 2-loop UPI designs. Nonetheless, the 2-loop plants have

unique phenomena associated with UPI in the LOCA transients relative to the 3- and 4-loop plant types. These phenomena are the focus for extending the existing FSLOCA EM to the UPI plants.

The approved FSLOCA EM (Kobelak et al. 2016) was developed following the Evaluation Model Development and Assessment Process (EMDAP) documented in Regulatory Guide (RG) 1.203 (USNRC, 2005), as laid out in Figure 1-1. The EMDAP is based on the Code Scaling, Applicability and Uncertainty (CSAU) (Boyack et al. 1996) roadmap for defining and qualifying a best-estimate thermal hydraulic code and quantifying the uncertainties in a LOCA analysis.

To extend the FSLOCA methodology to UPI plants, the FSLOCA EM development processes, which were mapped to the EMDAP, were reviewed to identify each step needed to be modified for application to UPI plants. In addition, the differences between the 2-loop UPI CQD and 3-/4-loop CQD methodologies was reviewed for the important UPI-specific phenomena which require additional validation tests. The results of these reviews are summarized next, starting from the Phenomena Identification and Ranking Table (PIRT).

The PIRT in the approved FSLOCA EM covers the SBLOCA, Intermediate Break LOCA (IBLOCA) and LBLOCA transient scenarios for all Westinghouse and Combustion Engineering designed plants, including the 2-loop UPI plants. Based on the PIRT, the code assessment matrix either remains unchanged or is subject to modification depending the transient scenarios, detailed as follows:

- LBLOCA
  The [ ]^{a,c} tests are added to the existing validation matrix of the FSLOCA EM code, WCOBRA/TRAC-TF2, to verify its applicability to the 2-loop plants, as was done in developing the existing CQD UPI method (Dederer et al., 1999). Since the FSLOCA PIRT identified consistent rankings of the phenomena for the 2-loop UPI plants with those in the PIRT of the CQD UPI (Dederer et al., 1999), the additional tests provide adequate assessment for the unique phenomena of importance.

- SBLOCA
  [

  ]^{a,c}

- IBLOCA
  [

  ]^{a,c} The IBLOCAs present transitional characteristics between the SBLOCA and LBLOCA. They have shown to be non-limiting and much less significant than the SBLOCA and LBLOCA transients with the approved FSLOCA EM.

The UPI specific phenomena and validation tests lead to changes in the input model nodalization and options limited to the regions of the vessel adjacent to where UPI occurs, relative to those of the 3- and 4-

loop PWRs. These changes allow for improved modelling of the dominant UPI phenomena in the validation tests and plant calculations. Some of these changes are retained from those identified in the previous UPI CQD method, while there are also new changes introduced to enable more physical modeling of the critical UPI phenomena with the WCOBRA/TRAC-TF2 code. All the changes are consistently applied to SBLOCA, IBLOCA and LBLOCA transient scenarios in the extended UPI method.

In addition to the changes in the input model, important phenomena unique to UPI require careful consideration on the treatment of the uncertainties associated with the key computer models dominating the prediction of these phenomena. The uncertainties are evaluated through the simulation of the additional UPI validation tests and their treatment is determined based on the evaluation results.

1.3 ORGANIZATION OF THE REPORT

The organization of this report follows the main development steps for extension of the 3- and 4-loop FSLOCA method, which were guided mainly by the key thermal hydraulic phenomena of each plant type with reference to the EMDAP structured processes. Section 2 presents the discussion of additional validation tests unique to the UPI configuration and associated simulation results. Next, the plant scoping and sensitivity studies, including the conclusions regarding the plant type-specific Limitations and Conditions (L&Cs) on the approved FSLOCA EM (Kobelak et al., 2016) are discussed in Section 3. The summary and conclusion of the method development are then provided in Section 4.

1.4 REFERENCES

1. Bajorek, S. M., et al., 1998, “Code Qualification Document for Best Estimate LOCA Analysis,” WCAP-12945-P-A, Volume 1, Revision 2, and Volume 2 through 5, Revision 1.

2. Boyack, B., et al., 1989, “Quantifying Reactor Safety Margins: Application of Code Scaling, Applicability, and Uncertainty (CSAU) Evaluation Methodology to a Large-Break, Loss-of-Coolant Accident,” NUREG/CR-5249.

3. Code of Federal Regulation, Title 10, “Energy”, Part 50, “Domestic Licensing of Production and Utilization Facilities,” Appendix K, “ECCS Evaluation Models.”

4. Dederer, S. I., et al., 1999, “Application of Best Estimate Large Break LOCA Methodology to Westinghouse PWRs with Upper Plenum Injection,” WCAP-14449-P-A, Revision 1.

5. Kobelak, J. R., et al., 2016, “Realistic LOCA Evaluation Methodology Applied to the Full Spectrum of Break Sizes (FULL SPECTRUM LOCA Methodology),” WCAP-16996-P-A, Volume I through III, Revision 1.

6. Nissley, M., E., et al., 2005, “Realistic Large-Break LOCA Evaluation Methodology Using the Automated Statistical Treatment of Uncertainty Method (ASTRUM),” WCAP-16009-P-A, Revision 0.

7. USNRC, 2005, “Transient and Accident Analysis Methods,” Regulatory Guide 1.203.

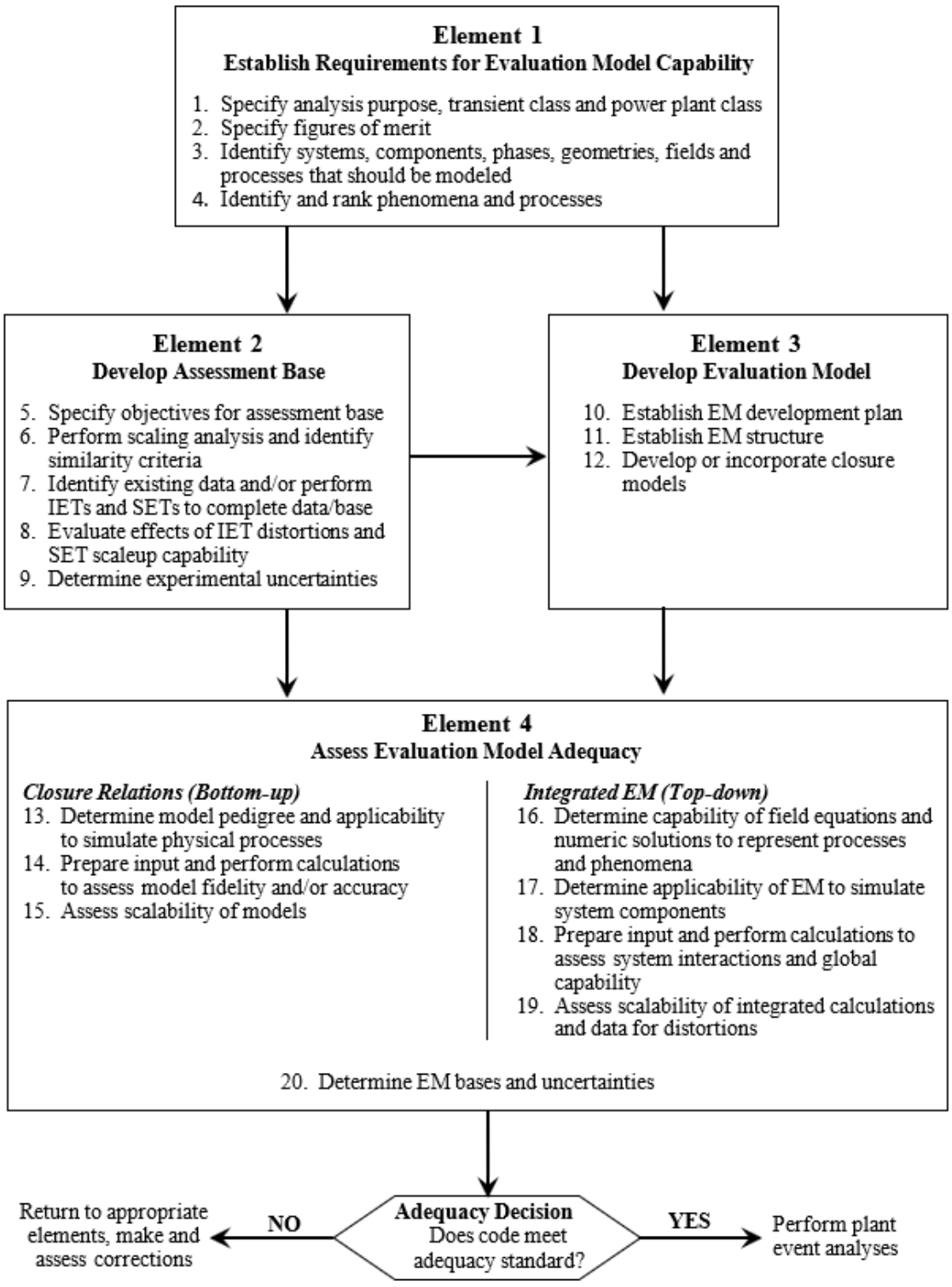

Figure 1-1 Evaluation Model Development and Assessment Process (EMDAP) – High Level Flow Chart (RG 1.203)

2 CODE ASSESSMENT BASE AND RESULTS FOR UPPER PLENUM INJECTION

2.1 INTRODUCTION

The capability of the WCOBRA/TRAC-TF2 code to simulate the expected behavior of Westinghouse-designed 3-loop and 4-loop and Combustion Engineering (CE)-designed pressurized water reactors (PWRs) during a loss-of-coolant accident (LOCA) has been assessed in Volume II of (Kobelak, et al., 2016). In this section, the application of WCOBRA/TRAC-TF2 to 2-loop PWRs equipped with upper plenum injection (UPI) will be assessed by analysis of UPI-specific phenomena. In Section 2.2, the assessment matrix is established to determine the capability of WCOBRA/TRAC-TF2 to realistically predict the UPI-dominant large break LOCA (LBLOCA) transient phenomena. The assessment results of the WCOBRA/TRAC-TF2 simulations of the validation tests are analyzed and discussed in Sections 2.3 through 2.7, and the conclusions regarding the code validation are summarized in Section 2.8.

2.2 ASSESSMENT MATRIX

The important LOCA transient processes for 3-loop, 4-loop and CE-designed plants are mostly applicable to the UPI plants (except phenomena related to the low head safety injection (LHSI) configuration). Thus, the assessment matrices developed in the FULL SPECTRUM LOCA (FSLOCA) Evaluation Model (EM) topical report (Kobelak, et al., 2016) are also applicable to UPI plants. Since these assessments have already been documented in Volume II of (Kobelak, et al., 2016), they will not be repeated here. This report will focus on those phenomena which were found to be unique in the UPI plant scenario.

The FSLOCA EM is capable of analyzing the full spectrum of possible LOCA break sizes. However, the assessment in this section is limited to the LBLOCA transient. Only the low head safety injection enters the reactor vessel upper plenum in 2-loop plants equipped with UPI; the higher pressure pumps inject into the cold legs similar to 3-loop and 4-loop Westinghouse-designed PWRs. As such, the UPI does not play a significant role in mitigating LOCAs with smaller break sizes.

Table 2.2-1 indicates rankings from the FSLOCA EM phenomenon identification and ranking table (PIRT) (Table 2-1 of (Kobelak, et al., 2016)) which differ for plants equipped with UPI. Blowdown phenomena are the same in UPI plants as in 3- and 4-loop plants since the low head safety injection does not begin until after the blowdown phase is complete. Therefore, the assessment in Volume II of (Kobelak, et al., 2016) is also applicable to UPI plants for blowdown.

A number of phenomena are highly ranked for UPI plants which were not so for other plant designs in the refill and reflood phases for LBLOCA. Some of the test facilities (i.e., the cylindrical core test facility (CCTF) and upper plenum test facility (UPTF)) comprising the validation case for the FSLOCA EM were reconfigured with hardware changes to provide data simulating UPI plant phenomena. There is another test (General Electric (GE) countercurrent flow limitation (CCFL) experiment) providing data for CCFL at the top nozzle (tie plate) with fuel rods. These tests are analyzed with the WCOBRA/TRAC-TF2 code as part of the refill and reflood assessments for the highly ranked phenomena in the UPI plant scenario, as shown in Tables 2.2-2 and 2.2-3.

Entrainment and condensation have been assessed previously in (Kobelak, et al., 2016), but the focus was on entrainment in the core and condensation in the downcomer and cold legs. CCFL was also assessed in the downcomer during emergency core cooling (ECC) bypass. There was an assessment of CCFL in (Kobelak, et al., 2016) for a range of geometries including perforated plates, and a flooding curve is applied at the upper core plate as described in Section 19.2 of (Kobelak, et al., 2016). However, both entrainment and condensation can affect the upper plenum drain distribution; that is, the delivery of the UPI flow to the core during the reflood phase of an LBLOCA transient. Due to the highly subcooled UPI flow, the ability of the code to predict the subcooled CCFL process at the top of the core also needs to be addressed. An assessment matrix was established to address these phenomena for the UPI application, as shown in Table 2.2-4. CCTF Tests 72 (Iguchi et al., 1985) and 76 (Iguchi et al., 1985a) provide verification of the overall effect of upper plenum injection on core thermal hydraulic behavior. These include CCFL and core heat transfer. The UPTF Test 20 (Siemens, 1988) was designed specifically for upper plenum injection simulations. The test results provide data for upper plenum entrainment and condensation, CCFL, and hot leg entrainment. The subcooled CCFL data are provided by a GE test (Jones, 1977). The GE test data can be used to verify the capability of WCOBRA/TRAC-TF2 in handling subcooled CCFL phenomena.

The ranges of conditions for the tests in Table 2.2-4 are listed in Table 2.2-5 along with estimated values for the predicted UPI plant ranges for the reflood period. **[**

][a,c]

When combined with the previous assessment matrix (Tables 2-2 through 2-6 of (Kobelak, et al., 2016)), the ability of WCOBRA/TRAC-TF2 to predict a LOCA transient for a PWR equipped with UPI can be assessed.

Table 2.2-1 FSLOCA EM PIRT Rankings which Differ for UPI Plants

[

]a,c

Notes:

1) L is Low importance, M is Medium importance, and H is High importance.

2) The first ranking in each cell is the ranking for non-UPI plants and the second is for UPI plants; a '---' indicates no difference in rankings.

Table 2.2-2 Additional FSLOCA EM UPI Refill Phenomena Assessment for LBLOCA

[ ]a,c

Table 2.2-3 Additional FSLOCA EM UPI Reflood Phenomena Assessment for LBLOCA

[

]a,c

Table 2.2-4 Additional Assessment Matrix for UPI-Unique Phenomena

Test	CCFL at Upper Core Plate	Subcooled CCFL	Upper Plenum Condensation	Upper Plenum Entrainment
CCTF 72	X			
CCTF 76	X			
UPTF 20	X		X	X
GE CCFL		X		

Table 2.2-5 Range of Test Parameters for UPI

[

]a,b,c

Note: Mass flow rates from the tests have been scaled by the following scaling factors based on comparison of core flow areas to plant: [

]a,b,c

2.3 GE CCFL

The GE CCFL tests were designed to determine the characteristics of subcooled CCFL in the upper region of a boiling water reactor (BWR) fuel bundle during safety injection. The tests were run at the General Electric's Zero Power Loop test facility. The objectives of the test program were to:

1. Obtain CCFL data for a wide range of inlet water flowrates and degree of subcooling,

2. Obtain temperature data from the pool of water which accumulates above the tie plate during CCFL, to determine the mixing profile of the pool, and

3. Evaluate the applicability of the existing CCFL correlations.

This test program is of interest for UPI applications because the source of water for the emergency core cooling system (ECCS) is significantly subcooled during the reflood of the core, following a hypothetical LOCA.

Despite some differences in the designs of BWR and PWR hardware, the GE data is generally applicable to a PWR UPI simulation. The characteristic dimensions relevant to CCFL, such as the hydraulic diameter of the tie plate, are generally similar between the two designs. For example, in a UPI PWR with a 14x14 fuel array bundle, the hydraulic diameter of the upper core plate (CCFL region) is about 0.43 inches, as compared to 0.455 inches in the GE test. On the other hand, the fuel bundles in a PWR are placed in an open lattice arrangement with the core, which permits some cross-flow; whereas in a BWR, the assemblies are enclosed within individual channels impermeable to cross-flow.

The WCOBRA/TRAC-TF2 prediction of the flooding characteristics will be compared to the GE test results.

2.3.1 Test Facility

The test section simulates a full-scale BWR fuel channel and the associated region of an upper plenum. The fuel bundle inside the channel is made up of 64 dummy fuel rods, shortened to approximately seven feet long. The rods are stainless steel tubes with a nominal outer diameter of 0.493 inches and are held together in an 8x8 square matrix by two grid spacers and a production type 8x8 upper tie plate. The plate is mated on top of the fuel channel to a specifically built flange which permits the fuel assembly to be easily removable. The lower surface of this flange is welded to a section of the channel less than three inches long, which simulates the channel extension above the tie plate in a BWR (Figures 2.3-1 and 2.3-2). The flange can also support additional sections of the channel extension into the upper plenum formed by bolting together a number of six inch sections of square tubing.

The upper tie plate region is enclosed in a large square box which is attached to the base plate of the upper plenum and is vented to the atmosphere by an orificed vent stack. The inlet water is piped in

through the base plate to the desired flow distribution system. The system can provide up to 8,000 lb/hr of water at temperatures ranging from 100°F to 205°F. The steam is supplied from a gas-fired boiler, which can provide up to 1,500 lb/hr steam at 80 psig. Figure 2.3-1 shows the general flow schematic of the test facility.

Three basic methods of inlet water injection were used during the tests. They are illustrated in Figure 2.3-2. The bypass slots method, intended to simulate the path of inlet water when the bypass region is flooded, was accomplished by cutting four 1/8 x 5-inch slots in a square pattern in the bottom of the flange at the base of the channel extension. A length of 1/2-inch tubing was connected from the water supply to each slot. The cross-flow method, intended to simulate the flow pattern near the peripheral bundles in a BWR when the sparger is flooded, was accomplished by piping the water through the side of the extended channel. On the side opposite from the water inlet, there were four small holes drilled in the channel wall. Four separate water lines provided the desired spray pattern through a set of removable 1-inch diameter plates at each connection to the channel. The flow pattern could be changed by installing a set of plates with different flow hole sizes and patterns. Finally, the spillover flow was accomplished by simply plugging the four bypass slots and injecting the water directly into the upper plenum. The water then accumulates until it spills over the channel extension into the test section.

Additional flexibility to the geometry of the test section was provided by adding extensions to the channel above the tie plate. Two extensions, one 6 inches and one 12 inches high, were used in these tests. The bypass tests were run without an extension and with the 6-inch and 12-inch extensions. The cross-flow tests were done with the 12-inch extension.

Three methods of injecting steam into the test section were also tested. They are illustrated in Figure 2.3-3. The capped sparger was a 2-inch pipe, 8 inches long, with four slots cut around its circumference and capped with a welded plate. To accommodate this sparger, the center 4x4 array of dummy rods was cut 8.5 inches shorter than the rest of the rods. The clarinet sparger was a 1-1/2-inch pipe with its end flared out in the shape of a bell. Again, the center 4x4 array of rods was cut shorter to accommodate the sparger. Finally, the lower tie plate sparger was fabricated using a prototypical lower tie plate nose piece, which has approximately the same flow area as the upper tie plate. A pipe was welded to the bottom of this nose piece and the 4x4 center array of rods was lengthened to the same dimension as the other rods.

The other major hardware variable changed was the configuration of the dummy fuel bundle. The configurations tested included the following:

1. Full 8x8 bundle of rods with tie plate and two spacers,
2. Full 8x8 bundle with two spacers but no tie plate,
3. Tie plate only, no bundle, and
4. Full 8x8 bundle with tie plate but no spacers.

These tests were performed to determine how the individual pieces of hardware on a fuel bundle affected the formation of the CCFL. The configuration of the tests to be analyzed with WCOBRA/TRAC-TF2 used the capped sparger steam injector, the 12-inch extension for the bypass slots method and the spillover flow method of water injection, and the 8x8 bundle of rods with the tie plate and two spacers. The selection of the capped sparger steam injection was made simply because the test data in Appendix C of (Jones, 1977) are mostly from the tests performed with this configuration.

2.3.2 Test Conditions

A full description and discussion of the results are found in (Jones, 1977). There was a total of 135 tests performed, divided into categories governed by basic hardware configurations and injection methods. Steady state tests were initiated by injecting subcooled water into the test section at a predetermined rate and temperature. After the initial set of data was recorded, increasing amounts of steam were added to the test section, in steps, until a complete CCFL was observed. The data was recorded at each step. After the CCFL was observed, the steam injection was reduced in reverse step increments while continuing to record the data.

Transient tests were run in a “steam first” mode. The steam was first injected at the desired rate. After the flow had stabilized, the inlet spray flow of water was initiated. With the steam flow held constant, the spray temperature was decreased from 205°F to a minimum of 80°F, and the data was recorded.

The selection of tests for simulation with WCOBRA/TRAC-TF2 was intended to cover a wide range of temperatures and injection rates, in order to bound the thermal-hydraulic conditions expected during core reflood in an UPI plant. The test data (Jones, 1977) that are judged to be applicable to a PWR simulation are from the tests performed in the steady state mode. The matrix of tests selected for WCOBRA/TRAC-TF2 simulation is listed in Table 2.3-1. Each test involved 30 or more steps (sub-tests) in which the water injection was held constant as the steam injection was increased in a step-wise manner. The precise steam conditions (i.e., pressure and temperature) were not reported in (Jones, 1977); however, the report does indicate that pressures in the sub-tests for Tests 60, 61, 62, 69, and 73 range from 14.7 to 23.2 psia. Over this pressure range the enthalpy of saturated steam varies from 1151 to 1160 Btu/lbm. Therefore, the WCOBRA/TRAC-TF2 simulations modeled a constant enthalpy of 1160.5 Btu/lbm to ensure slightly superheated steam was modeled for all tests.

The WCOBRA/TRAC-TF2 simulation of each test consisted of separate code executions performed for each steam flow rate step (sub-test). The first 50 seconds are used to establish the steady state conditions for the current sub-test, while the final 100 seconds are used to collect the results. The water injection flow rate is held constant for the entire simulation. The steam injection is delayed for 1 second, and then is ramped over the next 4 seconds to the flow rate for the previous step. This flow rate is held constant until 49 seconds after the start of the simulation, and is then ramped over the next 1 second to the flow rate for the current step. This flow rate is held constant for the final 150 seconds.

2.3.3 GE CCFL Nodalization

The test section at the GE facility consisted of an 8x8 simulated BWR fuel assembly inside a 5.27 inch square channel, shortened to 7 feet in length and connected to a scaled down section of the upper plenum. The steam injection occurred at the bottom of the test section, and subcooled water was injected into the upper plenum. Figure 2.3-1 provides a schematic of the GE CCFL facility.

Figure 2.3-4 shows the WCOBRA/TRAC-TF2 noding diagram of the test facility. The test section is modeled as a combination of vessel and loop components. The vessel components are broken into **[**

][a,c]

[

]a,c

2.3.4 GE CCFL Test Comparisons and Conclusions

The primary focus of the WCOBRA/TRAC-TF2 simulations was on the interfacial condensation and its impact on the flooding characteristics at the tie plate.

The test conditions for each of the five tests are summarized in Table 2.3-1. The first three tests [ ]a,c are similar, but the liquid injection rates are different. Test [ ]a,c is near saturation (pressure is at atmospheric conditions). Test [ ]a,c is unique in that it uses the spillover water injection method.

Figures 2.3-5 through 2.3-9 show the comparison of the [

]a,c

The predicted liquid drain rate vs. steam injection rate and the GE CCFL test data are compared against the subcooled CCFL correlations, which were obtained from tests performed on a perforated plate as investigated by (Bankoff, et al., 1981). The Bankoff correlation for a typical geometry of the upper tie plate becomes:

$$\left(K_{g,e}^{*}\right)^{1/2} + \left(K_{f}^{*}\right)^{1/2} = 2 \tag{2.3-1}$$

Where (K_f^*) is the Kutateladze number of dimensionless superficial velocity for liquid:

$$K_f^* = j_f \left(\frac{\rho_f{}^2}{g \cdot g_c \cdot \sigma(\rho_f - \rho_g)} \right)^{1/4} \quad (2.3\text{-}2)$$

Where,

j_f = Liquid superficial velocity, ft/s
ρ_f = Liquid density, lbm/ft^3
ρ_g = Vapor density, lbm/ft^3
σ = Surface tension, lbf/ft
g = Acceleration of gravity, 32.174 ft/s^2
g_c = Conversion factor, 32.174 lbm-ft/lbf-s^2

$K_{g,e}^*$ in Equation 2.3-1 is the effective dimensionless steam flow rate including the effect of steam condensation defined by:

$$K_{g,e}^* = K_g^* - \left(\frac{f C_p (T_{f,in} - T_{sat})}{h_{fg}} \right) \sqrt{\frac{\rho_f}{\rho_g}} K_{f,in}^* \quad (2.3\text{-}3)$$

Where,

f = Condensation efficiency
C_p = Liquid specific heat, Btu/lbm-°F
$T_{f,in}$ = Liquid temperature, °F
T_{sat} = Saturation temperature, °F
h_{fg} = Latent heat of enthalpy, Btu/lbm
K_g^* = Kutateladze number of dimensionless superficial velocity for vapor:

$$K_g^* = j_g \left(\frac{\rho_g{}^2}{g \cdot g_c \cdot \sigma(\rho_f - \rho_g)} \right)^{1/4} \quad (2.3\text{-}4)$$

Where,

j_g = Vapor superficial velocity, ft/s

For the saturated flooding case, the condensation efficiency term is not included as the inlet water temperature ($T_{f,in}$, °F) and saturation temperature (T_{sat}, °F) are equal.

[

]^{a,c}

[

]^{a,c}

Table 2.3-1 GE Tests Simulated with WCOBRA/TRAC-TF2

[

]a,c

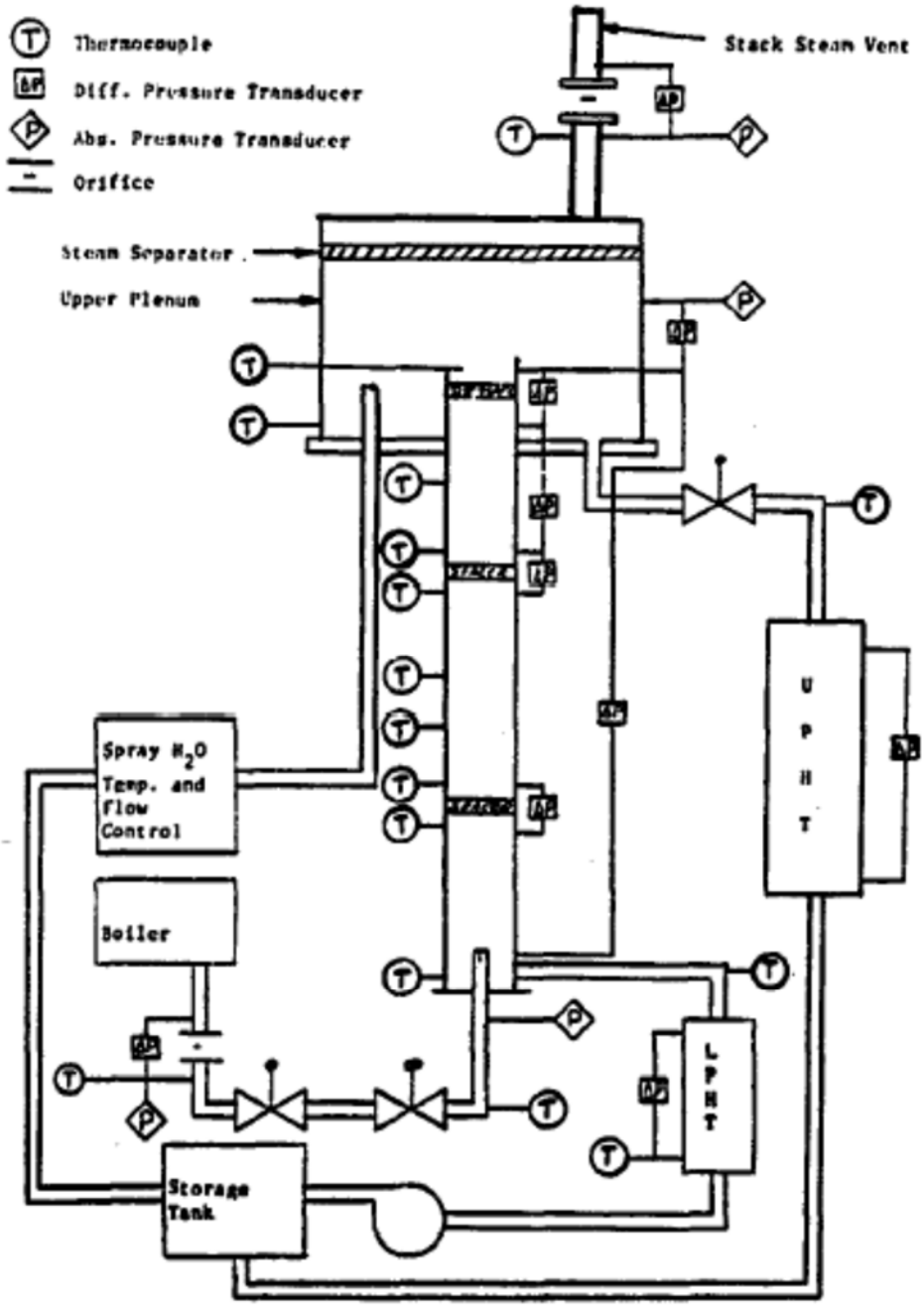

Figure 2.3-1 Schematic of GE CCFL Facility

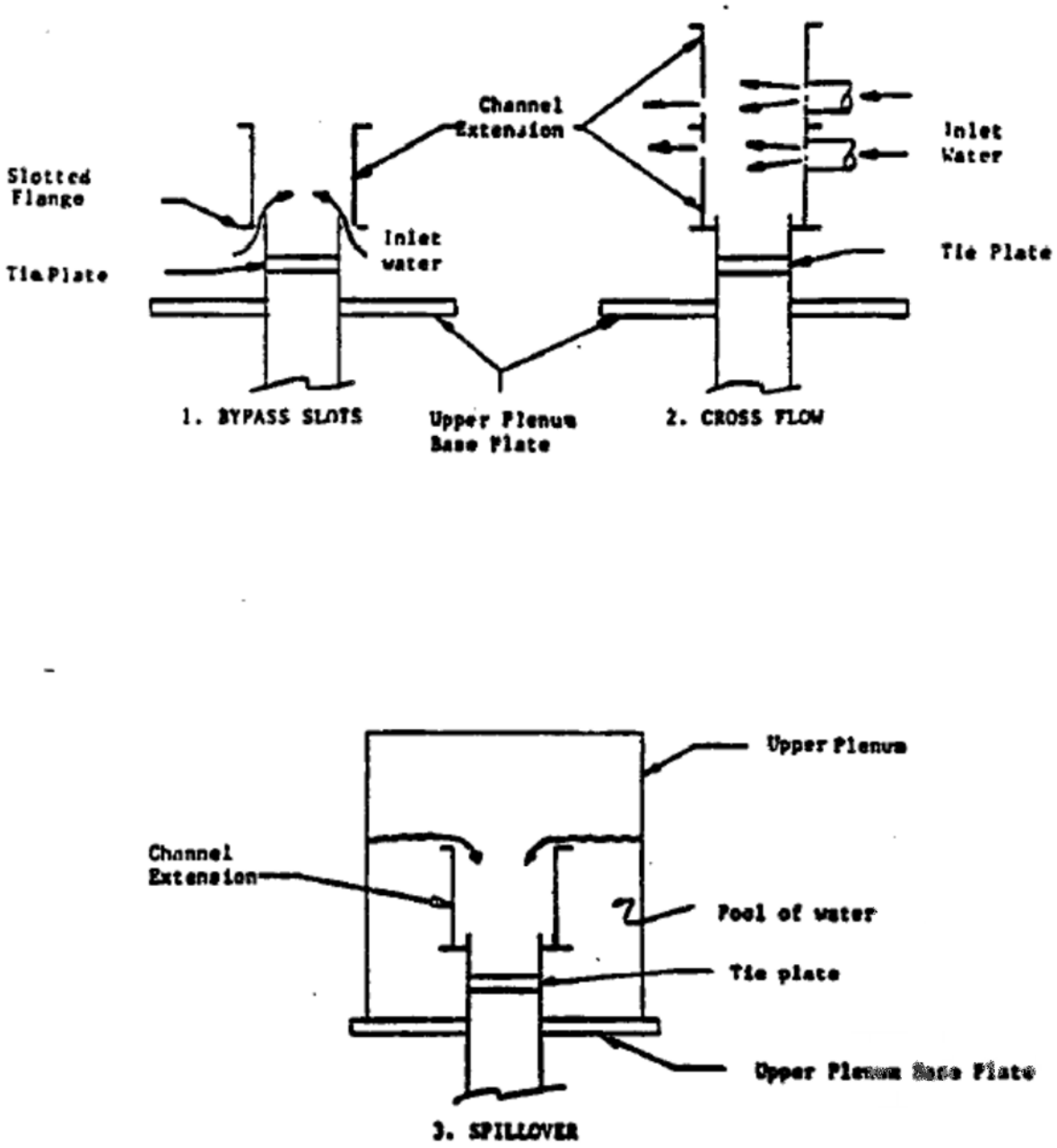

Figure 2.3-2 GE CCFL Tests – Water Injection Methods

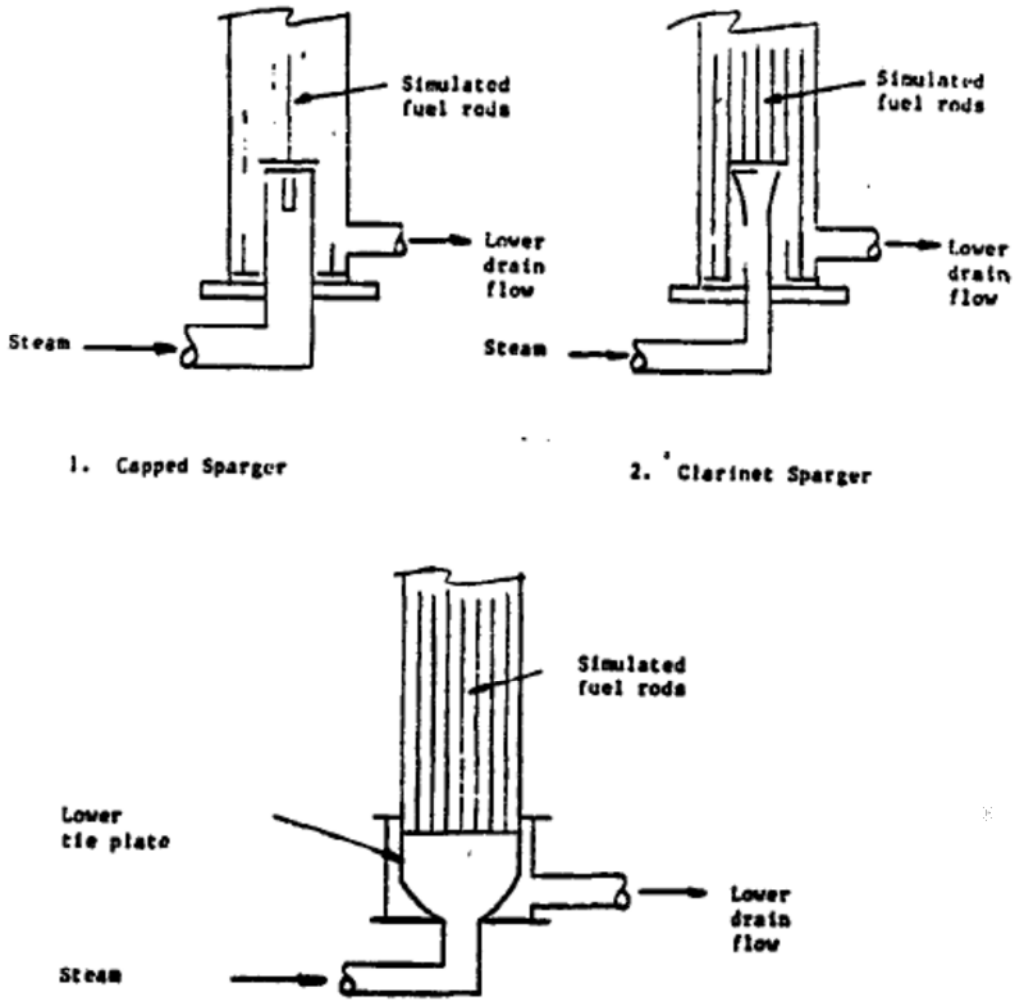

Figure 2.3-3 GE CCFL Tests – Steam Injection Methods

[**a,c**

]

Figure 2.3-4 WCOBRA/TRAC-TF2 Nodalization of GE CCFL Facility

[

]**a,c**

[a,b,c]

Figure 2.3-5 GE CCFL Test [ ]^{a,c} Liquid Drain Rate as a Function of Steam Injection Rate

[**a,b,c**

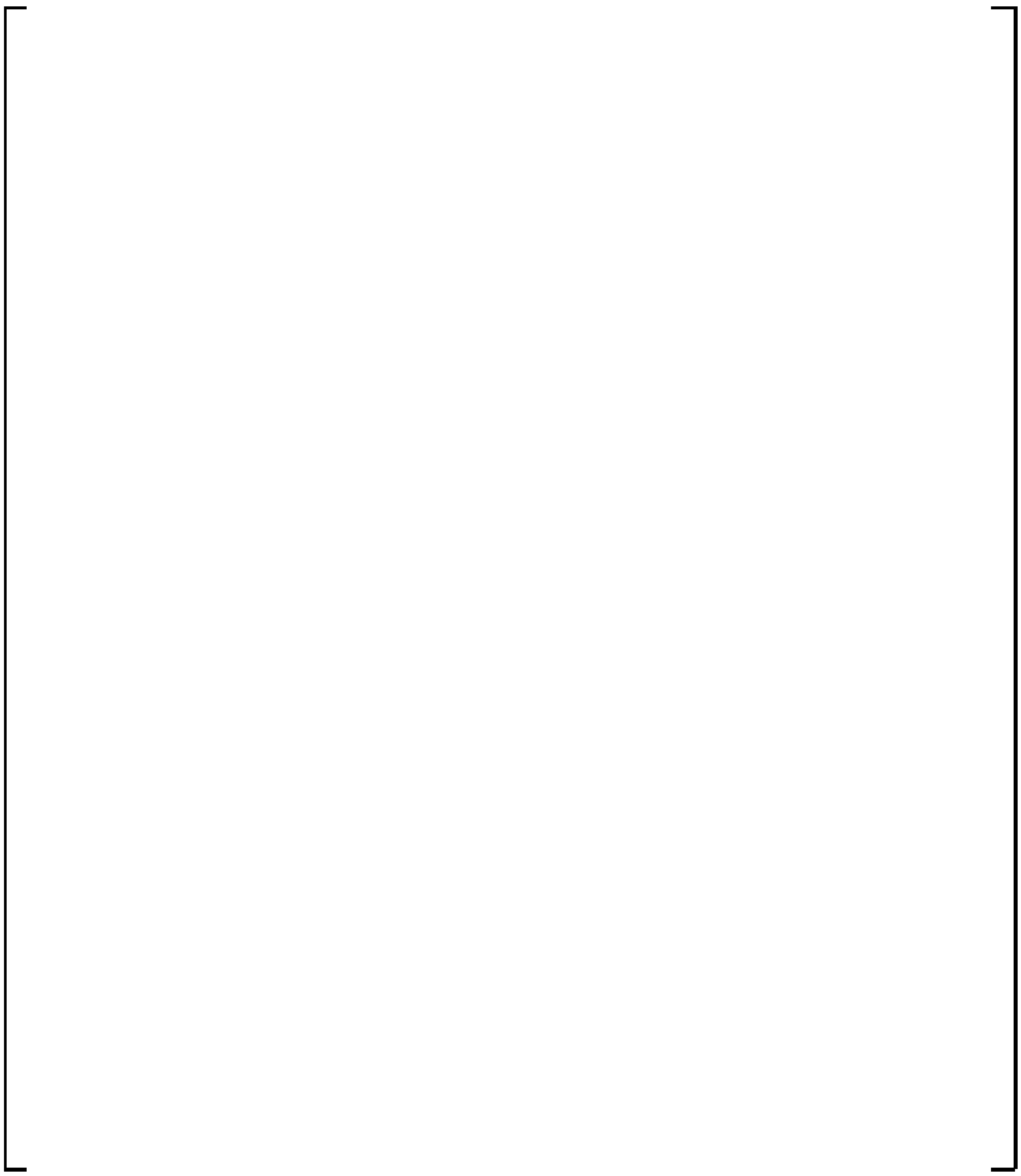

]

Figure 2.3-6 GE CCFL Test [ ]^{a,c} Liquid Drain Rate as a Function of Steam Injection Rate

a,b,c

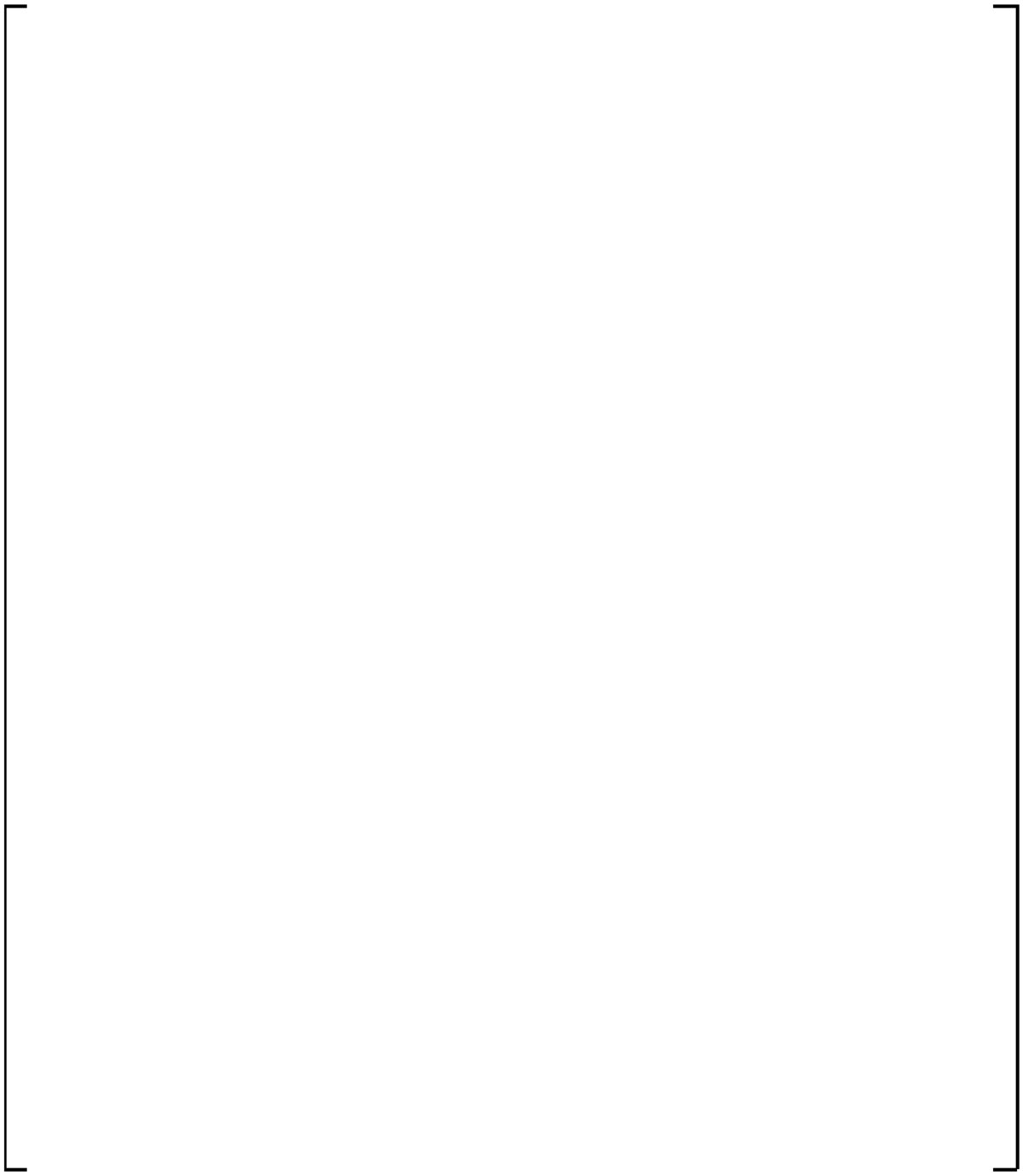

Figure 2.3-7 GE CCFL Test [ ]^{a,c} Liquid Drain Rate as a Function of Steam Injection Rate

[**a,b,c**

]

Figure 2.3-8 GE CCFL Test [ ]^{a,c} Liquid Drain Rate as a Function of Steam Injection Rate

[**a,b,c**

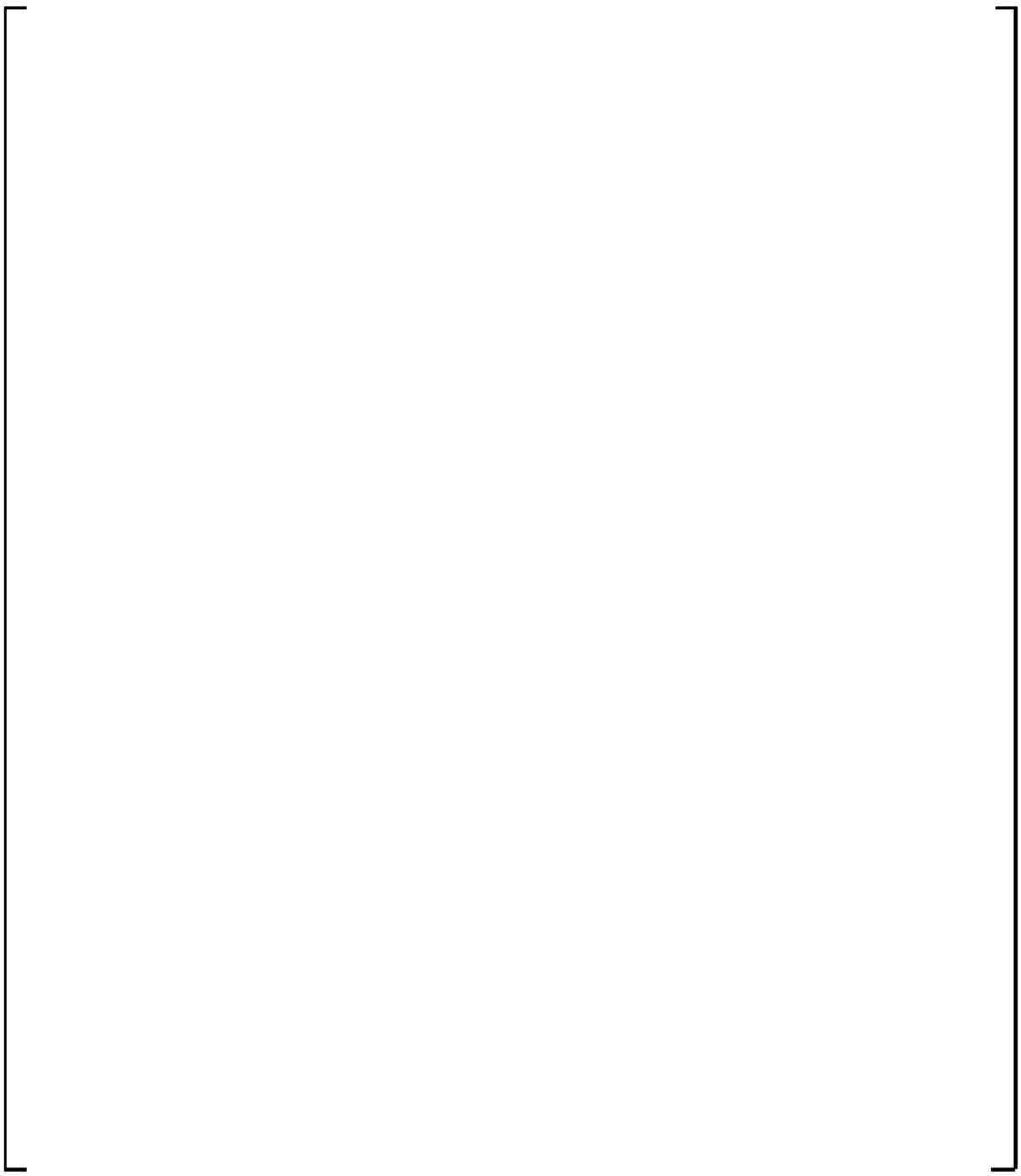

]

Figure 2.3-9 GE CCFL Test [ ]^{a,c} Liquid Drain Rate as a Function of Steam Injection Rate

[**a,b,c**

]

Figure 2.3-10 GE CCFL Test [ ]^{a,c} Prediction vs. Bankoff Flooding Correlation and Test Data

[**a,b,c**

]

Figure 2.3-11 GE CCFL Test [ ]^{a,c} Prediction vs. Bankoff Flooding Correlation and Test Data

a,b,c

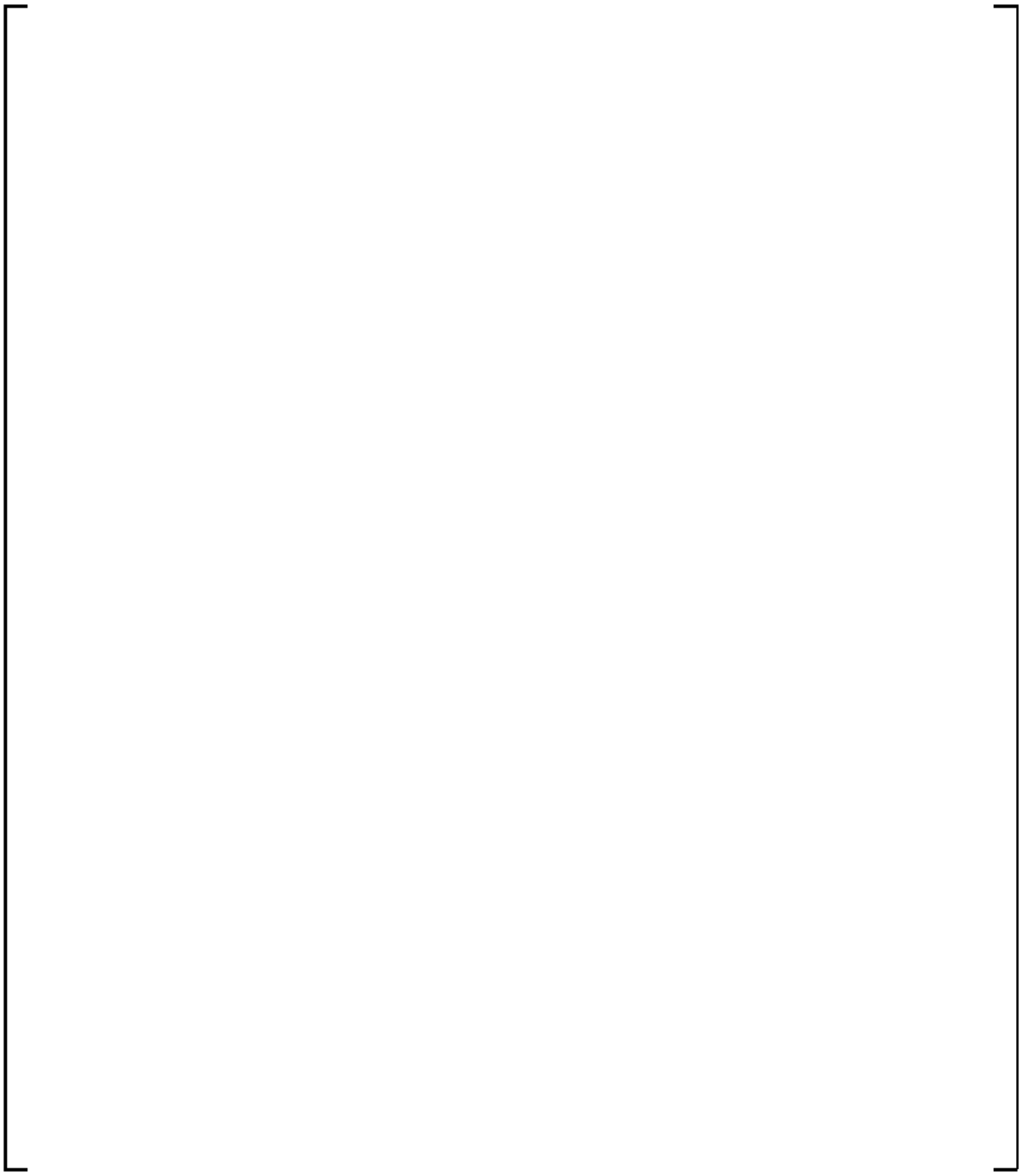

Figure 2.3-12 GE CCFL Test [ ]^{a,c} Prediction vs. Bankoff Flooding Correlation and Test Data

a,b,c

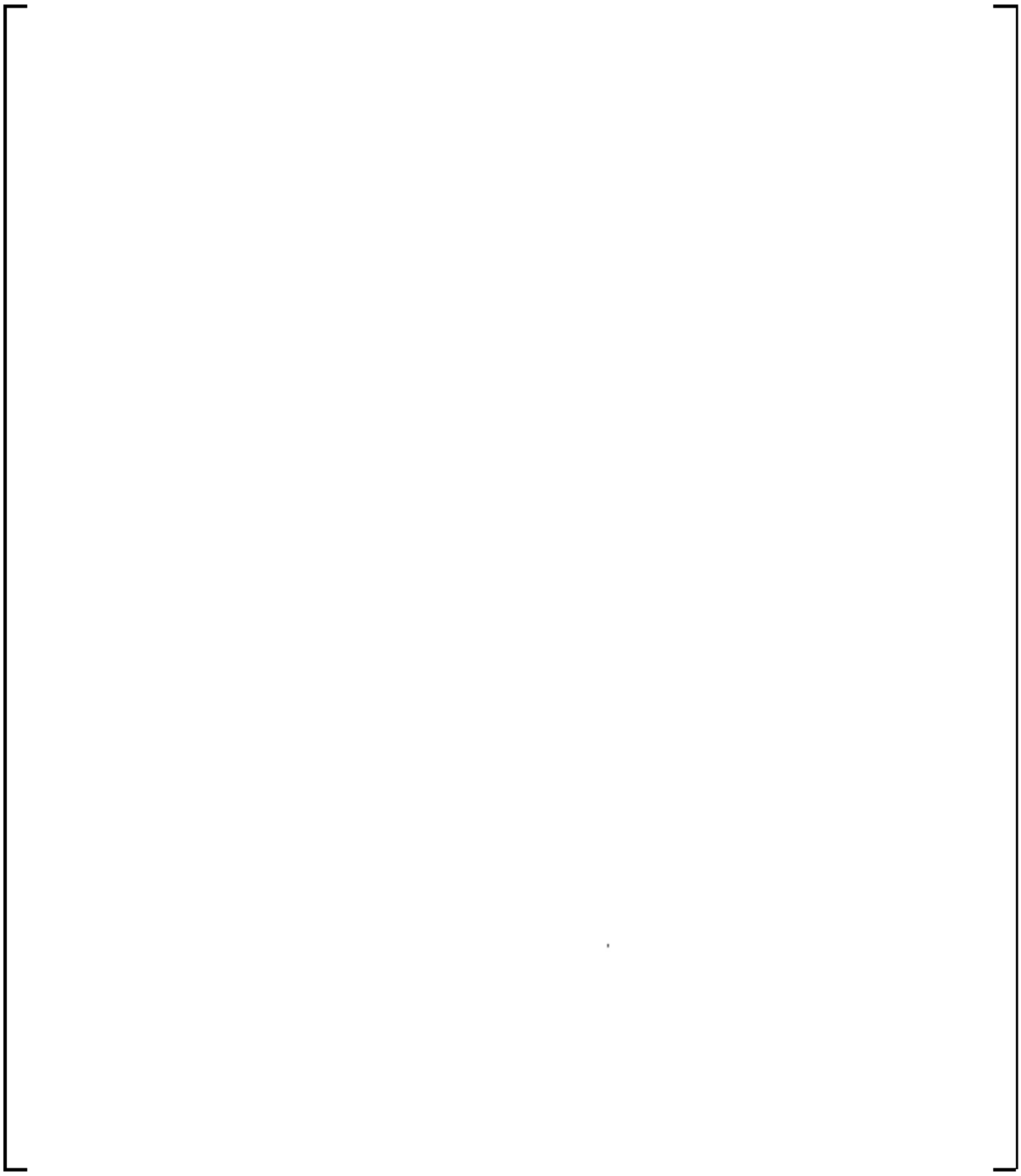

Figure 2.3-13 GE CCFL Test [ ]^{a,c} Prediction vs. Bankoff Flooding Correlation and Test Data

[**a,b,c**

]

Figure 2.3-14 GE CCFL Test [ ]^{a,c} Prediction vs. Bankoff Flooding Correlation and Test Data

2.4 CYLINDRICAL CORE TEST FACILITY TESTS WITH UPPER PLENUM INJECTION

The CCTF tests with upper plenum injection, CCTF Runs 72 and 76 (lguchi, et al., 1985 and 1985a), were analyzed with WCOBRA/TRAC-TF2 to assess the code application to a PWR equipped with UPI. Run 72 simulates no failure of low pressure coolant injection (LPCI) pumps, and the UPI water was injected through two injection pipes. Run 76 has a single failure of LPCI pump, and the UPI water was injected asymmetrically through one injection pipe.

Section 2.4.1 describes the WCOBRA/TRAC-TF2 noding of the CCTF tests. The **[ ]**[a,c] model in the CCTF simulations allows use of a similar WCOBRA/TRAC-TF2 model as for cold leg injection test (Run 62) from (Kobelak, et al., 2016). Although it is not strictly necessary to have a **[ ]**[a,c] model for Runs 72 and 76, it is judged that the impact of the modelling is insignificant on these UPI tests since the focus of Runs 72 and 76 was on the flow behavior in the upper plenum region and the core heat transfer, not the ECC bypass. Discussions of the test simulation results are presented in Sections 2.4.2 and 2.4.3, respectively, for Runs 72 and 76..

2.4.1 CCTF Noding

Figure 2.4-1 provides a schematic of the CCTF. The configuration of the upper plenum injection ports is illustrated in Figure 2.4-2. Figure 2.4-3 shows the cross-sectional view of the arrangement of the upper plenum injection pipe and the assemblies.

Figures 2.4-4 through 2.4-4c show the WCOBRA/TRAC-TF2 vessel noding diagrams for CCTF Runs 72 and 76. Section 1 is the lower plenum region. The region with the heater rods and simulated core is Section 2. The arrangement of **[**

][a,c]

Section 3 is the tie plate region. The CCTF top nozzle design **[**

][a,c] at the top of Section 3 in the CCTF 72 and 76 models. The channel modeling in this region is consistent with the UPI PWR model.

Section 4 is the noding for the first upper plenum region. There are **[ ]**[a,c] in Section 4, consistent with the standard model for UPI plants, to more accurately predict gravity-driven cross flows in the upper plenum region. **[**

][a,c]

[

]a,c This is consistent with the UPI PWR model.

Section 5 is the loop connection section. [

]a,c The guide tube (GT) channel remains in the inner global channel due to the guide tube wall which physically separates the flow from the global region. The combination of channels in Section 5 is consistent with that in the 3- and 4-loop model to the extent possible. Differences reflect structural differences of the test facility and the plants. Finally, the model contains [

]a,c

Figure 2.4-5 shows the loop noding diagram for CCTF Runs 72 and 76. The noding is similar to that employed by the 3- and 4-loop PWR models documented in the FSLOCA EM topical report (Kobelak, et al., 2016) with additional components added to model the UPI.

2.4.2 CCTF Run 72

One of the objectives of the CCTF test program was to study the effectiveness of the UPI system. CCTF Run 72 is a No Failure UPI test, that is, 100% of the LPCI was injected symmetrically into the upper plenum through the two UPI pipes located near the outside row of assemblies and pointing towards the center of the facility in the upper plenum (Figure 2.4-3). This is modelled with an UPI pipe connecting to channel 53, the upper plenum inner global channel at the loop elevation (Figure 2.4-4). The second source of ECCS water was the cold leg injection, which consisted of accumulator and high pressure coolant injection (HPCI) flows. The cold leg injection was modelled with FILLs and connecting PIPEs (Figure 2.4-5). The third source of the ECCS water was the lower plenum injection, which also modelled accumulator and HPCI flows. This was modelled with a flow boundary condition in channel 1. Figure 2.4-6 shows the timing and magnitude of the various ECCS water sources for test Run 72, taken from the JAERI report (Iguchi, et al., 1985).

[

]a,c

[

]a,c

[1] Note that a very small amount of weighted smoothing was applied to these figures for readability.

[

]a,c

2.4.3 CCTF Run 76

CCTF Run 76 (lguchi, et al., 1985a) was similar to Run 72, except that it was intended to study the effect of a single failure. As such, only about 50% of the LPCI flow was injected through one of the two UPI pipes. Figure 2.4-26 shows the test sequence of Run 76. The WCOBRA/TRAC-TF2 model for Run 76 was the same as that of Run 72 with the modifications of the flow boundary conditions to reflect the test flows. Comparing the data for Run 72 and Run 76, it was found that there was no significant difference in cladding temperature at the 6-foot elevation. A medium degree of cladding temperature difference occurred at the 8-foot elevation. The most cladding temperature difference can be seen at the 10-foot elevation.

[

]a,c

[

]a,c

[2] Note that a very small amount of weighted smoothing was applied to these figures for readability.

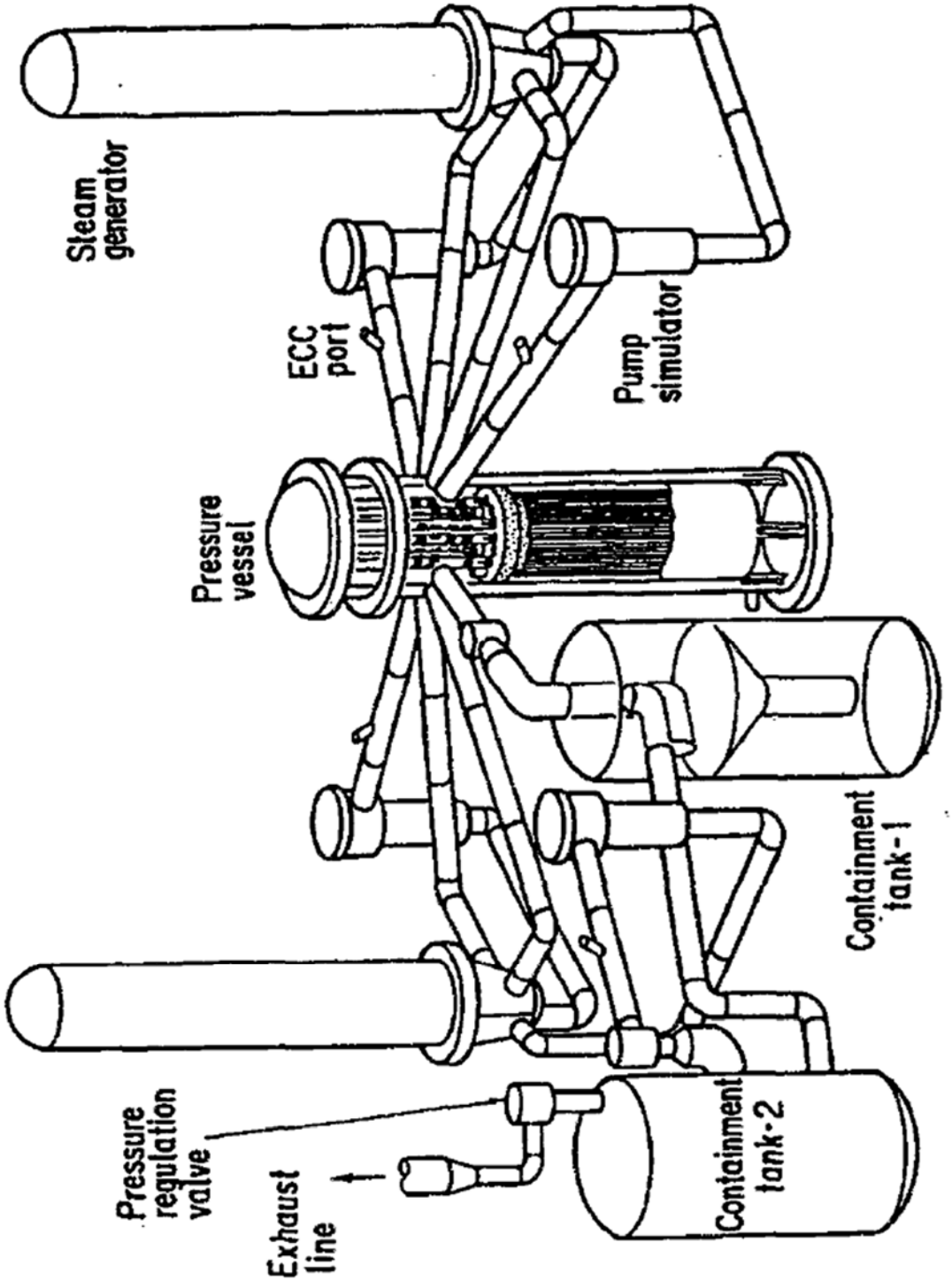

Figure 2.4-1 Schematic of CCTF

[a,b,c]

Figure 2.4-2 Configuration of Upper Plenum Injection Pipe for CCTF

a,b,c

Figure 2.4-3 Arrangement and Location of Upper Plenum Injection Pipe for CCTF

a,c

Figure 2.4-4 Vessel Noding Diagram for CCTF Run 72 and 76 (all units in inches)

a,c

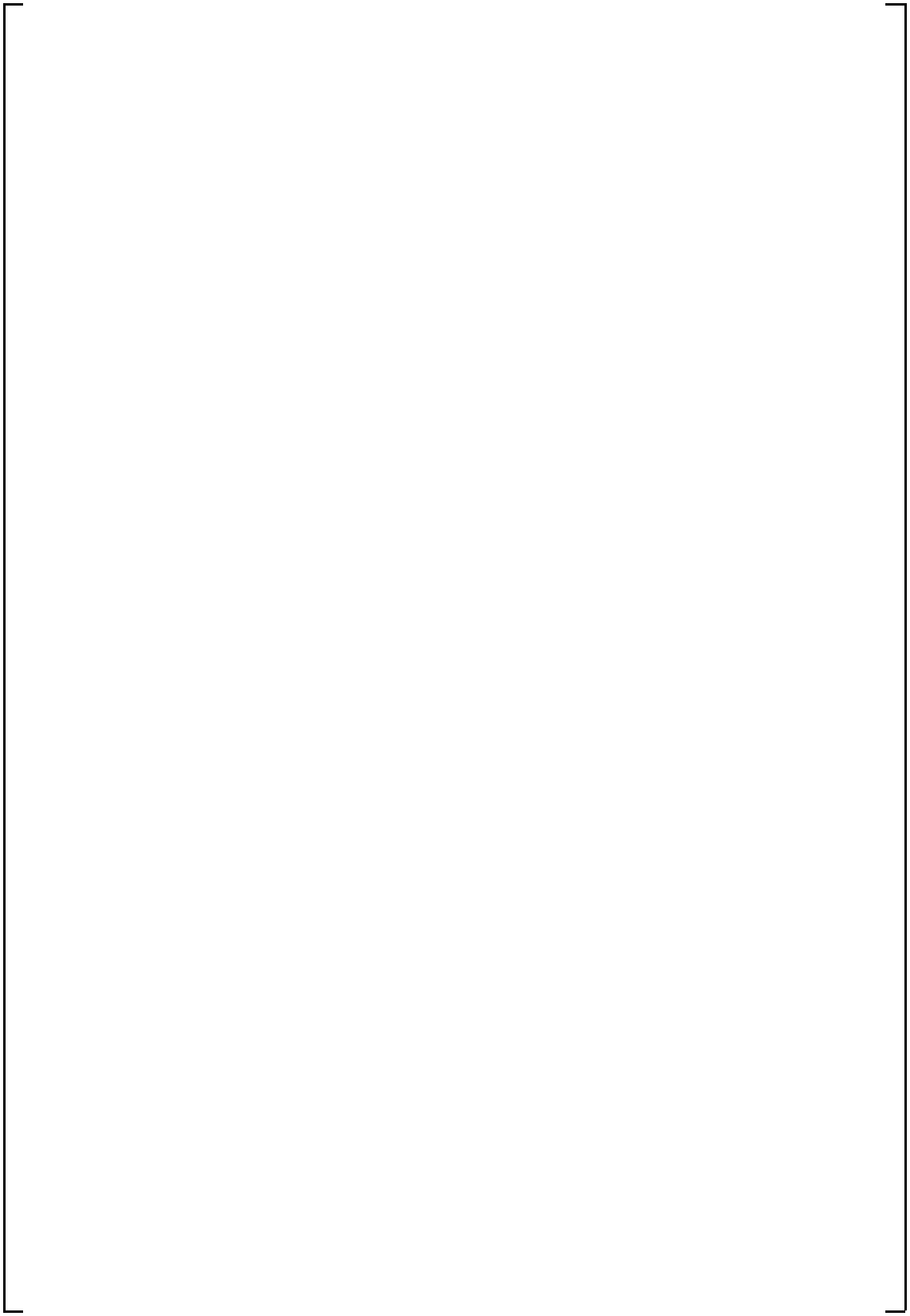

Figure 2.4-4a CCTF Run 72 and 76 Vessel Noding Diagram

a,c

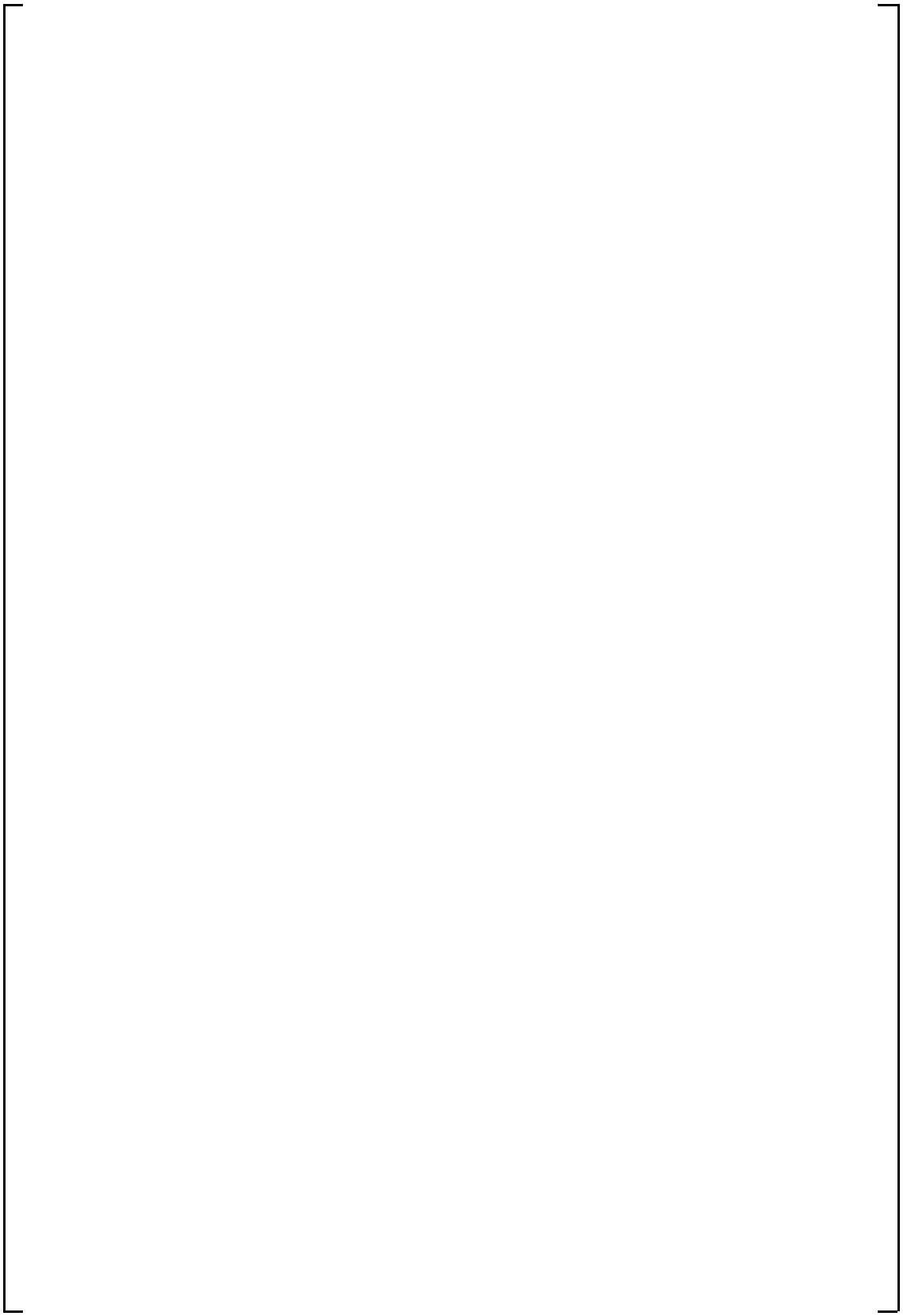

Figure 2.4-4b CCTF Run 72 and 76 Vessel Noding Diagram

a,c

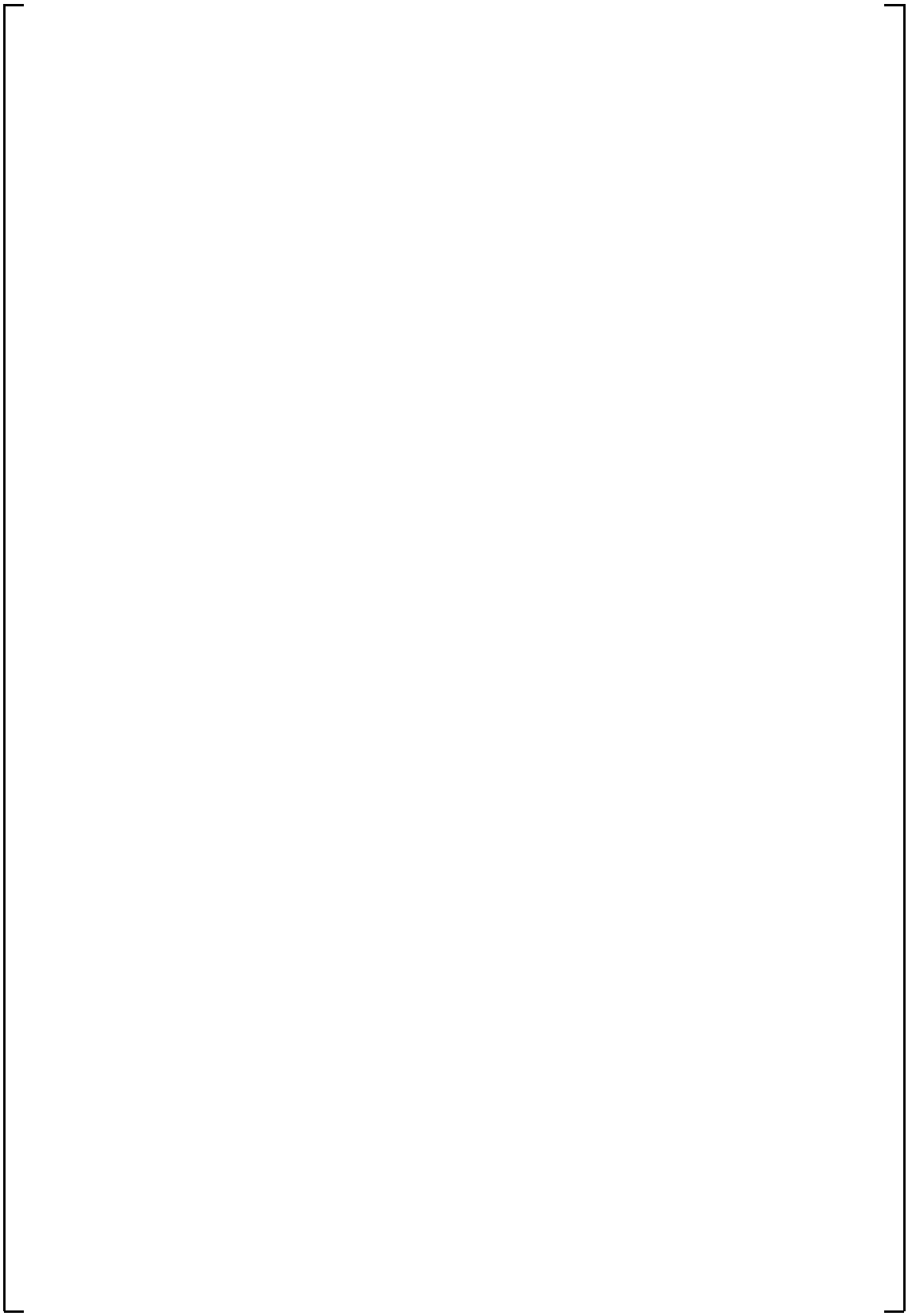

Figure 2.4-4c CCTF Run 72 and 76 Vessel Noding Diagram

a,c

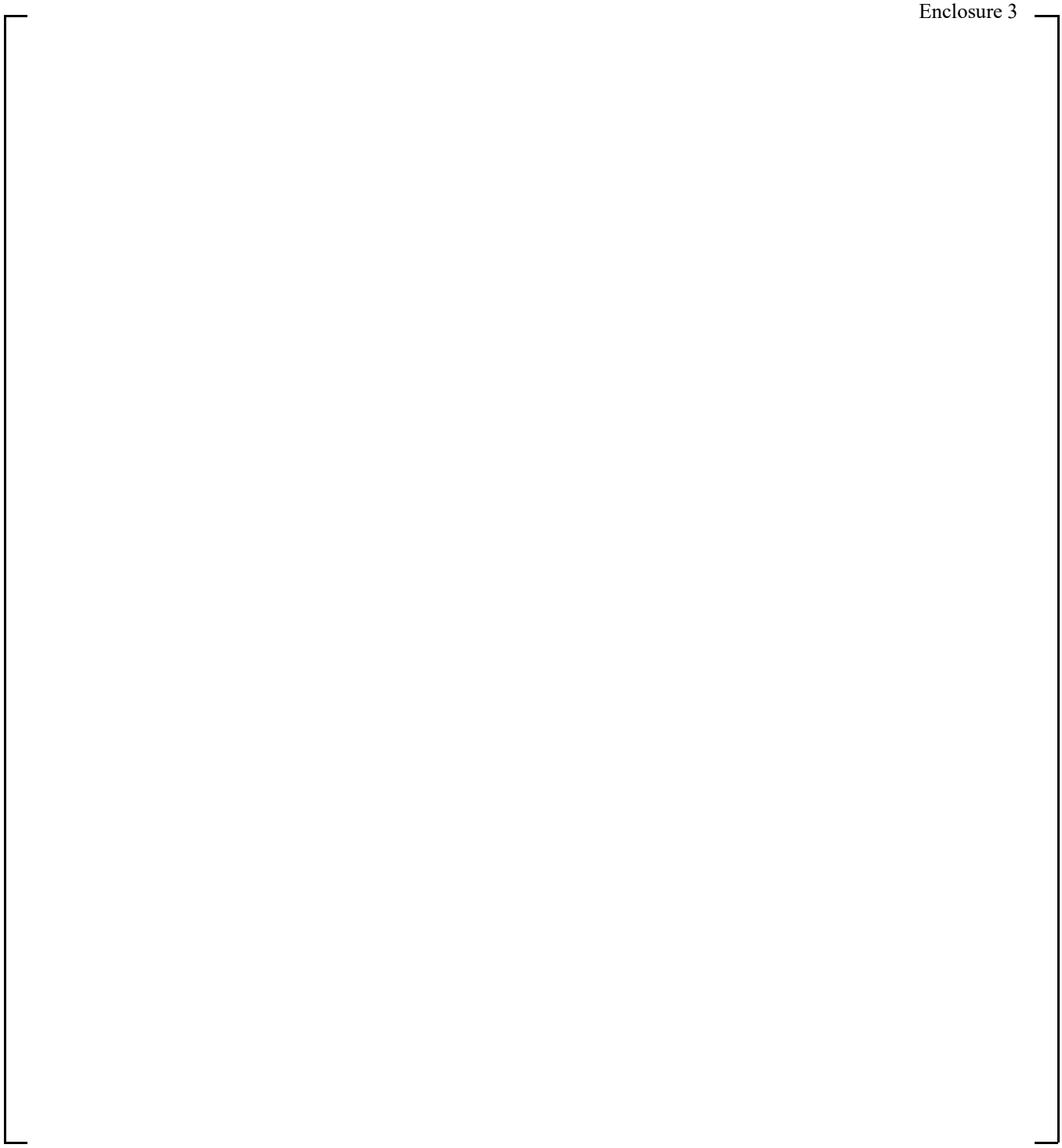

Figure 2.4-5 CCTF Run 72 and 76 Loop Noding Diagram

a,b,c

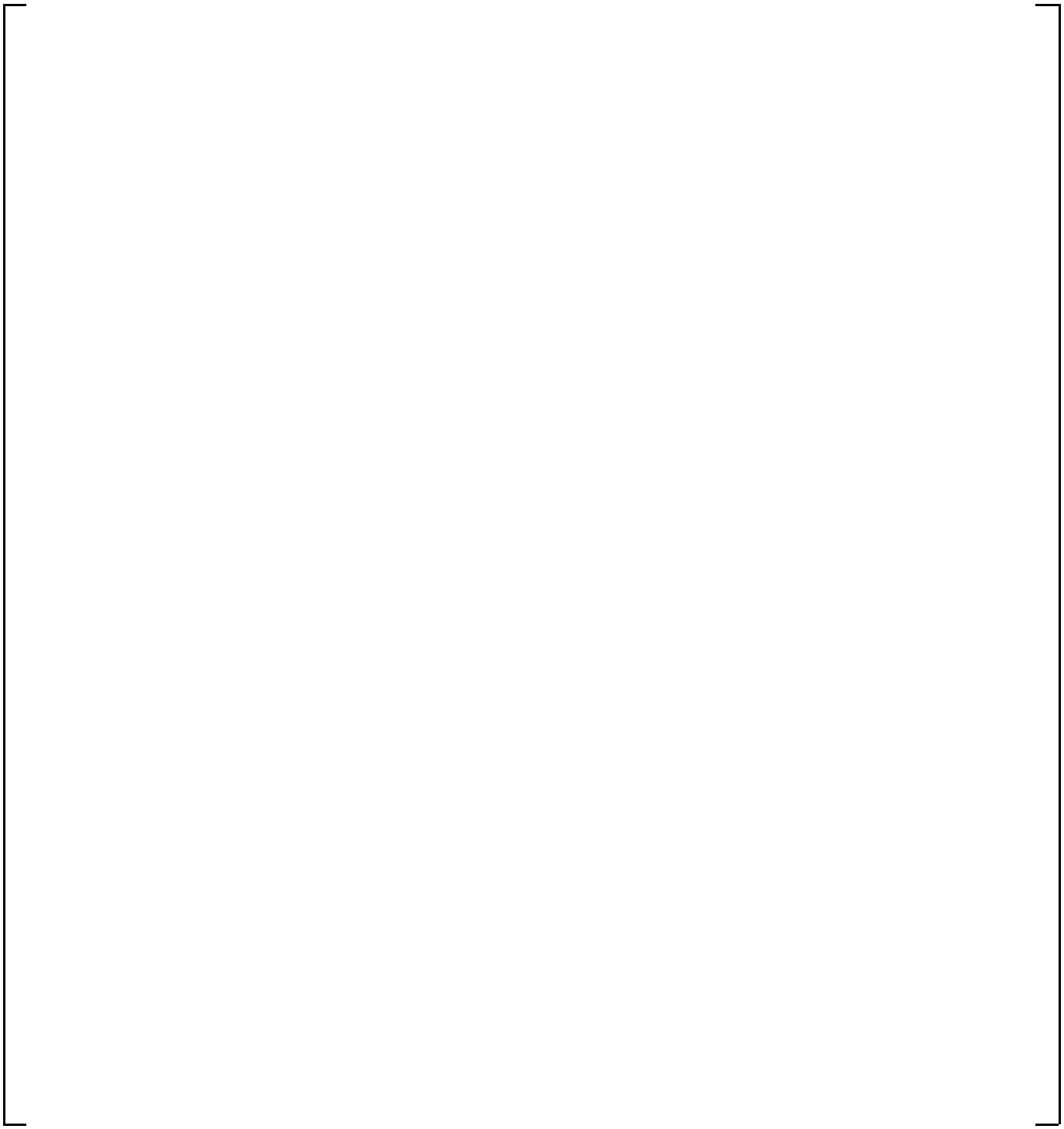

Figure 2.4-6 Schematic Sequence of C2-13 Test (CCTF Run 72)

[a,b,c]

Figure 2.4-7 CCTF Run 72 Broken Cold Leg Pressure Drop Comparison

a,b,c

Figure 2.4-8 CCTF Run 72 Upper Plenum Pressure Comparison

a,b,c

Figure 2.4-9 CCTF Run 72 Lower Plenum Pressure Comparison

a,b,c

Figure 2.4-10 CCTF Run 72 Hot Leg Vapor Mass Flow Rate Comparison

a,b,c

Figure 2.4-11 CCTF Run 72 Hot Leg Liquid Mass Flow Rate Comparison

a,b,c

Figure 2.4-12 CCTF Run 72 Cladding Temperature Comparisons at the 6-ft Elevation

a,b,c

Figure 2.4-13 CCTF Run 72 Cladding Temperature Comparisons at the 8-ft Elevation

a,b,c

Figure 2.4-14 CCTF Run 72 Cladding Temperature Comparisons at the 10-ft Elevation

a,b,c

Figure 2.4-15 CCTF Run 72 Hot Rod Quench Front Comparison

a,b,c

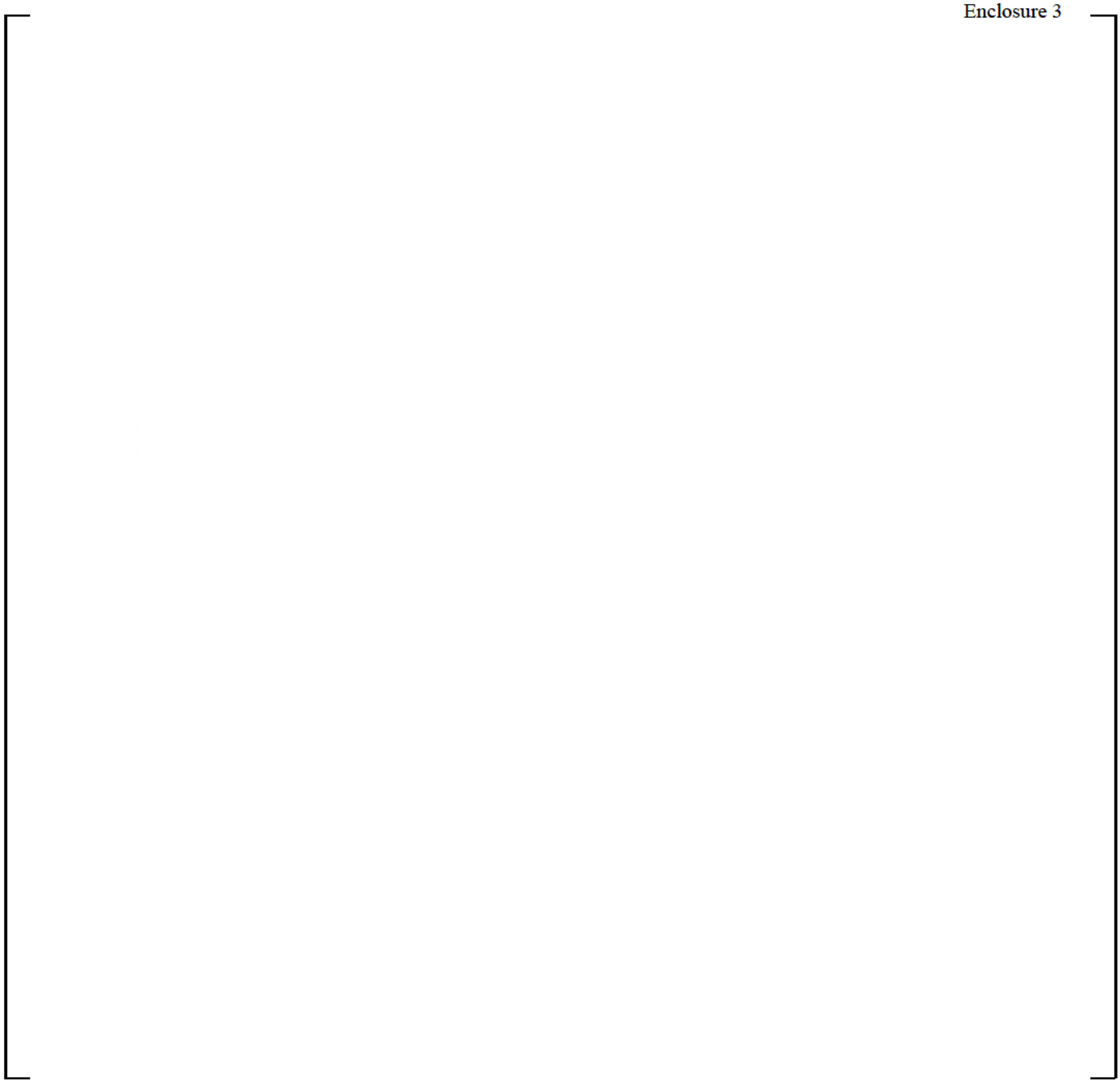

Figure 2.4-16 CCTF Run 72 Lower Plenum (0 to 6.9-ft Elevation) Void Fraction Comparison

a,b,c

Figure 2.4-17 CCTF Run 72 Core (6.9 to 8.9-ft Elevation) Void Fraction Comparison

a,b,c

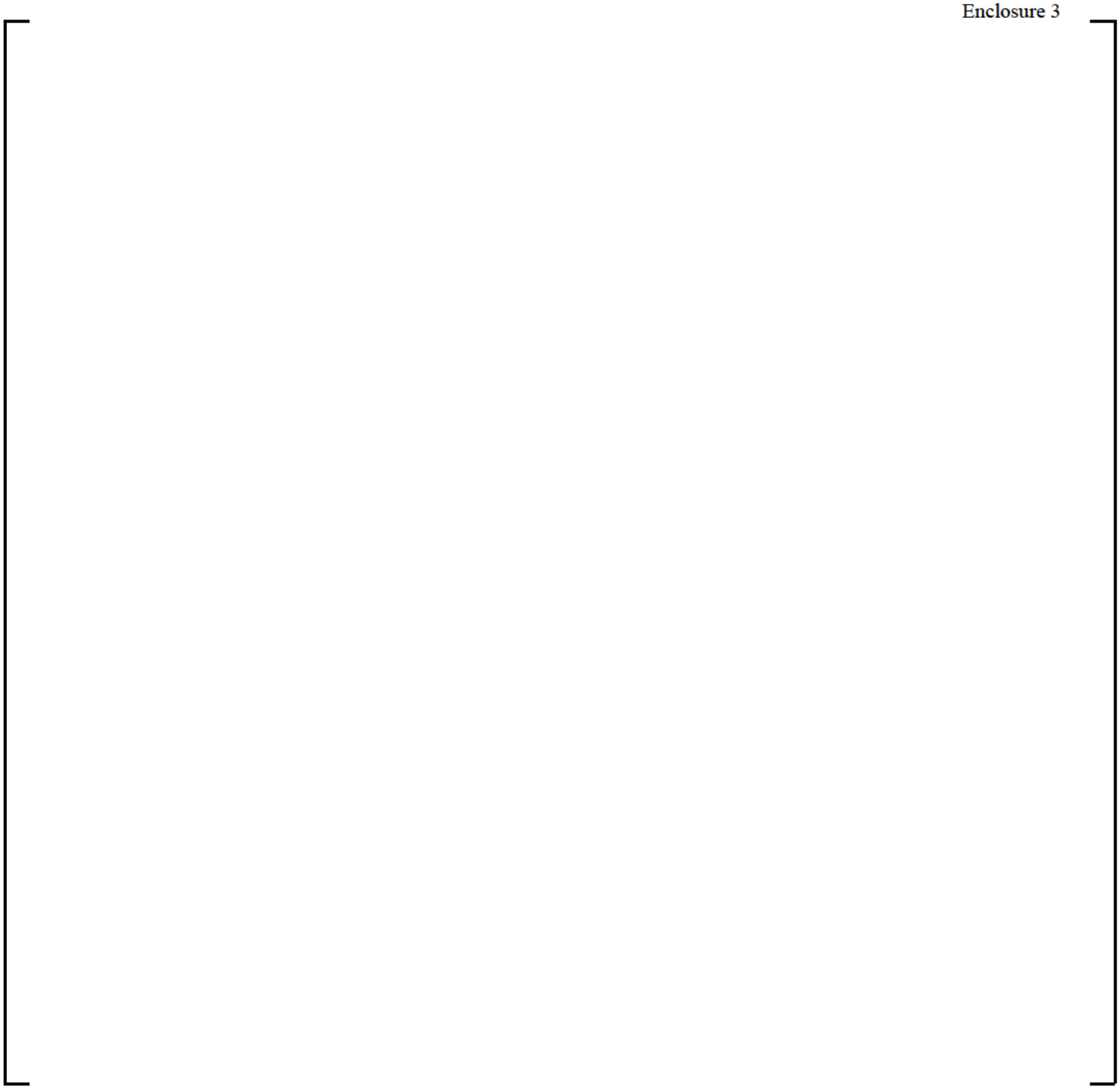

Figure 2.4-18 CCTF Run 72 Core (8.9 to 10.9-ft Elevation) Void Fraction Comparison

a,b,c

Figure 2.4-19 CCTF Run 72 Core (10.9 to 12.9-ft Elevation) Void Fraction Comparison

a,b,c

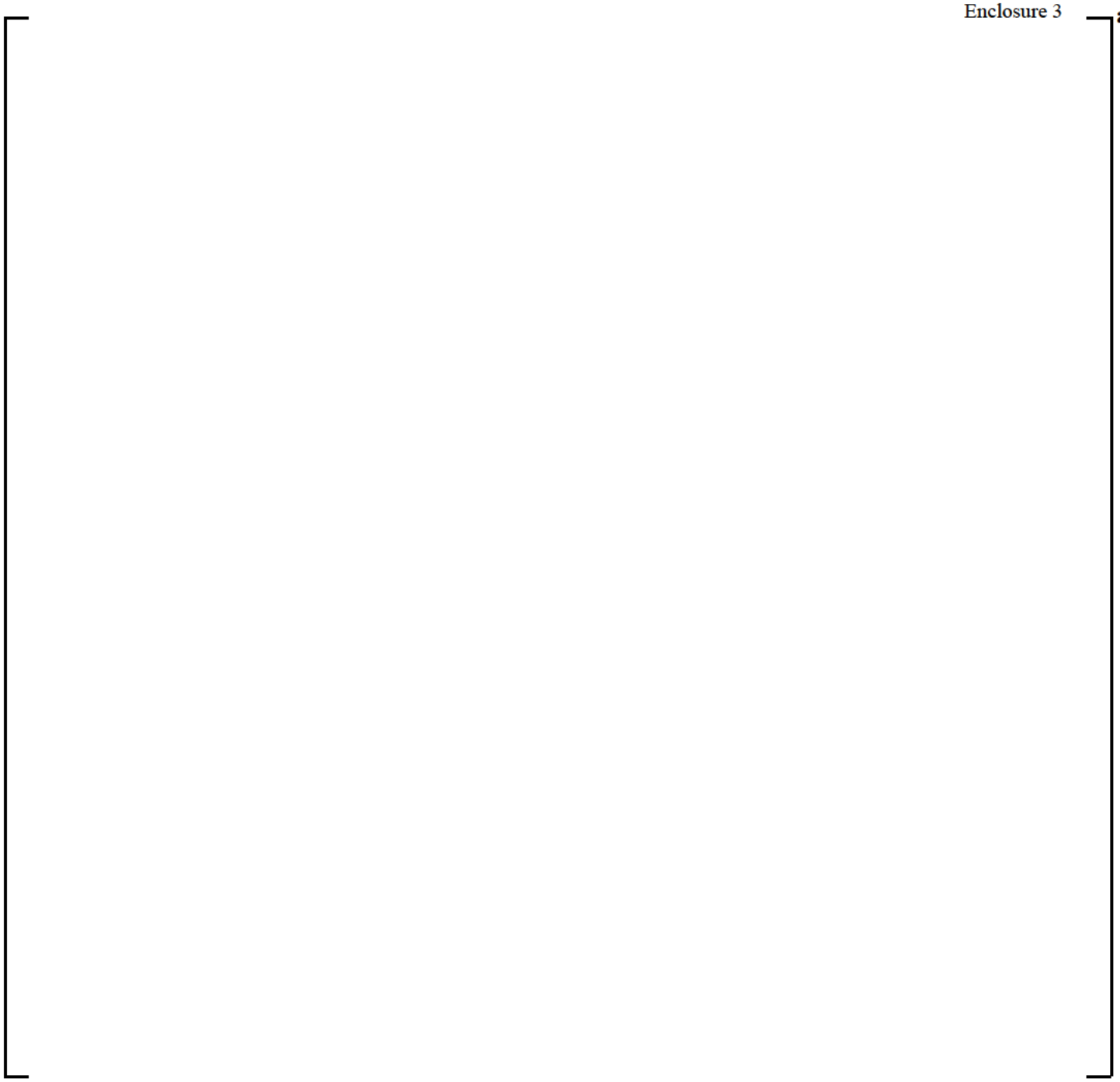

Figure 2.4-20 CCTF Run 72 Core (12.9 to 18.9-ft Elevation) Void Fraction Comparison

[a,c

]

Figure 2.4-21 Predicted Northwestern Dimensionless Volumetric Fluxes at the Top of High Power Channel 21 for CCTF Run 72

a,c

Figure 2.4-22 Predicted Northwestern Dimensionless Volumetric Fluxes at the Top of Channel 20 for CCTF Run 72

a,c

Figure 2.4-23 Predicted Northwestern Dimensionless Volumetric Fluxes at the Top of Channel 19 for CCTF Run 72

a,c

Figure 2.4-24 Predicted Northwestern Dimensionless Volumetric Fluxes at the Bottom of Channels 30 through 33 (Low Power Support Column Jet Channels in Each Quadrant) for CCTF Run 72

a,c

Figure 2.4-25 Flooding Behavior in CCTF Run 72 Above Low Power Core Channel at Tie Plate Elevation

a,b,c

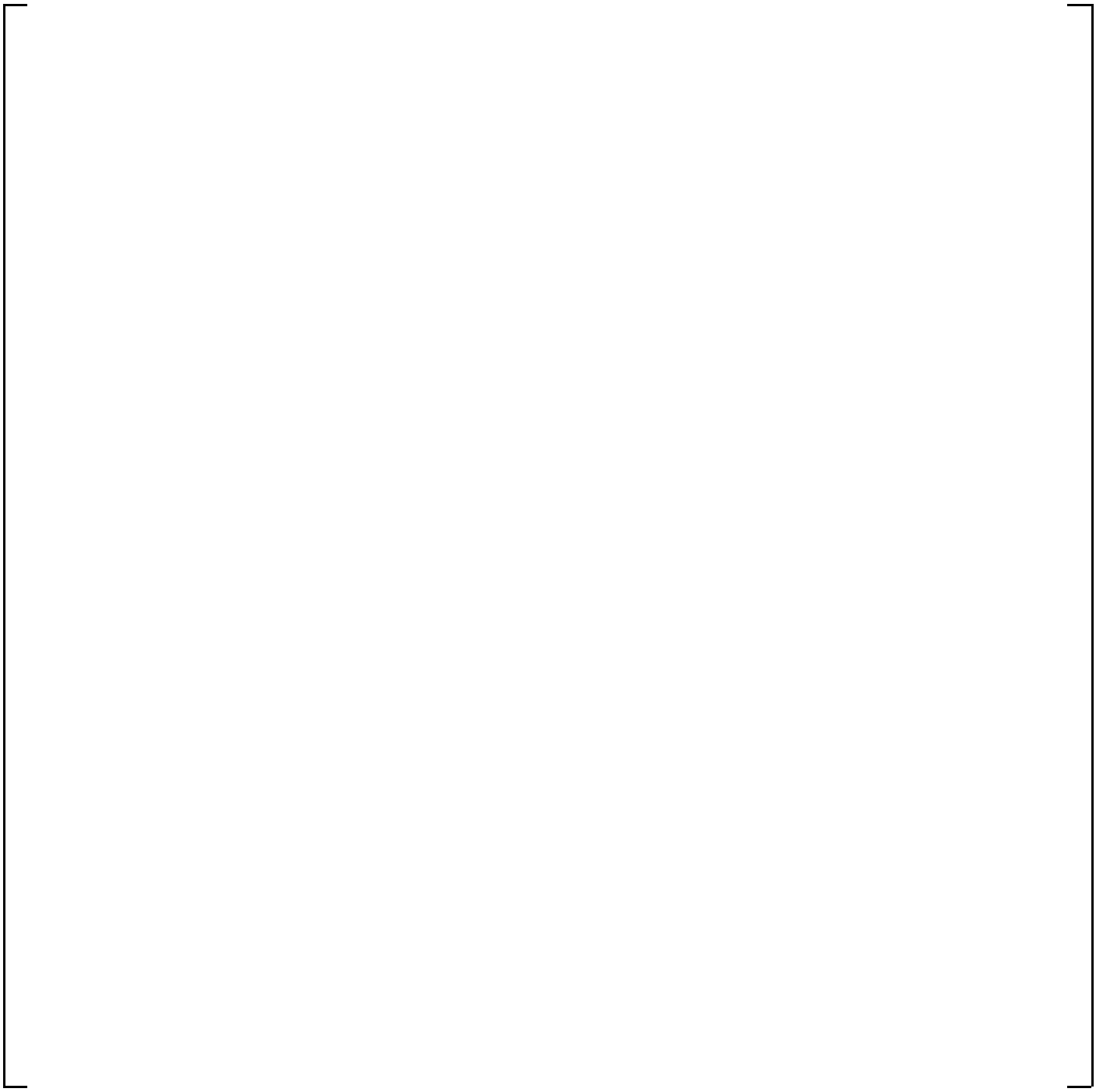

Figure 2.4-26 Schematic Sequence of C2-16 Test (CCTF Run 76)

a,b,c

Figure 2.4-27 CCTF Run 76 Broken Cold Leg Pressure Drop Comparison

a,b,c

Figure 2.4-28 CCTF Run 76 Upper Plenum Pressure Comparison

a,b,c

Figure 2.4-29 CCTF Run 76 Lower Plenum Pressure Comparison

a,b,c

Figure 2.4-30 CCTF Run 76 Hot Leg Vapor Mass Flow Rate Comparison

a,b,c

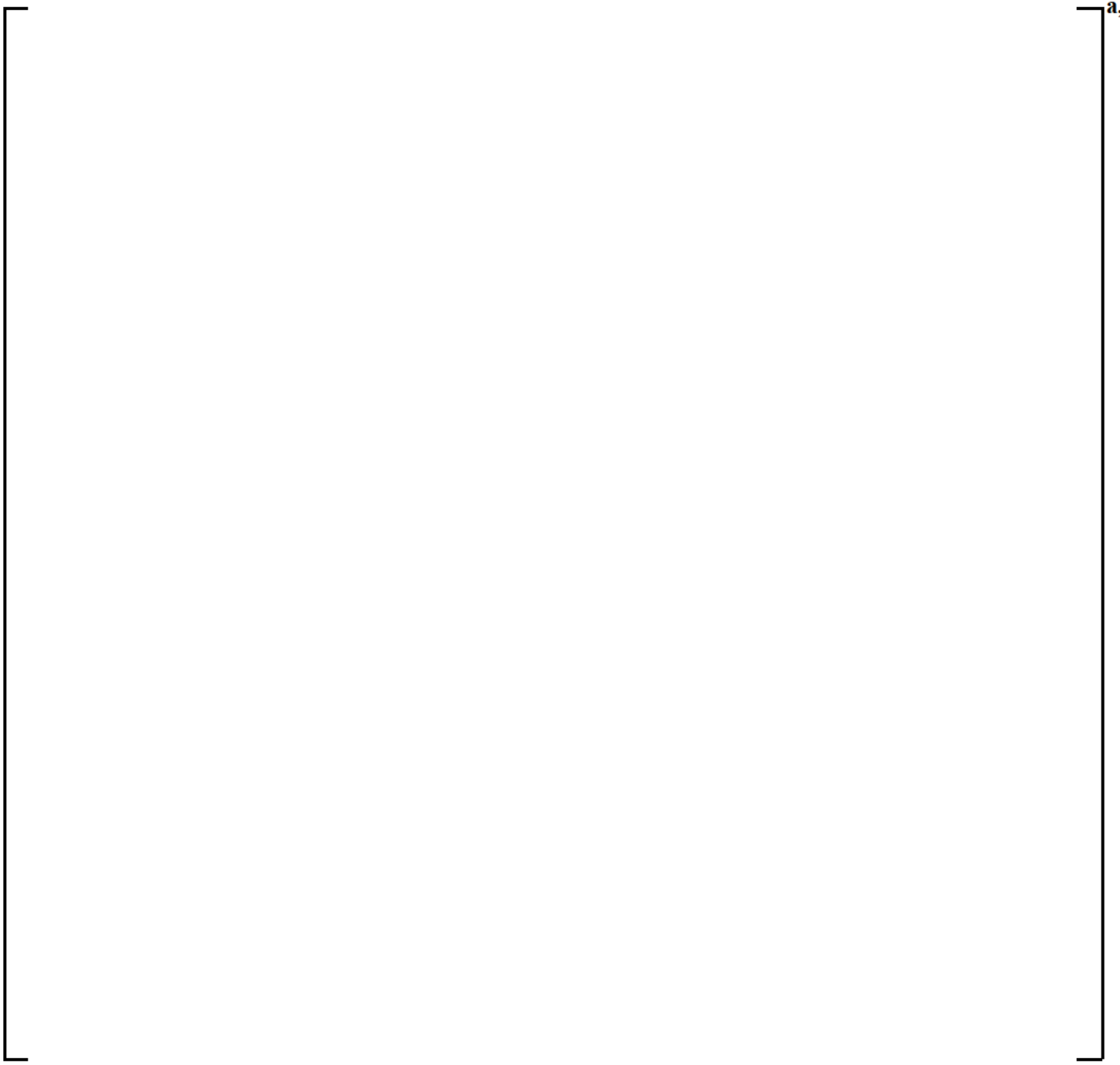

Figure 2.4-31 CCTF Run 76 Hot Leg Liquid Mass Flow Rate Comparison

a,b,c

Figure 2.4-32 CCTF Run 76 Cladding Temperature Comparisons at the 6-ft Elevation

a,b,c

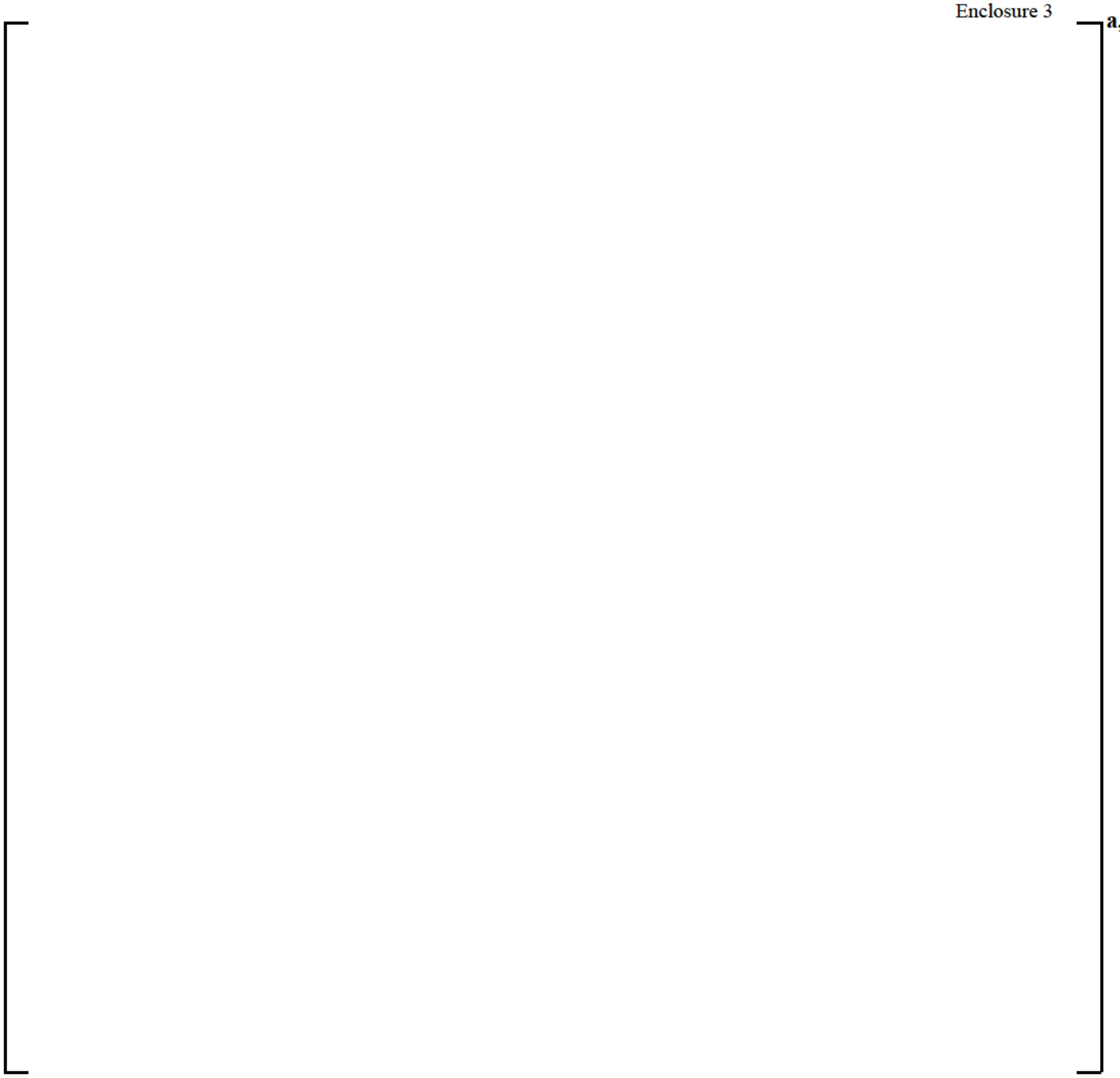

Figure 2.4-33 CCTF Run 76 Cladding Temperature Comparisons at the 8-ft Elevation

a,b,c

Figure 2.4-34 CCTF Run 76 Cladding Temperature Comparisons at the 10-ft Elevation

a,b,c

Figure 2.4-35 CCTF Run 76 Hot Rod Quench Front Comparison

a,b,c

Figure 2.4-36 CCTF Run 76 Lower Plenum (0 to 6.9-ft Elevation) Void Fraction Comparison

a,b,c

Figure 2.4-37 CCTF Run 76 Core (6.9 to 8.9-ft Elevation) Void Fraction Comparison

a,b,c

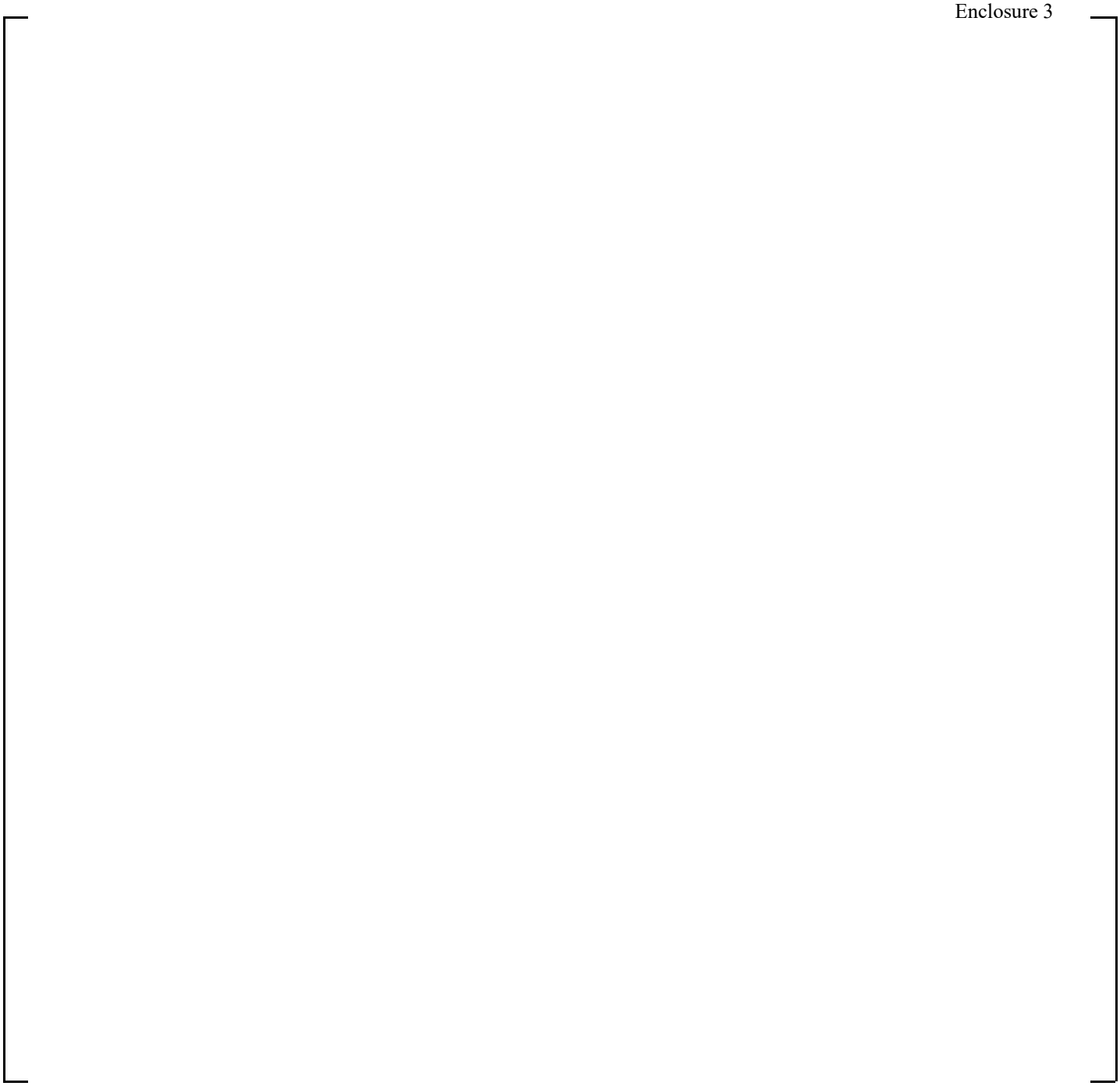

Figure 2.4-38 CCTF Run 76 Core (8.9 to 10.9-ft Elevation) Void Fraction Comparison

[a,b,c

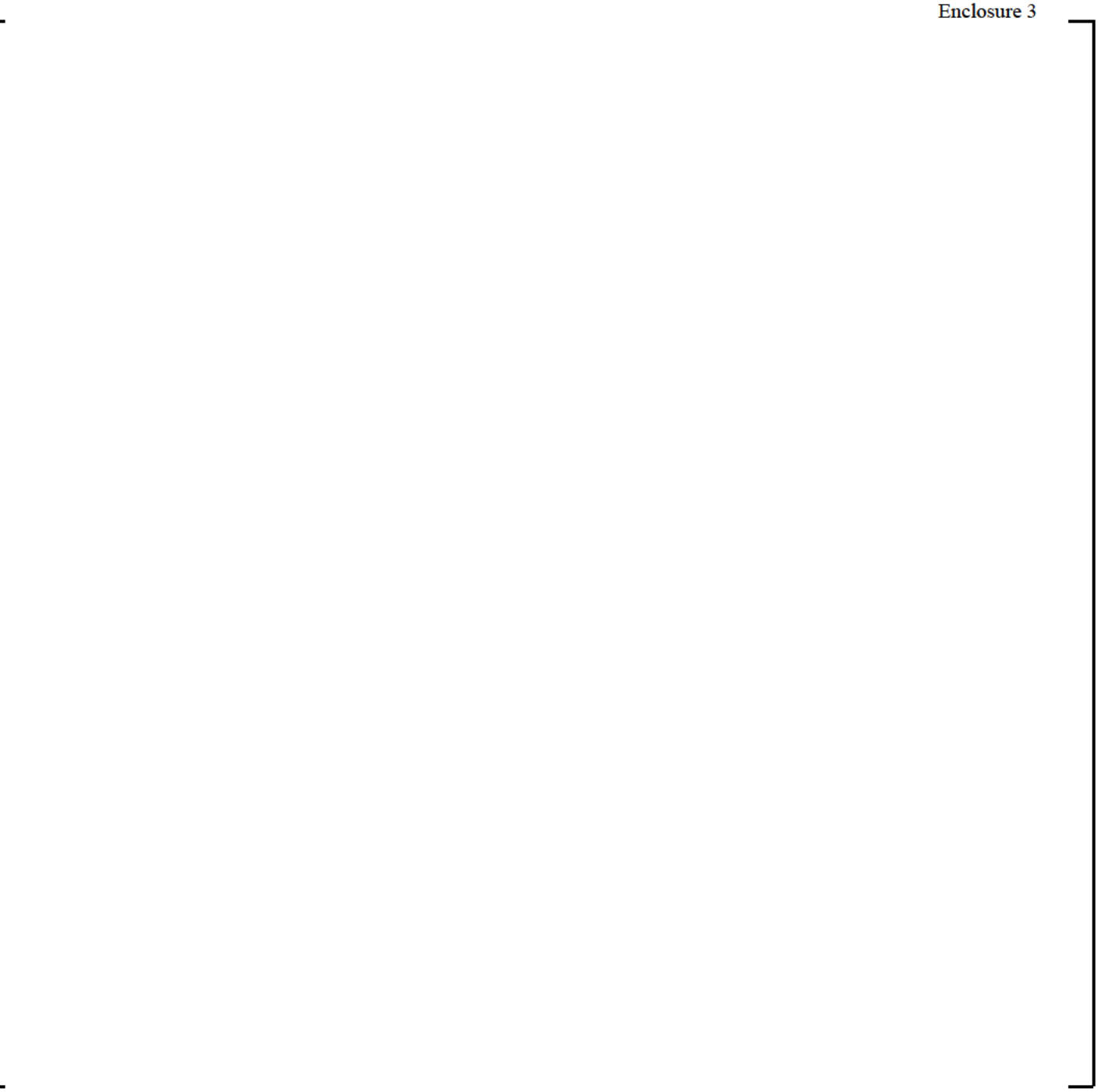

]

Figure 2.4-39 CCTF Run 76 Core (10.9 to 12.9-ft Elevation) Void Fraction Comparison

a,b,c

Figure 2.4-40 CCTF Run 76 Core (12.9 to 18.9-ft Elevation) Void Fraction Comparison

a,b,c

Figure 2.4-41 CCTF Run 76 Upper Plenum to Bottom of Hot Leg Nozzle Void Fraction Comparison

a,c

Figure 2.4-42 Predicted Northwestern Dimensionless Volumetric Fluxes at the Top of High Power Channel 21 for CCTF Run 76

[a,c

]

Figure 2.4-43 Predicted Northwestern Dimensionless Volumetric Fluxes at the Top of Channel 20 for CCTF Run 76

a,c

Figure 2.4-44 Predicted Northwestern Dimensionless Volumetric Fluxes at the Top of Channel 19 for CCTF Run 76

a,c

Figure 2.4-45 Predicted Northwestern Dimensionless Volumetric Fluxes at the Bottom of Channels 30 through 33 (Low Power Support Column Jet Channels in Each Quadrant) for CCTF Run 76

a,c

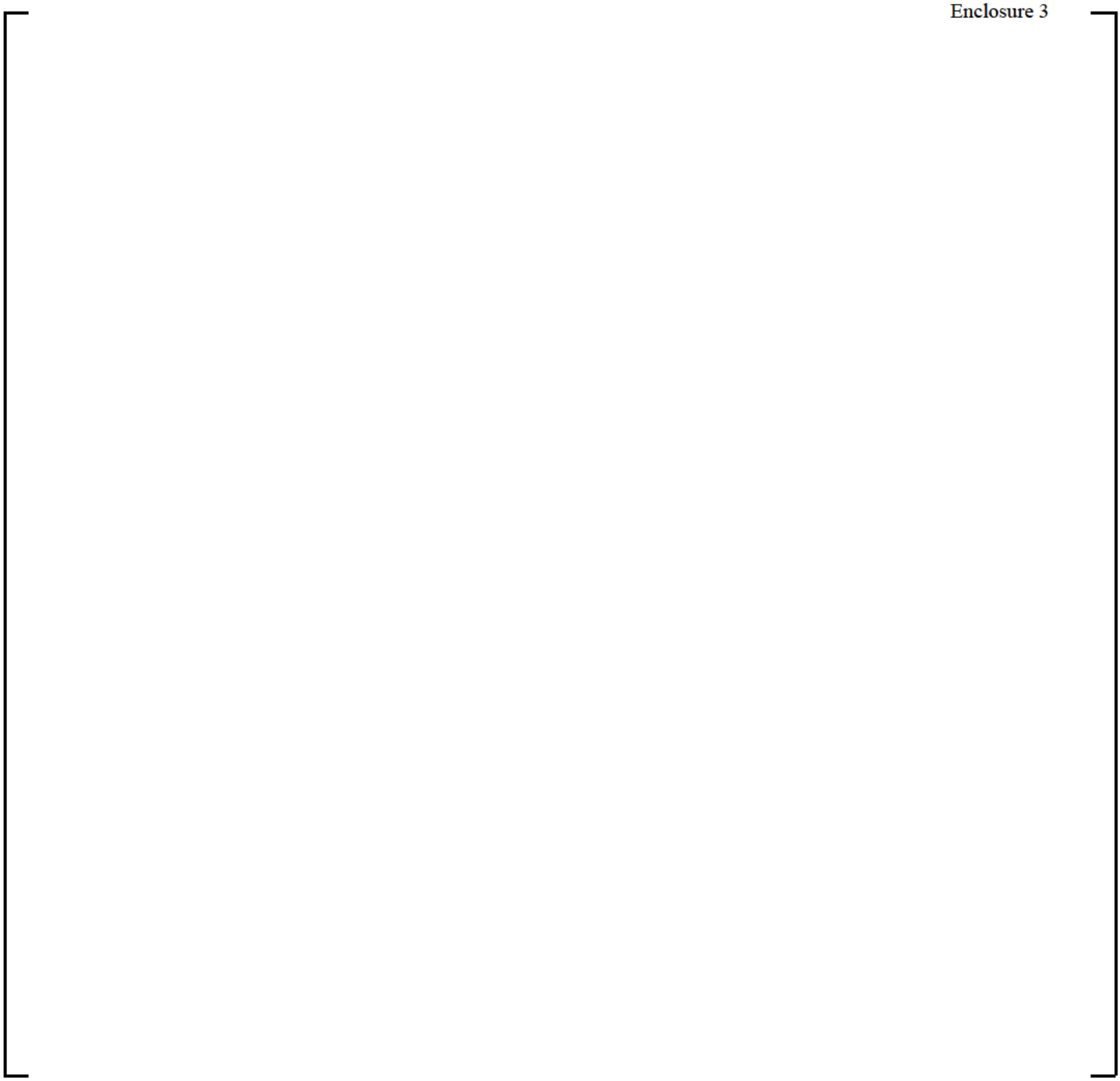

Figure 2.4-46 Flooding Behavior in CCTF Run 76 Above Low Power Core Channel at Tie Plate Elevation

2.5 UPPER PLENUM TEST FACILITY TESTS WITH UPPER PLENUM INJECTION

The UPTF was designed to obtain experimental data relative to the mu1ti-dimensional flows expected in a PWR during a LOCA. UPTF was the German contribution to the 2D/3D program established by the United States Nuclear Regulatory Commission (NRC), Japan (JAERI) and the Federal Republic of Germany (BMFT). Section 19.3 of the FSLOCA EM Topical Report (Kobelak, et al., 2016) describes the WCOBRA/TRAC-TF2 simulation of several UPTF tests, including Tests 6, 25A, 8A, and 29B.

This section will describe the modelling of Test 20, Phases A, B, and C, which simulated conditions in a PWR with UPI during the reflood phase of a cold leg large break LOCA. The objective of the Test 20 experiments was to investigate the steam/water-UPI flow interaction in the upper plenum during reflood following a postulated cold leg LOCA.

During the reflood portion of a LOCA, water rises through the core, and the hot fuel rods cause the water to boil. Steam generated in the core entrains droplets which are carried through the core into the upper plenum. These droplets will fall back to the core, de-entrain in the upper plenum, or pass through the upper plenum into the hot legs and the steam generators. In addition, the injection of cold ECC water into the upper plenum will cause some of the steam to condense. This condensed steam can mix with the ECC water and form a subcooled or saturated pool on top to the UCP. The amount of upper plenum water which passes through to the core is dependent on the amount of steam flow corning up and blocking the water downflow. This is called CCFL, and it usually occurs at the most restricted flow area.

Sections 2.5.1 and 2.5.2 describe the UPTF test facility and conditions, respectively. Section 2.5.3 describes the WCOBRA/TRAC-TF2 noding of the UPTF tests, with results in Section 2.5.4.

2.5.1 UPTF Test Facility

The UPTF facility simulated a full-scale 3900 MWt German PWR. The facility had four loops, each with a steam/water separator to simulate a steam generator and a variable resistance to simulate a reactor coolant pump. The upper plenum contained full-size internals in an arrangement typical of a KWU PWR. Figures 2.5-1 and 2.5-2 show an overall diagram of the UPTF test facility. A description of the test facility is included in Section 19.3.2 of (Kobelak, et al., 2016), and full details of the facility and its instrumentation are given in (Emmerling, et al., 1988).

The UPTF test facility was originally designed to examine separate effects during the refill and reflood periods of a 4-loop PWR LOCA transient. An integral system cannot be simulated with the UPTF because it is not equipped with heated core. MPR (MPR, 1985) investigated the suitability of using UPTF to perform tests which would be applicable to 2-loop UPI PWRs. It was concluded that separate effects of UPI related phenomena can be simulated with proper scaling considerations taken into account in the test conditions.

The objective of UPTF Test 20 was to investigate the following UPI phenomena:

1. Water entrainment and separation processes in the upper plenum,
2. Co-current and counter-current steam/water flow phenomena in the upper core tie plate region, including water break-through into the core,
3. Condensation and mixing processes in the hot legs of the loops, and in the upper plenum as a result of the injection of cold ECC water,
4. Subcooling in the upper plenum and below upper tie plate region, and
5. Upper plenum pool formation and distribution.

The range of investigation was achieved by varying the configuration of the facility.

There were three intact loops and one loop with a break in the cold leg. To simulate UPI, one hot leg was blocked for steam flow and the hot leg injector was used to inject the UPI water.

The entire vessel is shown in Figure 2.5-3. The upper plenum contained sixty-one guide tubes, eight support columns above fuel assemblies, and eight support columns outside the periphery of the core, as shown in Figure 2.5-4.

The UPTF facility simulated the upflow of steam and droplets through the core during reflood by injection of steam and water into dummy fuel rods. The dummy fuel rods represented the upper quarter of a core with 193 assemblies of 16x16 arrays of fuel rods. Sixty-one of the assemblies were below guide tubes and had control rod spider simulators (Figure 2.5-5). The remaining assemblies were below flow restrictors in the upper core plate. The water and steam injection nozzles are shown in Figure 2.5-6. There were seventeen independently controlled injectors to provide a separate nozzle for each dummy fuel rod assembly. The dummy control rods terminated at the bottom of the guide tubes, which were sealed to prevent flow from the upper plenum to the upper head. The upper head was thereby isolated from the rest of the vessel and had no effect on the test.

MPR (MPR, 1988) compared selected design parameters of UPTF and UPI PWR and developed an approximate scale factor of 2.1 (Table 2.5-1). Using this scale factor, the UPI flows and steam flows were set to match the 2-loop PWR.

[

]^{b}

[

]^{b} This factor will be important later as the results of the WCOBRA/TRAC-TF2 simulation of Test 20 are examined.

Phase A of UPTF Test 20 simulated a uniform radial power distribution by using a uniform steam injection rate. Phases B and C of Test 20 simulated a radial power distribution effect by using a 20 percent lower steam injection rate in the outside channels as compared to the inside (inner channel steam flow rate at 1.13 times average, outer channel steam flow rate at 0.90 times average), a reasonable approximation for a PWR with a relatively high amount of power in the low power periphery. For PWR core designs with lower relative power in the core periphery, it will be easier for the UPI water to penetrate into the outer assemblies compared to the test because the steam flow in the outside region would be relatively lower.

2.5.2 UPTF Test Conditions

A full description of the test and presentation of the results is given by (Siemens, 1988 and 1988a). The water and steam injected into the vessel at the core simulator flows upward through the dummy rods into the upper plenum. Part of this mixture flows through the intact loops into the downcomer and out into the containment via the broken cold leg. Part of the mixture flows through the broken hot leg to the containment. The remainder of the mixture builds up a liquid level in the upper plenum. The UPI water is injected into the upper plenum through one of the hot leg connections. The reactor vessel contains sufficient water to cover the bottom of the core barrel. This creates a seal, such that injected steam cannot pass under the core barrel directly into the downcomer and can only flow upward into the upper plenum, as it would during the reflood stage of a LOCA in a UPI plant. As steam is injected, the pressure in the core region rises and the water level falls in the core region and rises in the downcomer. The original vessel water inventory is selected to ensure that a downcomer seal is maintained.

The core water and steam injection rates for the three phases of Test 20 are shown in Table 2.5-2. Each phase has a different combination of steam and water flow, with a rest period between each phase, to allow water to drain back from the upper plenum to the lower plenum. At low steam flows, injected water can fall back into the core simulator, rather than being carried into the upper plenum. Condensation is also occurring as the mixture passes through the core simulator and upper plenum. These effects have been analyzed by (MPR, 1988) and are shown in Figures 5-8 to 5-10 of the MPR report (MPR, 1988). The liquid and vapor core flowrates presented in Table 2.5-3 are those at the bottom of the upper plenum, which are obtained from Figures 5-11 to 5-13 of the MPR report.

[

]^{b}

[

]b

2.5.3 UPTF Noding

The philosophy used in modelling the UPTF was to use the same level of noding detail as in the UPI PWR calculation, described in Section 3.2 and shown in Figure 3-1.

Figure 2.5-7 shows the axial noding diagram for the UPTF vessel, and Figures 2.5-8 through 2.5-10 show the vessel cross-section noding for each axial section. The WCOBRA/TRAC-TF2 model of the UPTF reactor vessel is divided into [

]a,c

Just as for the 3- and 4-loop PWR model, the UPTF model includes a [

]a,c

The WCOBRA/TRAC-TF2 model of the UPTF facility includes a [

]a,c

In vessel section [

]a,c

[

]a,c

The WCOBRA/TRAC-TF2 component noding for the loops of the UPTF facility is shown in Figure 2.5-11. There are two identical intact loops in the facility, which are modelled individually. The core simulator injects droplets and steam below the dummy fuel rods. These are modelled with PIPE and FILL components connected to the [

]a,c

[

]a,c

The pump simulators and steam generator simulators are represented by PIPE components which have the appropriate frictional loss and area variation. The water separator in the vessel side of the broken loop is modelled by a constant area PIPE with an appropriate frictional loss coefficient. The containment simulator is modelled by BREAK components at the ends of the broken loop to give the correct back pressure.

2.5.4 Test Results and WCOBRA/TRAC-TF2 Predictions

All three phases (A, B, and C) of UPTF Test 20 were simulated with WCOBRA/TRAC-TF2. The simulations were conducted for the full test time to ensure that the calculations had reached a quasi-steady state, and to allow for comparison with the mass balance results obtained by the (MPR, 1988) analysis of the test.

Table 2.5-3 summarizes the results of the WCOBRA/TRAC-TF2 calculations compared with the actual test results for net core drain rate and hot leg flows. It also compares the test simulated steam mass flowrates to calculated steam flows for a typical PWR LOCA analysis using best-estimate assumptions. The steam mass flowrates simulated in Test 20 Phase C are most representative of the UPI plant steam flowrates when the 2.1 scale factor is included. The Test 20 results are taken from the mass balance results obtained by the (MPR, 1988) analysis of the test.

The WCOBRA/TRAC-TF2 calculations for Phases A, B, and C displayed the same overall characteristics observed in the experiments:

1. The tests show that UPI water preferentially drains near the injection location,
2. There is some pooling of water on the UCP, and
3. Some of this water is entrained and flows out the hot legs.

WCOBRA/TRAC-TF2 predictions of these aspects are discussed in more detail below for Test 20 Phase C.

The void fractions just above the UCP in the upper plenum inner global channel 29 and outer global channels 21 to 24 are shown in Figures 2.5-12 and 2.5-13, indicating that the [

]a,c The flow rates at the UCP are shown in Figure 2.5-14 for channels 10 through 16, excluding channel 12, individually. These figures show [

]a,c

[

]a,b,c

Figure 2.5-15 shows the hot leg gap flows for the two intact and broken loop nozzles. Adding these flows together yielded the summaries shown in Table 2.5-3. The net vapor flow out the hot legs is [ ]a,c The net liquid outflow is approximately [ ]a,c the value reported for the test, indicating that WCOBRA/TRAC-TF2 is [

]a,c

Figures 2.5-16 through 2.5-19 show the upper plenum liquid levels in the outer global upper plenum channels. These liquid levels range from [ ]a,c, with the highest level calculated in the quadrant beneath the UPI injection. The corresponding liquid levels from Test 20 are Figures B-8 through B-11 in the Siemens test report (Siemens, 1988a). The test liquid levels range from [ ]b, again with the highest level being below the injection quadrant. The code is calculating [

]a,c

Phase A of Test 20 had core simulator flows which were comparable to Phase C, but the injection rates were radially uniform. The UCP drain distribution for Phase A is shown in Figure 2.5-20, with the overall mass balance summarized in Table 2.5-3. The core drain rate is [ ]a,c, the hot leg vapor flows are [ ]a,c and the hot leg entrainment is [

]a,c

Phase B of Test 20 had core simulator flows which were 20 percent higher than Phase C. The UCP drain distribution for Phase B is shown in Figure 2.5-21 with the mass balance summarized in Table 2.5-3. The core drain rate is [ ]a,c, the hot leg vapor flows are [

]a,c, and the hot leg entrainment is [ ]a,c These results indicate that [

]a,c

Table 2.5-1 Comparison of Selected UPTF and UPI Plant Parameters (MPR, 1988)

[ ]b

1. Thermal rating of the KWU PWR that UPTF replicates.
2. Total area within core barrel. Actual flow area is dependent on internal configuration.
3. Three loops only: One loop is isolated to be the UPI injection port.
4. Hot Leg Hutze flow area (UPI injection area).
5. Updated from (MPR, 1988) to reflect current US PWR range.

Table 2.5-2 Core Simulator Injection Rates into Upper Plenum* for UPTF Test 20

[

]b

* From Figures 5-11 to 5-13 of (MPR, 1988)

Table 2.5-3 UPTF Test 20 Results Summary

[

]a,b,c

*Data from Figures 5-11 to 5-13 of (MPR, 1988), at upper core plate

**Data from Figures 5-8 to 5-10 of (MPR, 1988)

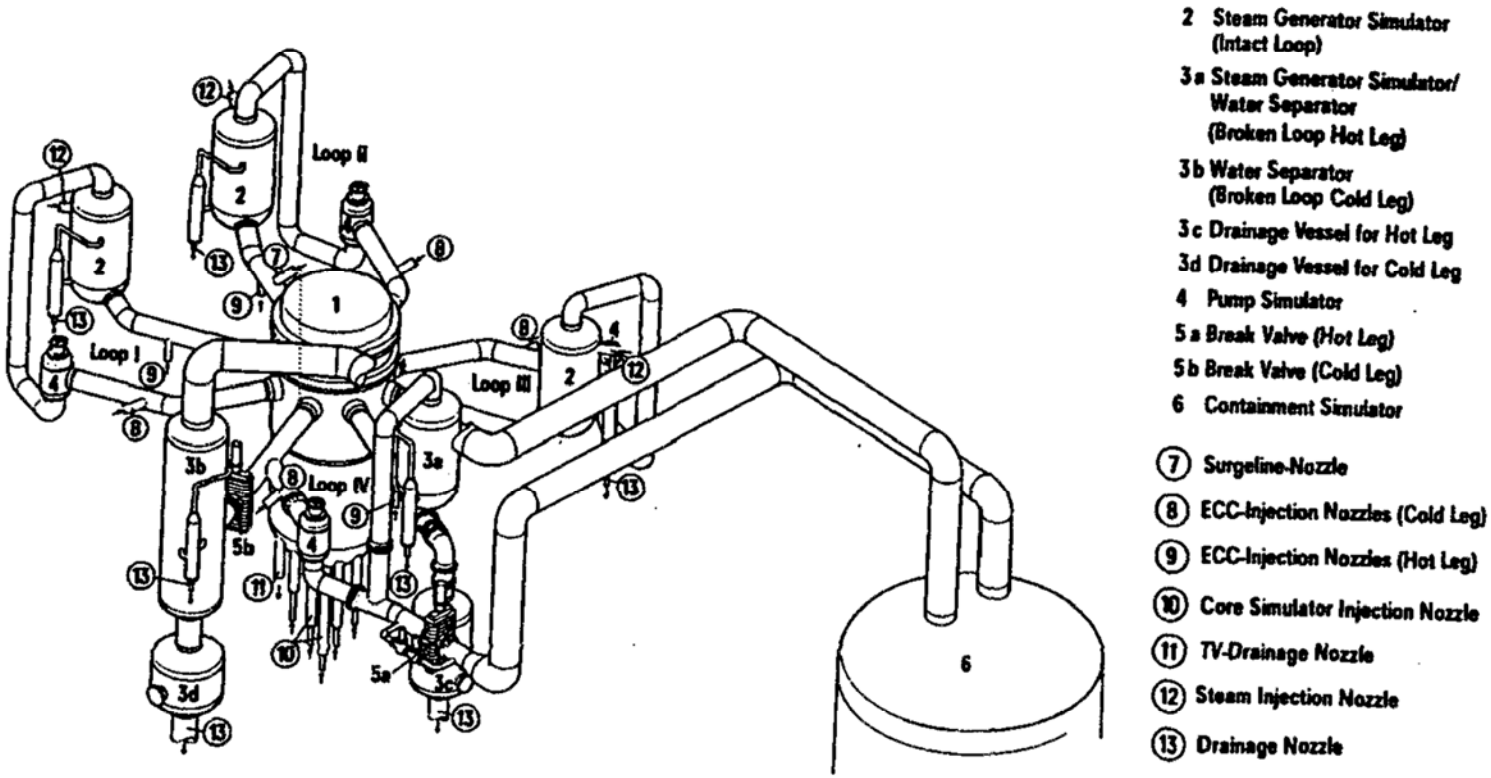

Figure 2.5-1 UPTF Plan View

b

Figure 2.5-2 UPTF Test Vessel and Primary Loop

[b

Figure 2.5-3 UPTF Reactor Vessel

[ ]b

Figure 2.5-4 UPTF Upper Plenum Structures

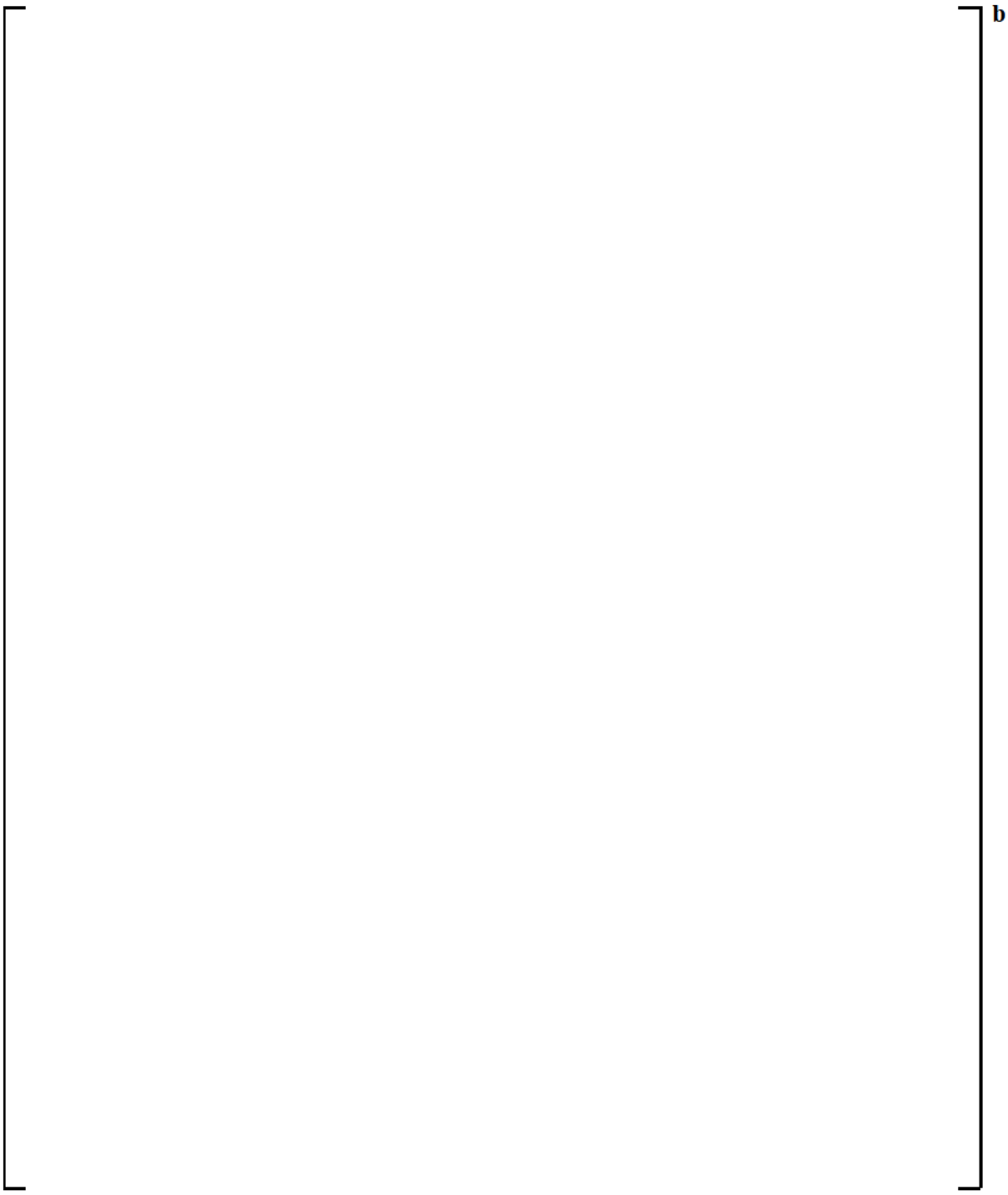

Figure 2.5-5 Dummy Fuel Assembly and End Box with Flow Restrictor (A) or Spider (B)

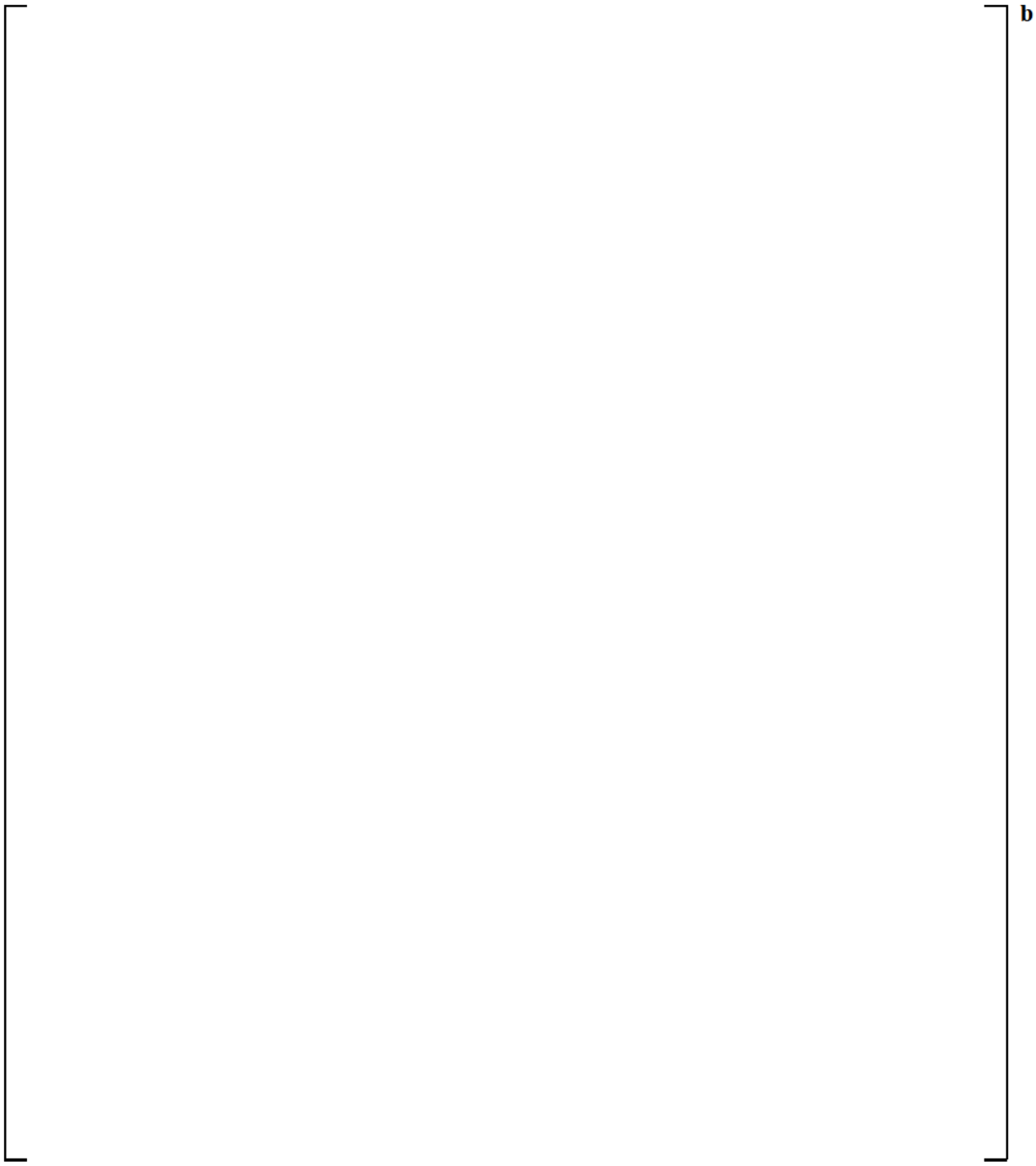

b

Figure 2.5-6 UPTF Core Simulator Injection Assembly

[a,c

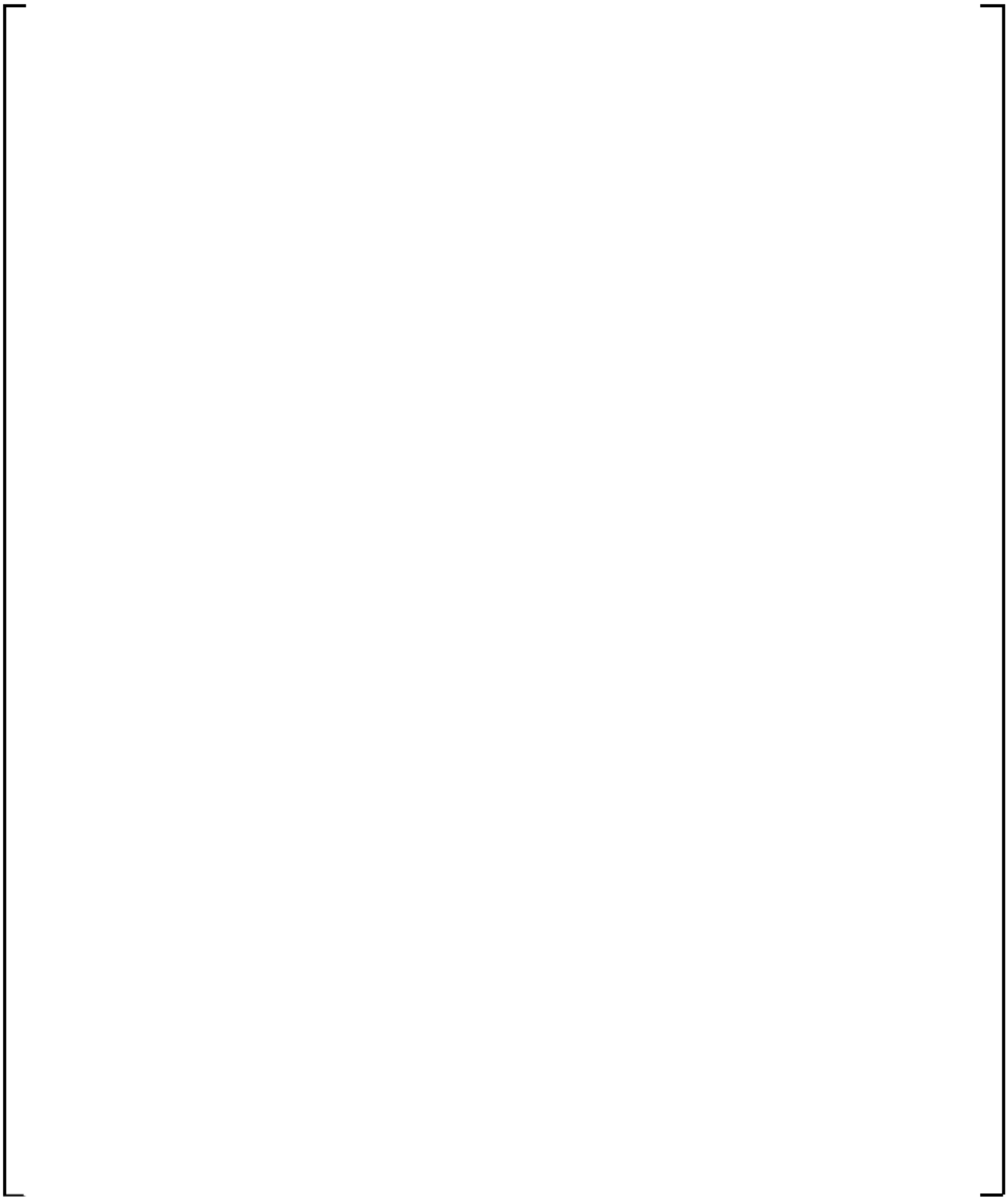

]

Figure 2.5-7 WCOBRA/TRAC-TF2 Vessel Component Axial Noding for UPTF Test 20 (Elevations in meters)

a,c

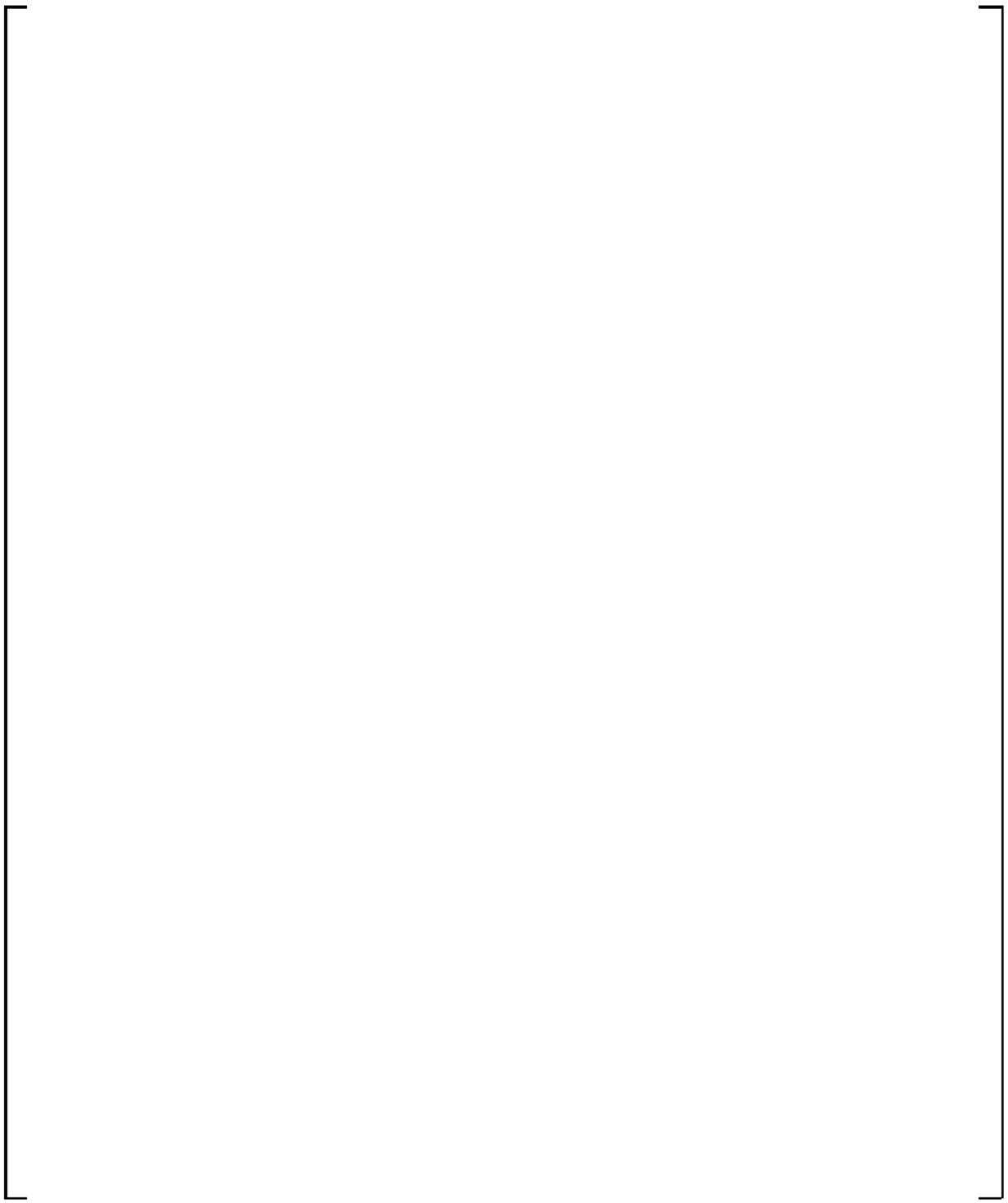

Figure 2.5-8 WCOBRA/TRAC-TF2 Vessel Cross-Section Diagram for UPTF Test 20 (Sections 1 through 3)

a,c

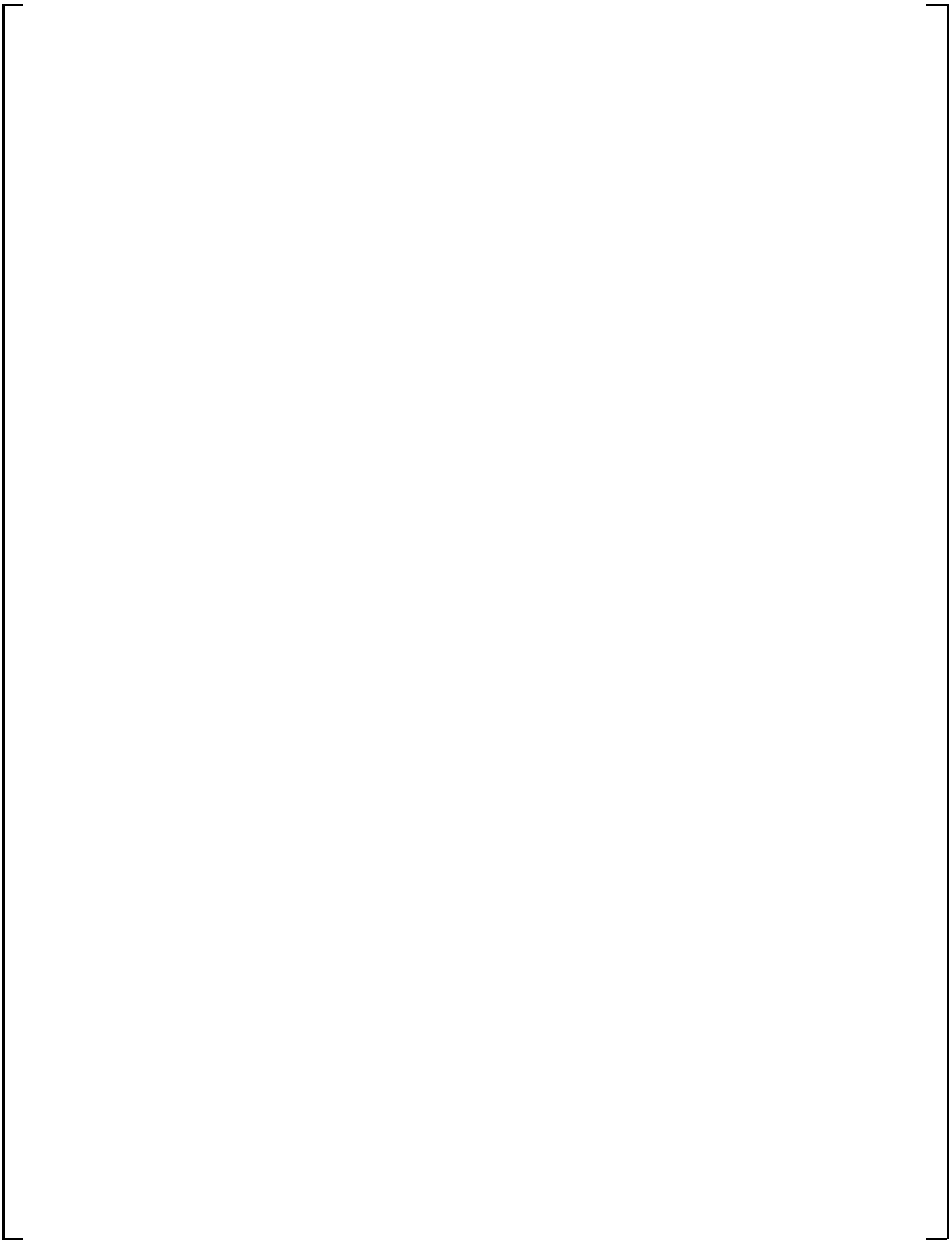

Figure 2.5-9 WCOBRA/TRAC-TF2 Vessel Cross-Section Diagram for UPTF Test 20 (Sections 4 and 5)

a,c

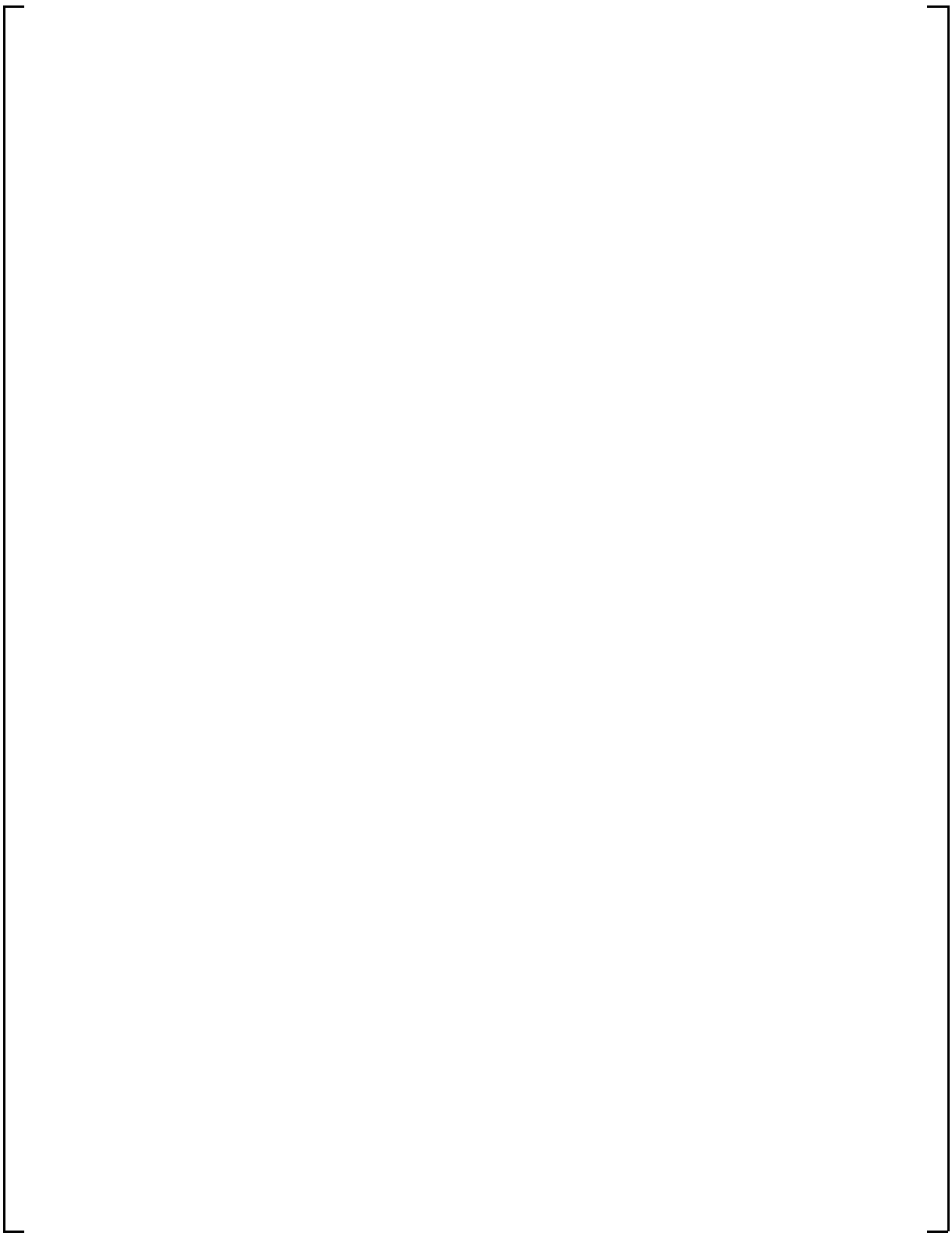

Figure 2.5-10 WCOBRA/TRAC-TF2 Vessel Cross-Section Diagram for UPTF Test 20 (Sections 6 and 7)

a,c

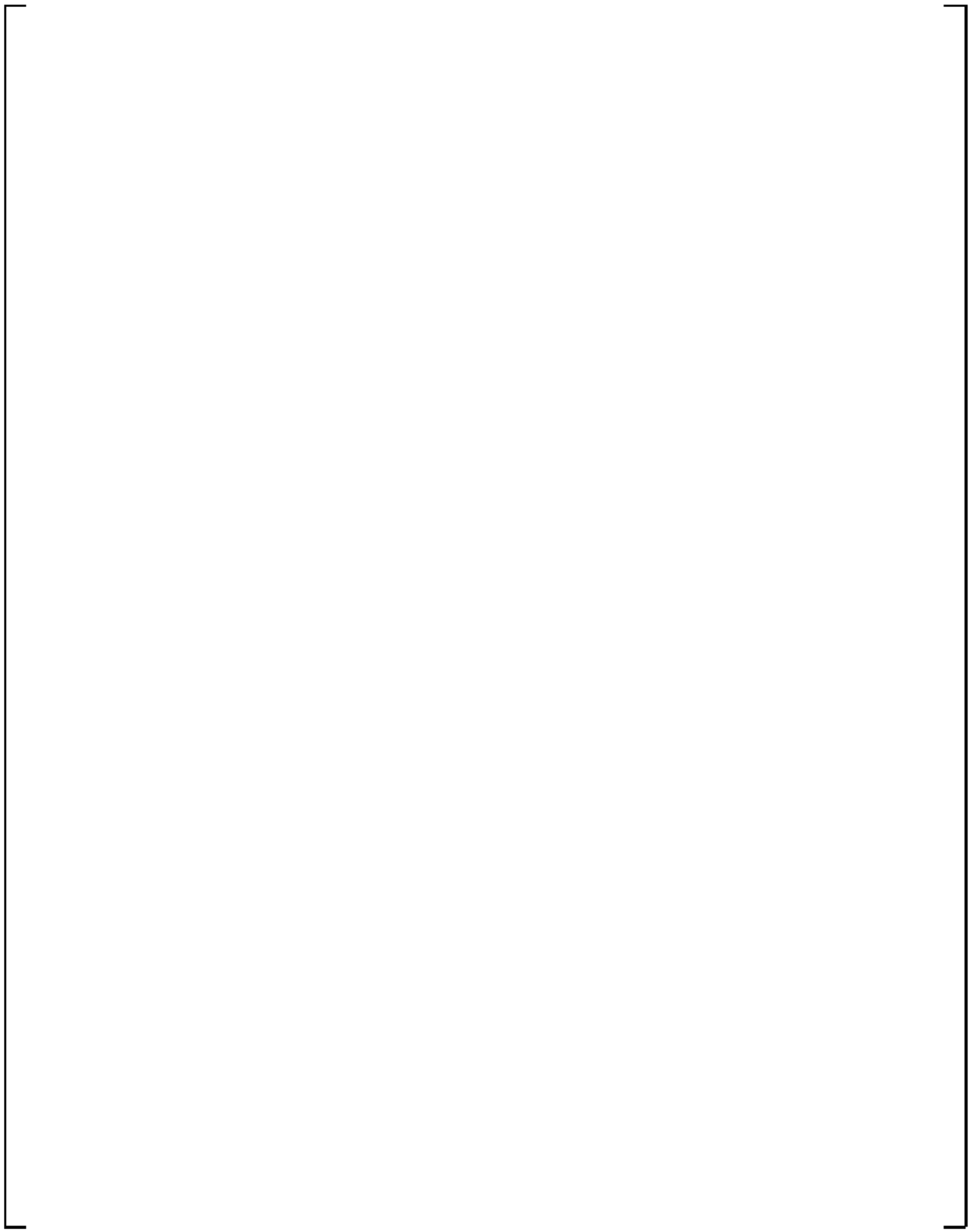

Figure 2.5-11 UPTF 20 Loop Noding Diagram

[a,c

]

Figure 2.5-12 UPTF Test 20, Phase C Void Fraction in Inner UP Global Channel 29

[a,c]

Figure 2.5-13 UPTF Test 20, Phase C Void Fraction in Outer UP Global Channels

a,b,c

Figure 2.5-14 UPTF Test 20, Phase C Liquid Drain Distribution at UCP

a,b,c

Figure 2.5-15 UPTF Test 20, Phase C Hot Leg Liquid and Vapor Flows

[a,c]

Figure 2.5-16 UPTF Test 20, Phase C Collapsed Liquid Level in Outer Injection Loop UP Quadrant (Channels 21, 36, 51)

[a,c]

Figure 2.5-17 UPTF Test 20, Phase C Collapsed Liquid Level in Outer Intact Loop UP Quadrant (Channels 22, 37, 52)

[a,c]

Figure 2.5-18 UPTF Test 20, Phase C Collapsed Liquid Level in Outer Intact Loop UP Quadrant (Channels 23, 38, 53)

a,c

Figure 2.5-19 UPTF Test 20, Phase C Collapsed Liquid Level in Outer Broken Loop UP Quadrant (Channels 24, 39, 54)

a,b,c

Figure 2.5-20 UPTF Test 20, Phase A Liquid Drain Distribution at UCP

[a,b,c]

Figure 2.5-21 UPTF Test 20, Phase B Liquid Drain Distribution at UCP

2.6 SCALING EFFECTS

A discussion of the effects of scale was provided for the various facilities utilized in the validation of WCOBRA/TRAC-TF2 in Volume II of (Kobelak, et al., 2016). The approach taken to evaluate scale effects was generally to examine the predicted trends of key LOCA processes as scale was increased. The full scale UPTF data was available to address the scaling distortions identified by Code Scaling, Applicability, and Uncertainty (CSAU) / the Evaluation Model Development and Assessment Process (EMDAP). This data was used to assess ECC bypass, upper plenum entrainment/de-entrainment, and condensation. **[**

][a,c] Also, the additional full scale data available from the UPTF facility was used to compare to the 1/15 and 1/5th scaled ECC bypass experiments, and to the CCTF (1/21 scale) upper plenum de-entrainment behavior. The UPTF facility also provided full scale data for cold leg steam/water mixing and condensation.

Scaling problems and issues related to the UPI have been addressed and tests were performed as a part of the 2D/3D program, established by the United States (Nuclear Regulatory Commission), Japan (Japan Atomic Energy Research Institute), and the Federal Republic of Germany (BMFT). The test facilities used various sizes of core flow area: UPTF (scaling factor 2.1), Slab Core Test Facility (SCTF) (scaling factor 0.091), the Oak Ridge National Laboratory (ORNL) Instrument Development Loop (IDL) scaling factor 0.011, 0.033), Dartmouth (scaling factor 0.0091), CCTF (scaling factor 0.091), and Semiscale (scaling factor 0.0017). The scaling effects of UPI tests were obtained through data analyses and summarized in (Damerell and Simons, 1993). The quantities of interest are:

1. Breakthrough Flow Area as Percentage of Core Flow Area,
2. Downflow Rate as Percentage of Available Water (Defined as ECC Injection, Core Liquid Upflow plus Steam Condensation Rate),
3. Net Hot Leg Water Carryover Rate as Percentage of the Available Water, and
4. Collapsed Liquid Level/Height to Hot Leg Centerline.

Thus, scaling trends of these phenomena have been deduced from the test data and made available. The physical phenomena unique to UPI plants are condensation of steam in the upper plenum, pooling of subcooled water on the top of UCP, the CCFL due to steam upflow which restricts liquid downflow into the core, and entrainment/de-entrainment of the pooled water, resulting in liquid carry over into the hot leg and steam binding. Such phenomena were captured and quantified by the above scaling parameters.

The scaling trends are obtained from the earlier analysis results of CCTF Test Run 72 and Run 76, UPTF Test 20 Phases A, B, and C, and a typical UPI plant (scaling factor 1.0). The scaling trends predicted for the above quantities are compared with the test data in Figures 2.6-1 through 2.6-4.

The data and predictions indicate that the **[**

][a,c]

[

]^{a,c}

Table 2.6-1 Scaling of Upper Plenum Injection

[

]b

[a,b,c]

Figure 2.6-1 Scaling Predictions and Test Data for Breakthrough Area

[a,b,c]

Figure 2.6-2 Scaling Predictions and Test Data for Downflow into Core

[a,b,c]

Figure 2.6-3 Scaling Predictions and Test Data for Hot Leg Water Carryover

[a,b,c]

Figure 2.6-4 Scaling Predictions and Test Data for Liquid Level in the Upper Plenum

2.7 COMPENSATING ERRORS

In Section 24 of (Kobelak, et al., 2016), potential compensating errors were identified and assessed for the FSLOCA EM, which is approved for application to 3- and 4-loop cold leg injection (CLI) plants. This section reviews those assessment results applicable to the 2-loop plants equipped with UPI. In addition, compensating errors associated with the important phenomena unique to the UPI plants are discussed based on the simulation results of the validation tests presented in Sections 2.3 through 2.6.

The highly ranked phenomena are identified in the FSLOCA EM PIRT for **[**

][a,c]

The review of this PIRT and assessment base (Sections 1.2 and 2.2) indicates that important phenomena governing 2-loop plants response to LOCA events of all scenarios are **[**

][a,c]

The UPI plants have **[**

][a,c]

The intermediate-break LOCA (IBLOCA) of UPI plants generally **[**

][a,c]

Based on the rationale discussed, the assessment in this section will focus on the key phenomena of **[** **]**[a,c] In the approved FSLOCA method, the potential compensating errors were assessed in **[**

][a,c] The compensating error assessment for the 2-loop UPI plants is discussed in the **[** **]**[a,c] based on the important phenomena for the 2-loop plants, of which **[** **]**[a,c] as will be further elaborated later in this section. The key phenomena unique to UPI occur in the upper plenum during the **[** **]**[a,c] thus they can be suitably discussed in areas of the **[**

][a,c]

2.7.1 [ ]a,c

The compensating error assessment for 3- and 4-loop plants in the FSLOCA EM concluded that [ ]a,c This conclusion is applicable to UPI plants, as the [ ]a,c

The timing of the UPI relative to the transient evolution of a LBLOCA of the 2-loop R. E. Ginna plant is demonstrated in Figure 2.7.1, which shows the reactor vessel lower plenum and core liquid levels and the mass flow rates of accumulator injection, HHSI, and UPI. The selected transient is [ ]a,c for the plant. During this transient, the system pressure drops below the accumulator cover pressure and accumulator injection begins at about [ ]a,c The accumulator liquid fills the lower plenum and [ ]a,c The liquid begins entering the core region at about [ ]a,c

The UPI could initiate [ ]a,c as shown for this transient. There is a [ ]a,c not expected to significantly impact the LBLOCA transient and the timing for UPI initiation relative to the beginning of reflood remains approximately the same.

The overview of these transient phases confirms that the UPI specific phenomena occur [ ]a,c

2.7.2 [ ]a,c

The conclusions of the compensating error analysis resulting from the 3- and 4-loop plants is first reviewed. It is then demonstrated that the [ ]a,c for 2-loop plants.

Three- / Four-Loop Plants

Potential compensating errors in the [ ]a,c are investigated in the approved FSLOCA EM for the 3- and 4-loop plants using the [ ]a,c It was concluded that [ ]a,c In the approved FSLOCA method, this issue was addressed by [ ]a,c

The assessment of the [ ]a,c tests in the FSLOCA EM for the 3- and 4-loop plants concluded [ ]a,c

UPI Plants

As mentioned earlier, the phenomena that influence **[**

][a,c]

The core wide flow pattern is **[**

][a,c] However, the **[**

][a,c] The core flow pattern of the R. E. Ginna UPI plant is investigated for the same **[** **]**[a,c] LOCA transient that was previously shown in Figure 2.7-1.

The reactor vessel core region is modeled with **[**

][a,c]

Details of the WCOBRA/TRAC-TF2 input model for the R. E. Ginna plant are discussed in Section 3, and the nodalization is presented in Figure 3.2-6. The entire core has **[**

][a,c] as shown in Figures 2.7-2a through 2.7-2d for the **[**

][a,c] of the core.

Recall from Figure 2.7-1 that UPI **[**

][a,c]

Furthermore, it is demonstrated that the **[**

][a,c]

A sensitivity study of core **[**

][a,c]

First, **[**

][a,c] Figure 2.7-9 contains a comparison plot of the peak clad temperature transients. Figures 2.7-10 and 2.7-11 show the **[**

][a,c] The results of this study show that **[**

][a,c] effect on the peak clad temperature.

Next, another **[**

][a,c] The sensitivity calculations modeled **[**

][a,c] Figure 2.7-12 contains a comparison plot of the peak clad temperature transients. The results of this study show that **[**

][a,c] effect on the transient.

Since the **[**

][a,c] is expected and reasonable.

The discussion on the UPI plant **[**

][a,c]

2.7.3 **[** **]**[a,c]

Three- / Four-Loop Plants

[
][a,c] were used to assess the potential for compensating errors in the prediction of the **[**

][a,c]

UPI Plants

The previous assessment of **[**

][a,c] The

assessment of **[**

][a,c] However, the previous assessment is **[**

][a,c]

Westinghouse has performed calculations of the GE CCFL tests, CCTF Tests 72 and 76, and UPTF Test 20 to assess the ability of WCOBRA/TRAC-TF2 to predict **[**

][a,c] The following assessment of the potential for compensating errors in the prediction of phenomena unique to UPI plants will use the results of those calculations, as presented in Sections 2.3 through 2.6, compared with the experimental data.

- **[**

][a,c]

[

][a,c]

The sensitivities of the predicted draining flow discussed above for the **[** **]**[a,c] are consistent with what are expected in the physical phenomena. Therefore, they add confidence that no significant compensating errors occur in the prediction of CCFL at the top of the core of a UPI plant.

- **[** **]**[a,c]

The WCOBRA/TRAC-TF2 predictions of **[**

][a,c] Figures 2.4-10, 2.4-11, 2.4-30, and 2.4-31 show the **[**
][a,c] and Figure 2.4-15 and 2.4-35 plot the **[** **]**[a,c]

The predicted cladding temperatures were compared with the available test data at different elevations, which indicated WCOBRA/TRAC-TF2 **[**

][a,c] These observations are **[**

][a,c] There is no evidence of significant compensating errors in any of these comparisons.

The comparisons are shown in Figures 2.7-17 through 2.7-26 for the **[**
][a,c]

- **[** **]**[a,c]

The WCOBRA/TRAC-TF2 predictions of **[** **]**[a,c] showed that the code **[**
][a,c] as shown in Table 2.5-3. The predicted **[**
][a,c] These are all self-consistent and give no indication of compensating errors.

- Assessment of Scale

Finally, the effect of scale on the ability of WCOBRA/TRAC-TF2 to predict phenomena relevant to UPI plants was assessed (Section 2.6). It was shown that the **[** **]**[a,c] are predicted, adding further confidence that there are no significant compensating errors present in the prediction of phenomena unique to UPI plants.

2.7.4 Applicability of FSLOCA EM Conclusions Regarding Compensating Error Assessment

The conclusions drawn from the evaluation of the compensating errors in the 3- and 4-loop plant applications of FSLOCA EM (Section 24.9 of Kobelak, et al., 2016) are discussed in this section, in terms of their applicability to the UPI plant simulations. Each FSLOCA EM conclusion is repeated in italicized text, followed by an assessment of its applicability for UPI plants.

1. *[*

][a,c]

This assessment **[**

][a,c]

This assessment and resolution **[**

][a,c]

[a,c

]

Figure 2.7-1 [ ]a,c

[a,c

]

Figure 2.7-2a [ ]a,c

[a,c

]

Figure 2.7-2b [ ]a,c

[a,c

]

Figure 2.7-2c [ ]^{a,c}

[a,c

]

Figure 2.7-2d [ ]a,c

[a,c

]

Figure 2.7-3 [ ]a,c

[a,c

]

Figure 2.7-4 [**]a,c**

[a,c

]

Figure 2.7-5 [**]a,c**

[a,c

]

Figure 2.7-6 [ ]a,c

[a,c

]

Figure 2.7-7 [ ]a,c

[a,c

]

Figure 2.7-8 [ ]a,c

[a,c

]a,c

Figure 2.7-9 [

]a,c

[a,c

]

Figure 2.7-10 [

]a,c

[a,c

]a,c

Figure 2.7-11 [

]a,c

[**a,c**

]

Figure 2.7-12 [

]a,c

[a,b,c

]

Figure 2.7-13 [**]a,c**

[a,b,c

]

Figure 2.7-14 [ ]^{a,c}

[a,b,c

]

Figure 2.7-15 [ ]^{a,c}

[a,b,c

]

Figure 2.7-16 [

]^{a,c}

[a,b,c

]

Figure 2.7-17 [**]a,c**

[a,b,c

]

Figure 2.7-18 [ ]^{a,c}

[a,b,c

]

Figure 2.7-19 [ ]^{a,c}

[a,b,c

]

Figure 2.7-20 [**]a,c**

[a,b,c

]

Figure 2.7-21 [**]a,c**

[a,b,c

]

Figure 2.7-22 [**]a,c**

[a,b,c

]

Figure 2.7-23 [**]a,c**

[a,b,c

]

Figure 2.7-24 [**]a,c**

[a,b,c

]

Figure 2.7-25 [**]a,c**

[a,b,c

]

Figure 2.7-26 [**]a,c**

2.8 CONCLUSIONS

WCOBRA/TRAC-TF2 simulations of the **[**

][a,c]

The compensating error assessment **[**

][a,c] No significant compensating errors were identified. For all cases where **[**

][a,c]

2.9 REFERENCES

1. Bankoff, S. G., et al., 1981, "Countercurrent Flow of Air/Water and Steam/Water through a Horizontal Perforated Plate," *Int. Journal Heat Mass Transfer*, Vol. 24, No. 8, pp. 1381 – 1395.

2. Damerell, P. S. and Simons, J. W., 1993, "Reactor Safety Issues Resolved by the 2D/3D Program," NUREG/IA-0127.

3. Dederer, S. I., et al., October 1999, "Application of Best Estimate Large Break LOCA Methodology to Westinghouse PWRs with Upper Plenum Injection," WCAP-14449-P-A, Revision 1.

4. Emmerling, R., et al., 1988, "UPTF Program and System Description," Siemens Report U941, 4/88/023.

5. Hsieh, C., et al., 1980, "Countercurrent Air/Water and Steam/Water Flow above a Perforated Plate," NUREG/CR-1808.

6. Iguchi, T., et al., July 1985, "Data Report on Large Scale Reflood Test-96, CCTF Core-II Test C2-13 (Run 072)," JAERI-memo 60-157.

7. Iguchi, T., et al., February 1985a, "Data Report on Large Scale Reflood Test-99, CCTF Core-II Test C2-16 (Run 076)," JAERI-memo 60-158.

8. Jones, D. D., 1977, "Subcooled Counter-Current Flow Limiting Characteristics of the Upper Region of a BWR Fuel Bundle," GEAP-NEDG-23549.

9. Kobelak, J. R., et al., November 2016, “Realistic LOCA Evaluation Methodology Applied to the Full Spectrum of Break Sizes (FULL SPECTRUM LOCA Methodology),” WCAP-16996-P-A, Revision 1.

10. MPR, 1985, “Upper Plenum Injection (UPI) of Emergency Core Coolant (ECC) -- Previous Tests and Analyses, and Capabilities of the Upper Plenum Test Facility (UPTF) to Perform UPI Tests.”

11. MPR, 1988, “Summary of Results from the UPTF Upper Plenum Injection (UPI) Separate Effects Test, Comparison to Previous Scaled Tests, and Application to US Pressurized Water Reactors.”

12. Siemens, 1988, “2D/3D Program UPTF Quick Look Report, Test Number 20, Upper Plenum Injection Simulation Test,” Siemens Report U9 316/88/07.

13. Siemens, 1988a, “2D/3D Program UPTF Experimental Data Report, Test Number 20 Upper Plenum Injection Simulation Test,” Siemens Report U9 316/88/08.

3 PLANT SCOPING AND SENSITIVITY STUDIES

3.1 INTRODUCTION

In this section, the input model for the R. E. Ginna (RGE) plant is developed and exercised using the WCOBRA/TRAC-TF2 code to determine the sensitivity of the large and small break Loss-of-Coolant Accident (LOCA) transients to the key modeling parameters and assumptions. The intent of these plant sensitivity studies is to demonstrate reasonable predicted transient behavior in response to the critical phenomena and parameters identified and to support aspects of the analysis methodology for the plant type. Ultimately, these studies will confirm the applicability of the extended FULL SPECTRUM LOCA (FSLOCA) Evaluation Model (EM) to the 2-loop pressurized water reactors (PWRs) equipped with upper plenum injection (UPI). Section 3.2 describes the development of the Ginna plant input model in detail. The sensitivity studies for the large and small break LOCA transients are discussed in Sections 3.3 and 3.4, respectively.

3.2 UPI PLANT INPUT MODEL (NODALIZATION)

The vessel and loop portions of a UPI PWR are modeled with significant detail for WCOBRA/TRAC-TF2 within the Westinghouse FSLOCA EM.

R. E. Ginna is a 2-loop upper plenum injection plant containing Westinghouse 14x14 Vantage+ fuel. The modeled nominal core power for this plant is 1,811 MWt. The R. E. Ginna vessel geometry as modeled in WCOBRA/TRAC-TF2 is described in Section 3.2.1, the core modeling is described in Section 3.2.2, the loop geometry is described in Section 3.2.3, and the emergency core cooling system (ECCS) modeling is described in Section 3.2.4.

3.2.1 Vessel Model

Figure 3.2-1 shows the vessel drawing for the R. E. Ginna 2-loop UPI PWR. Figure 3.2-2 shows the vessel major internal component elevation layout. The elevations shown on the right are relative to the inside bottom of the vessel. This vessel elevation layout contains most of the information needed to divide the vessel into nine vertical sections. These sections are described in turn starting at the bottom of the vessel.

Proceeding up the vessel, the bottom of vessel Section 1 is the inside vessel bottom. The bottom of vessel Section 2 is defined by the elevation at which the outside of the core barrel, if extended down into the lower plenum, would intersect the vessel wall. The bottom of vessel Section 3 is defined as the beginning of the active fuel. The bottom of vessel Section 4 is defined as the top of the active fuel. The bottom of vessel Section 5 is the elevation at the bottom of the upper core plate. The bottom of vessel Section 6 is the bottom elevation of the hot leg inner wall. The bottom of vessel Section 7 is equal to the elevation of the top of the hot leg inner wall. The bottom of vessel Section 8 is the elevation at the top of the upper support plate. The bottom of vessel Section 9 is the elevation at the top of the upper guide tubes in the upper head. The top of vessel Section 9 is the inside top of the vessel upper head.

The UPI modeling of the lower plenum, core, barrel/baffle region, and upper head regions is basically the same as the modeling in 3- and 4-loop PWRs as described in the FSLOCA EM topical report (Kobelak et

al., 2016). The difference in noding for the UPI model is seen in the region between the top of the core and the upper core plate (known as the counter-current flow limitation, or CCFL, region) and in the upper plenum and downcomer. **[**

][a,c]

An additional change to vessel Section 5 in the upper plenum is to incorporate four axial levels instead of two. This enables WCOBRA/TRAC-TF2 to more accurately predict the flow distribution at the upper core plate, specifically the ability to discern in what fashion, or to what extent, the UPI injection will either flow axially downward into the CCFL and core region or accumulate at the upper core plate elevation where it then becomes available to flow laterally into the inner region of the upper plenum. The extent to which these flow patterns occur can affect the upper plenum drain distribution during refill/reflood transient. The basis for the UPI upper plenum nodalization is consistent with the nodalization used for the test simulations performed specifically to address UPI phenomena.

Figures 3.2-3 through 3.2-12 illustrate the R. E. Ginna vessel noding. Figure 3.2-3 is a vertical section noding diagram. Figures 3.2-4 through 3.2-12 are the horizontal views of each section. In these figures, the numbers within the squares are the channel numbers and the numbers within the circles with arrows attached to them are the gap numbers. A gap is used to define a horizontal flow path between channels. Positive flow is in the direction indicated by the arrow. It is assumed within WCOBRA/TRAC-TF2 that a vertical flow path for vertically stacked channels exists unless specified in the input. Upward axial flow is considered as positive flow.

As can be seen in Figures 3.2-3 through 3.2-12, 87 channels and 100 gaps are used for R. E. Ginna to define the vessel. Note that two of these channels (Channels 21 and 24) and seven gaps (Gaps 21 through 27) are fully blocked within the model and so are not included in any of the vessel noding diagram figures. Other gaps may be fully or partially blocked due to physical flow restrictions within the vessel but are shown in the noding diagrams. It can be seen in Figure 3.2-3 that several of the nine vertical sections are sub-divided into two or more levels. For example, the active fuel region, vessel Section 3, is divided into 15 vertical levels. By accounting for the vertical sub-division within vessel Sections 2, 3, 5, and 7, the vessel model for R. E. Ginna has a total of 325 fluid cells.

Vessel Section 1 models the vertical section of the vessel from the inside bottom of the vessel to the elevation at which the outside of the core barrel, if extended down into the lower plenum, would intersect the vessel wall. This section contains one vertical level. The modeling of this section is relatively simple

since there is one channel (designated as Channel 1) and no horizontal flow gaps (Figures 3.2-3 and 3.2-4). Channel 1 completely represents Section 1 of the vessel. The top flow area of Channel 1 represents the net flow area through the upper tie plate.

Vessel Section 2 models the vertical section of the vessel from the top of vessel Section 1 to the bottom of the active fuel region. This section contains two vertical sub-levels. The intermediate level interface is set at the radius of curvature point for the lower plenum. This section contains 7 channels (designated 2 through 6, 76, and 77) and 12 horizontal flow gaps (numbered 1 through 8, 85, 86, 97, and 98), as shown in Figures 3.2-3 and 3.2-5.

Channels 2 through 5, 76, and 77 each represent one-sixth of the annulus outside the core barrel and its extension; Channel 6 models the volume inside the core barrel. The top cell of Channel 6 contains the lower core plate, bottom fuel nozzle, non-active portion of the fuel rods, etc. **[**

][a,c]

The area at the top of Channel 6 is equal to the sum of the areas modeled at the bottom of Channels 11 through 15 in vessel Section 3. Gaps 1 through 4, 85, and 86 model the lateral connections between the peripheral channels (Channels 2 through 5, 76, and 77) in the extended downcomer region, and Gaps 5 through 8, 97, and 98 model the horizontal radial connections between the peripheral channels and Channel 6. Because this section has two sub-levels, each channel has two cells and each gap has two levels. The upper level of the radial gaps, however, is blocked since there is no flow across the core barrel extension (sometimes referred to as the flow skirt). The lower level of the radial gaps models the flow below the lower support plate in this section. Area variation inputs are used to vary the axial and gap flow areas in this section to account for the area changes due to the barrel wall and other structure blockages.

Vessel Section 3 models the vertical section of the vessel from the bottom to the top of the active fuel region. The modeling is effectively accomplished using 15 axial levels in 11 channels (designated 7 through 15, 78, and 79) and 10 lateral flow gaps (designated 9 through 16, 87, and 88), as shown in Figures 3.2-3 and 3.2-6. Channels 7 through 10, 78, and 79 each represent one-sixth of the downcomer annulus volume between the vessel inner wall and the core barrel outer wall. Channel 11 is the volume between the core barrel inner wall and the baffle plates, which is designated as the barrel/baffle channel. For R. E. Ginna, flow travels downward through this region during normal operation, which is referred to as a downflow barrel/baffle design.

Channels 12 through 15, combined, represent the total volume within the baffle plates, i.e., the entire core active fuel region for all 121 assemblies in the R. E. Ginna nuclear power plant. Channel 12 includes assemblies on the periphery of the core, which have relatively low power. **[**

][a,c] A map of the different structures in the upper plenum is presented in Figure 3.2-13. There are four types of upper internals in the R. E. Ginna upper plenum: guide tubes, open holes, source plates, and support columns (of which two types are noted in Figure 3.2-13). **[**

][a,c]

The hot assembly is a single assembly in the core model, and the particular type was chosen so as to limit axial flow, most importantly during blowdown, but with consideration to limit UPI downflow into the hot assembly during refill/reflood. **[**

][a,c]

The gaps modeled in vessel Section 3 are illustrated in Figure 3.2-6. The 143.25-inch active fuel length is divided into 15 axial cells. The grids and their associated form losses are modeled within this length range at their specified elevations. **[**

][a,c]

Vessel Section 4 includes the vertical section of the vessel from the top of the active fuel to the bottom of the upper core plate. Vessel Section 4 of the model is referred to as the CCFL region, where CCFL is the acronym for counter-current flow limitation. This section has 1 vertical level and uses 12 channels (designated 16 through 20, 22, 23, 25 through 27, 80, and 81) and 12 horizontal flow gaps (17 through 20, 81 through 84, 89, 90, 99, and 100) to model this portion of the vessel. Figures 3.2-3 and 3.2-7 illustrate the vertical and radial representation of this section of the vessel model.

Channels 16 through 19, 80, and 81 each represent one-sixth of the downcomer annulus volume between the vessel inner wall and the core barrel outer wall. Channel 20 represents the extension of the barrel/baffle region into this section. R. E. Ginna is a downflow design with the radial Gaps 81 through 84, 99, and 100 modeled to direct a fraction of the downcomer flow to the barrel/baffle. The barrel/baffle region ends at the top of Channel 20, and due to the presence of the upper core plate, no axial flow is allowed at the top of this channel.

[

][a,c]

Vessel Section 5 extends vertically from the bottom of the upper core plate to the bottom of the hot leg inner wall. This section contains four levels with 22 channels (designated 28 through 47, 82, and 83) and 25 lateral flow gaps (numbered 28 through 50, 91, and 92) as shown in Figures 3.2-3 and 3.2-8. Channels 28 through 31, 82, and 83 each represent one-sixth of the downcomer annulus volume between the vessel inner wall and the core barrel outer wall. **[**

][a,c]

Vessel Section 6 models the vertical section of the vessel from the bottom of the hot legs to the top of the hot legs (inner diameter). The WCOBRA/TRAC-TF2 input uses 1 level in 15 channels (designated 48 through 60, 84, and 85) and 17 horizontal flow gaps (designated 51 through 65, 93, and 94) to model this section, as shown in Figures 3.2-3 and 3.2-9. Channels 48 through 51, 84, and 85 each represent one-sixth of the downcomer annulus volume between the vessel inner wall and the core barrel outer wall, excluding the volume of the hot leg which passes through this region. Channels 49 and 51 are connected to the broken and intact loop cold leg nozzles, respectively. **[**

][a,c]

[

]^{a,c} Channels 59 and 60 model the broken and intact loop hot leg nozzles, respectively. Gap 64 models the transverse flow between the outer global channel and the broken loop hot leg channel. Gap 65 models the transverse flow between the outer global channel and the intact loop hot leg channel. The upper plenum injection system delivers low head safety injection into the periphery region of this section. Two injection ports can be modeled, with injection into Channels 53 and/or 55 (Figure 3.2-9). The residual heat removal (RHR) pumps have separate injection lines (not headered) such that the assumption of a single failure loss of an RHR pump results in asymmetric injection into the upper plenum. Therefore, with a single failure assumption, either channel could receive UPI flow. Since these quadrants are equidistant to the quadrant where the broken loop hot leg nozzle is attached, no differentiation is necessary and either injection cell can be used. Channel 55 was chosen to be the UPI injection location.

Vessel Section 7 extends vertically from the top of the hot leg inner wall to the top of the upper support plate. This section has 2 levels and uses 13 channels (designated 61 through 71, 86, and 87) and 15 horizontal flow gaps (designated 66 through 78, 95, and 96) to model this region, as shown in Figures 3.2-3 and 3.2-10. Channels 61 through 64, 86, and 87 each represent one-sixth of the downcomer annulus. The interface at the top of the downcomer in vessel Section 7 with the upper head is via the spray nozzles; a loss coefficient is modeled to reflect the flow through this interface. Channels 65 through 71 model the same regions as Channels 52 through 58, respectively, in vessel Section 6. The OH/SP/SC channel, inner global channel, and outer global channels (Channels 65 through 70) are bounded on the top by the upper support plate and have no axial flow connections at the top. Guide tube Channel 71 connects vertically to vessel Section 8 through the guide tube extension. The elevation of the end of the free volume in the Type II support columns is chosen as the elevation of the intermediate level in vessel Section 7.

Vessel Section 8 extends vertically from the top of the upper support plate to the top of the upper guide tubes. This section has one level and uses three channels (designated 72 through 74) and two horizontal flow gaps (designated 79 and 80) to model this region, as shown in Figures 3.2-3 and 3.2-11. The axial flow from the six downcomer channels in vessel Section 7 is incorporated into a single channel in vessel Section 8 (Channel 72) and models the flow through the spray nozzles. The boundary between Channels 72 and 73 is formed by the cylinder which intersects the inside of the upper head sphere at the top of the upper guide tube elevation. Channel 72 includes the volume of the upper head outside this imaginary boundary, while Channel 73 models the volume inside this imaginary boundary, excluding the volume of the upper guide tubes. There is no flow into Channel 73 from below, since the upper support plate prevents direct flow communication between the upper head and upper plenum. Channel 74 models the volume of the inside of the upper guide tubes and communicates flow axially with Channel 71 in vessel Section 7. Flow slots in the upper guide tube enclosure allow for the modeling of the transverse flow through Gap 80.

Vessel Section 9 extends vertically from the top of the upper guide tubes to the inside top of the vessel head. This section uses one axial level, one channel (designated 75), and no horizontal flow gaps to

model this region, as shown in Figures 3.2-3 and 3.2-12. This channel models the fluid volume above the top of the guide tubes and communicates axially with Channels 73 and 74 of vessel Section 8.

3.2.2 Core Model

Rod 1 is the **[**

][a,c]

The nuclear fuel rods are initialized with internal gas compositions and fuel average temperatures from the PAD5 code (Bowman et al., 2017).

[

][a,c]

3.2.3 Loop Model

The R. E. Ginna loop model is presented in Figure 3.2-14, with a more detailed noding for the steam generators shown in Figure 3.2-15. As with the vessel inputs, each component in the one-dimensional loop has various cells to allow for specific changes in geometry along the component. Each component is identified by a module title, a unique component number, and connections to numbered junctions. The two loops are defined using 56 components and 50 junctions. Components and junctions are indicated by rectangles and circles, respectively, in Figures 3.2-14 and 3.2-15.

Loop 1 is the loop that contains the pressurizer. Component 11 is the hot leg and was modeled with a TEE module. Component 19, the pressurizer (PRIZER module), is connected to the secondary branch of the hot leg TEE. **[**

][a,c]

The primary side of the steam generator is modeled as Component 12, with the secondary side consisting of several components (see Figure 3.2-15). TEE Component 112 is the shell of the steam generator secondary side. The feedwater connection is modeled as TEE Component 113, and the downcomer of the steam generator is PIPE Component 114. The feedwater is injected through FILL Component 115, and the steam flows through TEE Component 118 and then exits via either the Main Steam Isolation Valve (MSIV) (VALVE Component 218 and BREAK Component 116) or Main Steam Safety Valve (MSSV) (VALVE Component 318 and BREAK Component 418). **[** **]**[a,c]

[

]a,c

Continuing around the loop are the crossover leg (PIPE Component 13) and reactor coolant pump (PUMP Component 14). It is noted that flow stratification is allowed in the loop seal bends via the use of the STRTX input. The Loop 1 cold leg is modeled using three PIPE components (Components 15, 16, and 17).

Loop 2 is set up similarly to Loop 1. Component 21 is the hot leg and was modeled with a PIPE module since there is no pressurizer connection. The steam generator, crossover leg, and reactor coolant pump of Loop 2 are modeled the same as Loop 1. The cold leg modeling is different for Loop 2 as safety injection is modeled.

The cold leg is modeled by one TEE component (Component 25) and two PIPE components (Components 26 and 27). Component 25 models the cold leg (TEE module) immediately downstream of the reactor coolant pump. The secondary branch of the TEE connects to VALVE Component 79 and then to TEE Component 78 which models the safety injection and accumulator discharge lines. The secondary branch of this TEE connects to SI FILL Component 77. The other side of the primary branch of TEE Component 78 connects to VALVE Component 74, which models the accumulator check valve. The accumulator tank itself (Component 75) is modeled with a PIPE component and an associated input which causes an accumulator module to be invoked.

The accumulator and pressurizer components have two junctions, although they only have a single communication path with the reactor coolant system (RCS). As such, zero FILL Components 119 and 76 are provided as boundary conditions for the junction not in communication with the RCS.

[

]a,c BREAK Component(s) 4 and/or 6 are used to model containment conditions for the transient (depending on the break type, either one or both of the components are required). [

]a,c

Thimble bypass is modeled using three separate PIPE modules (Components 50, 51, and 52) connected to the bottom cells of the low power assembly, OH/SP/SC assembly, and guide tube assembly channels, respectively, in vessel Section 3 and the corresponding CCFL channels in vessel Section 4. The low head safety injection is modeled with a FILL module (Component 58) that injects through a PIPE module (Component 57) and then into the vessel at the hot leg nozzle elevation.

3.2.4 Emergency Core Cooling Safety Injection Model

The Safety Injection System (SIS) for R. E. Ginna consists of two accumulator tanks, three high head safety injection (HHSI) pumps, and two low head safety injection (LHSI) pumps. The HHSI and the accumulator inject into the cold leg through the same injection line. The LHSI injects into the upper plenum at the same elevation as the hot leg centerline. The loss of one train of safety injection (one LHSI and one HHSI) is considered as the limiting single failure assumption.

[

]^{a,c}

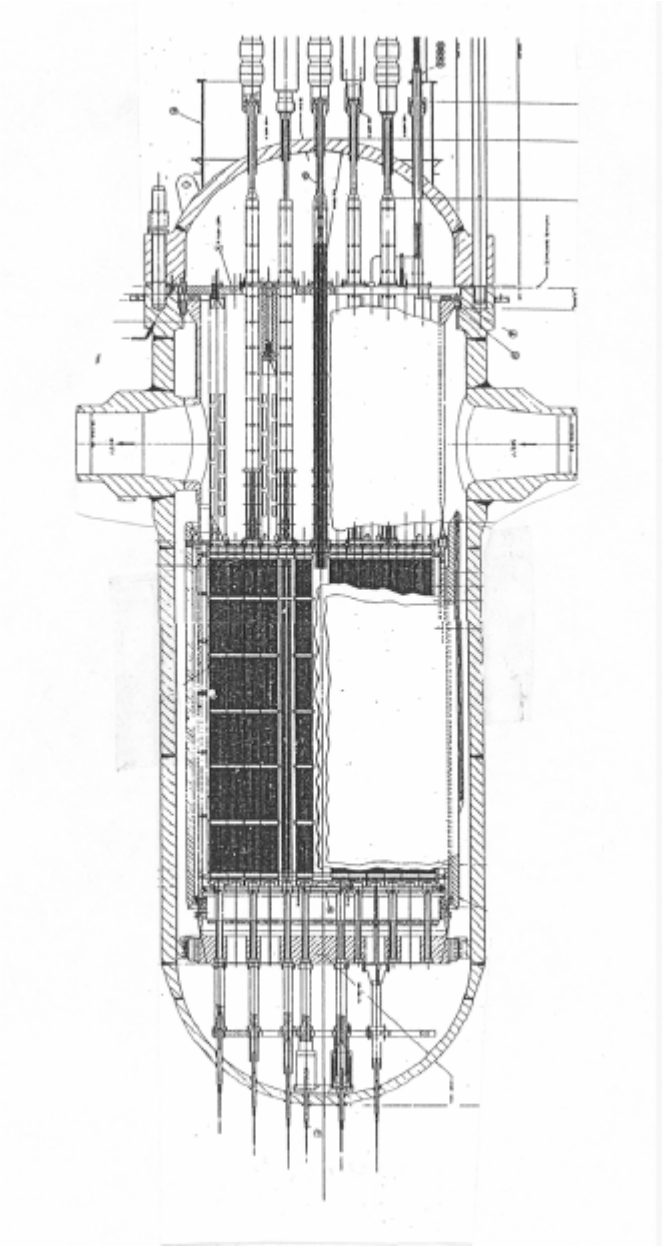

Figure 3.2-1 R. E. Ginna Vessel Profile

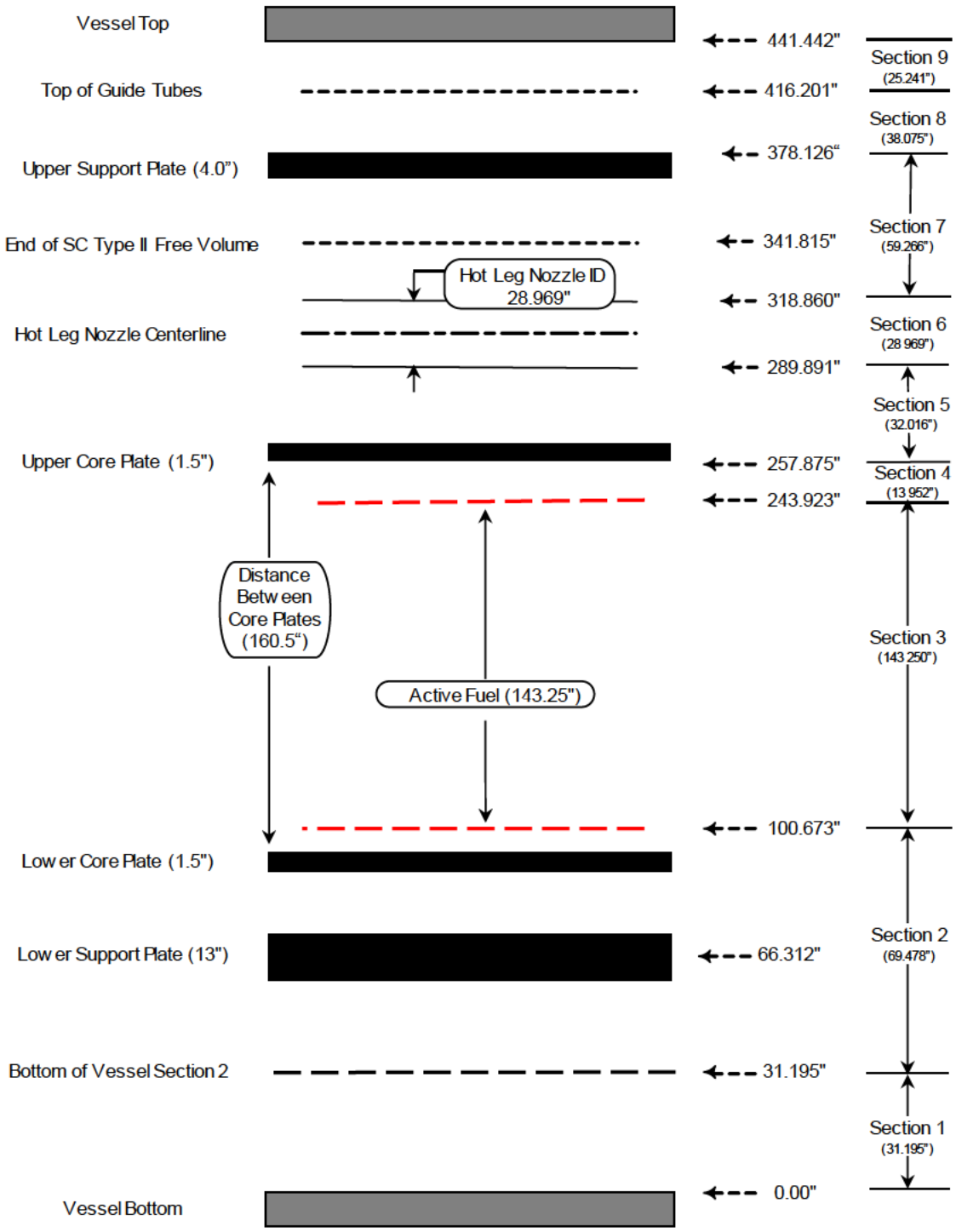

Figure 3.2-2 R. E. Ginna Vessel Component Elevations

a,c

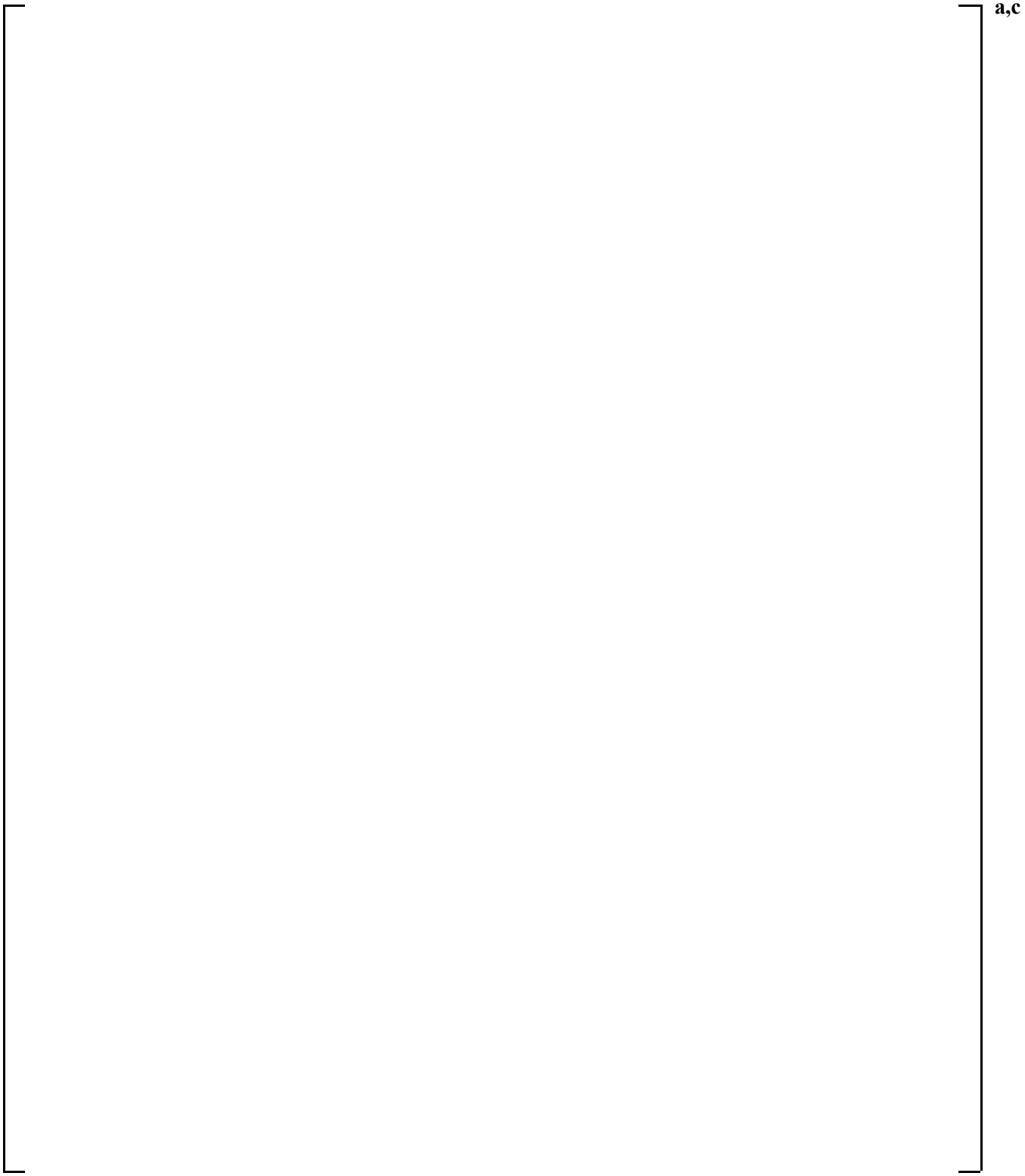

Figure 3.2-3 R. E. Ginna Vessel Model Noding Diagram

[**a,c**]

Figure 3.2-4 R. E. Ginna Vessel Section 1

a,c

Figure 3.2-5 R. E. Ginna Vessel Section 2

a,c

Figure 3.2-6 R. E. Ginna Vessel Section 3

[**a,c**

]

Figure 3.2-7 R. E. Ginna Vessel Section 4

[a,c]

Figure 3.2-8 R. E. Ginna Vessel Section 5

[**a,c**

]

Figure 3.2-9 R. E. Ginna Vessel Section 6

[a,c]

Figure 3.2-10 R. E. Ginna Vessel Section 7

[a,c]

Figure 3.2-11 R. E. Ginna Vessel Section 8

[**a,c**]

Figure 3.2-12 R. E. Ginna Vessel Section 9

[a,c]

Figure 3.2-13 R. E. Ginna Upper Internals Configuration

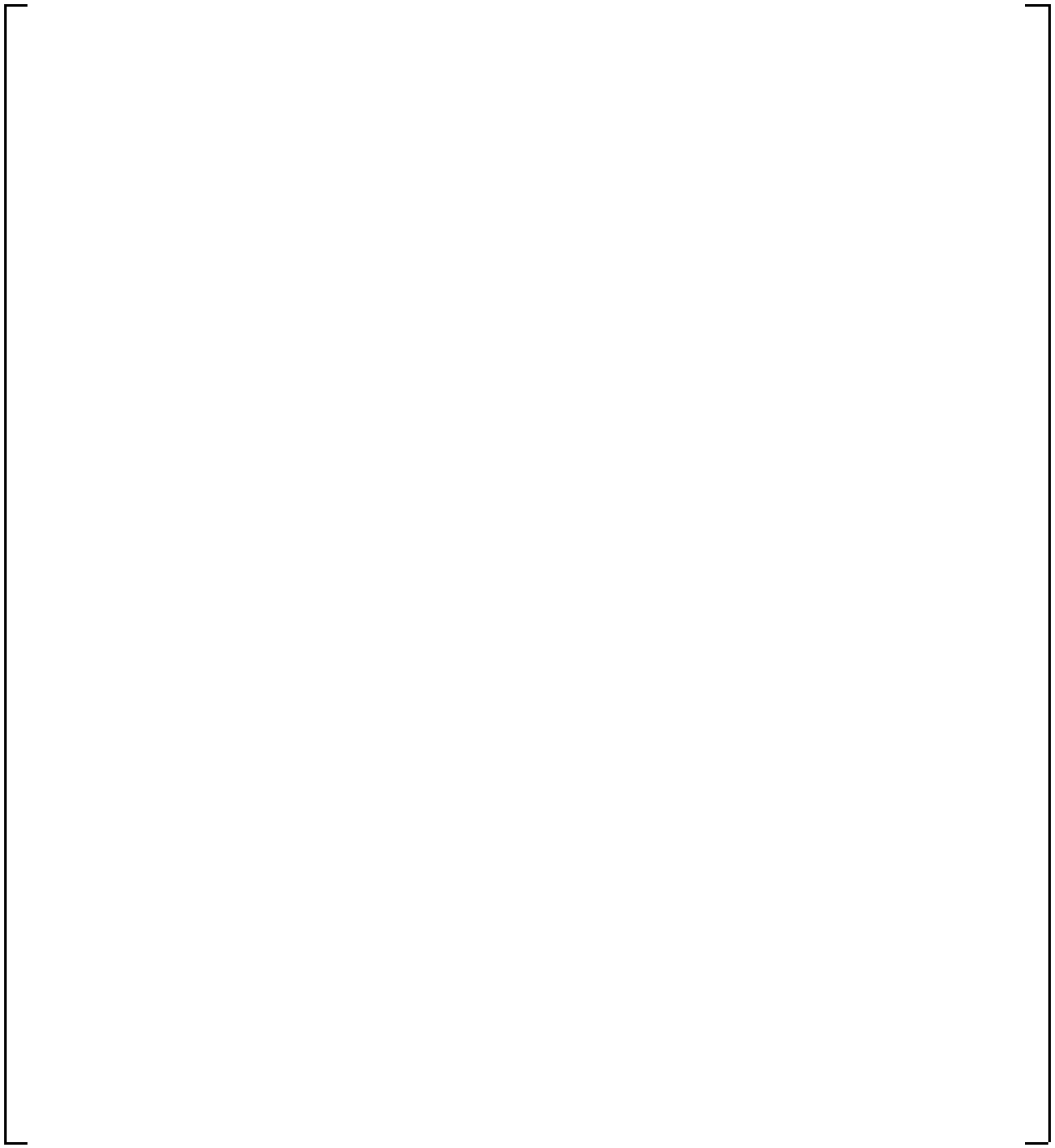

a,c

Figure 3.2-14 R. E. Ginna Loop Model Noding Diagram

a,c

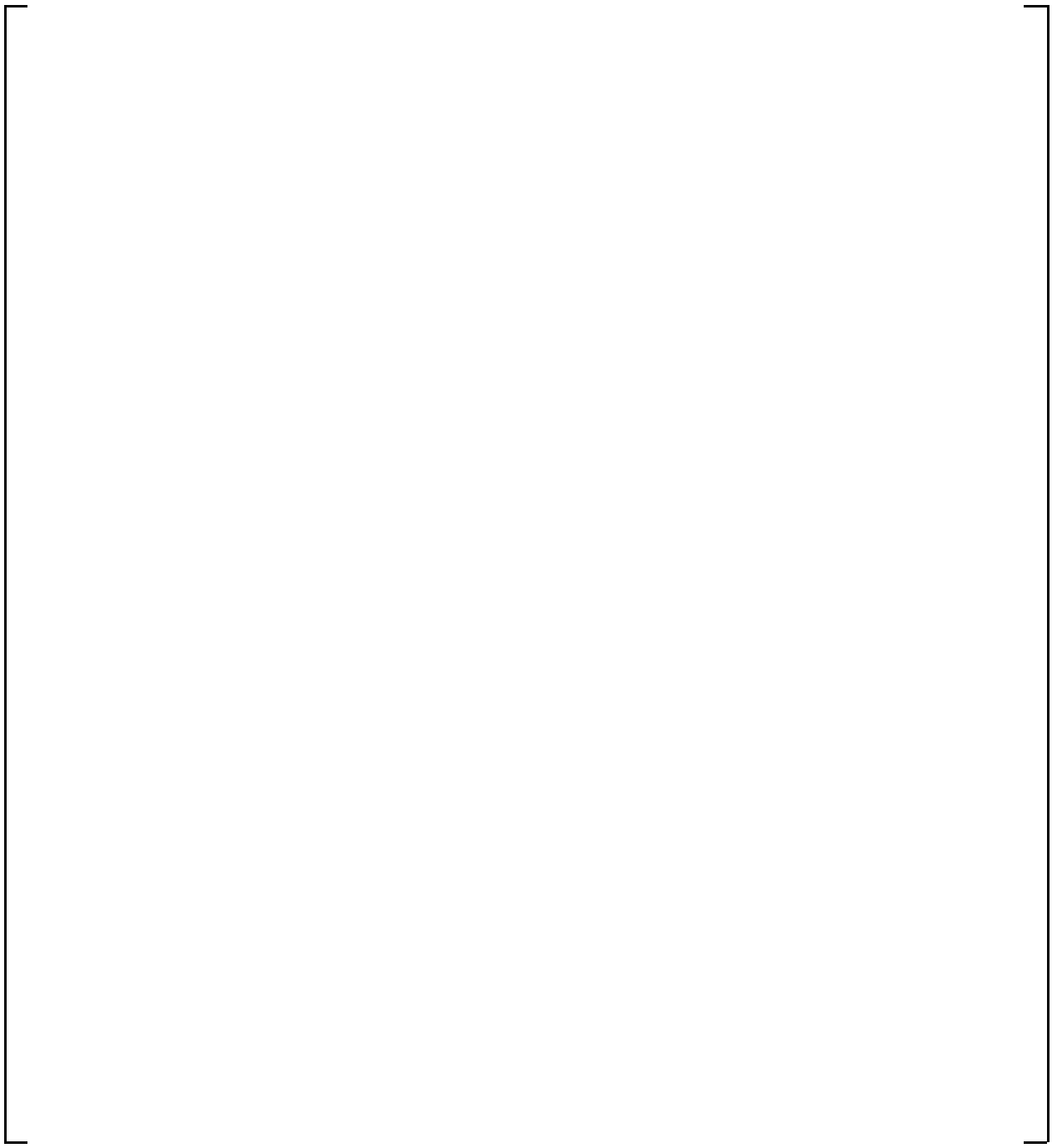

Figure 3.2-15 R. E. Ginna Steam Generator Component Noding Diagram

3.3 LARGE BREAK SCOPING STUDY RESULTS

In this section, the R. E. Ginna plant model is exercised using the WCOBRA/TRAC-TF2 code to determine the effect of variations in key LOCA parameters on the large break LOCA results. The goal of the studies is to evaluate the effects of parameters of interest and demonstrate reasonable system thermal hydraulic behavior is predicted. The intent is to confirm that the treatment of certain parameters, already approved for the FSLOCA EM (Kobelak et al., 2016), is also appropriate for 2-loop UPI plants.

3.3.1 Break Path Resistance Study

To demonstrate that **[**

][a,c]

[

]^{a,c}

[

]a,c

Table 3.3.1-1 Scenarios for Break Path Resistance Sensitivity Study

[

]a,c

[a,c

]

Figure 3.3.1-1 [ ]a,c

[a,c

]

Figure 3.3.1-2 [ ]a,c

[a,c

]

Figure 3.3.1-3 [ ]a,c

[a,c

]

Figure 3.3.1-4 [ ]a,c

[ ]a,c

Figure 3.3.1-5: [ ]a,c

[a,c

]

Figure 3.3.1-6 [ ]a,c

[ ]a,c

Figure 3.3.1-7 [ ]a,c

[a,c

]

Figure 3.3.1-8 [ ]a,c

[ ]a,c

Figure 3.3.1-9 [ ]a,c

[a,c

]

Figure 3.3.1-10 [

]a,c

[a,c

]

Figure 3.3.1-11 [

]a,c

[a,c

]

Figure 3.3.1-12 [ ]a,c

[a,c

]

Figure 3.3.1-13 [ ]a,c

[a,c

]

Figure 3.3.1-14 [ ]a,c

[ ]a,c

Figure 3.3.1-15 [ ]a,c

[a,c

]

Figure 3.3.1-16 [

]a,c

[ ]a,c

Figure 3.3.1-17 [ ]a,c

[a,c

]

Figure 3.3.1-18 [ ]a,c

[a,c

]

Figure 3.3.1-19 [**]a,c**

[a,c

]

Figure 3.3.1-20 [

]a,c

[a,c

]

Figure 3.3.1-21 [ ]a,c

[a,c

]

Figure 3.3.1-22 [ ]a,c

3.3.2 Steam Generator Tube Plugging Sensitivity Study

For a large break, the additional resistance through the steam generator tubes as a result of tube plugging increases the relative pump-side break path resistance and has two primary effects. First, it alters the conditions in the vessel regarding flow stagnation and core flow reversal during blowdown. Second, higher steam generator resistance inhibits steam venting during reflood, thus aggravating the effects of steam binding and reducing the rate at which the vessel fills with liquid.

To assess the impacts of steam generator tube plugging (SGTP), the limiting split break (Case 6) in Table 3.3.1-1 in Section 3.3.1 was analyzed at the high (10%) and low (0%) SGTP level.

For this particular sensitivity, **[**

][a,c]

[a,c

]

Figure 3.3.2-1 [

]a,c

[ ]a,c

Figure 3.3.2-2 [ ]a,c

[ ]a,c

Figure 3.3.2-3 [ ]a,c

3.3.3 Peripheral Assembly Power (PLOW) Study

Standard core design practice is to minimize neutron leakage from the reactor core by placing assemblies on the periphery that have already been irradiated for at least one cycle. The power in the low power peripheral region of the core is determined from the core design and can vary from **[ ]**[a,c] percent of the core average power; however, it typically varies by only a small amount from cycle to cycle. A relative power **[ ]**[a,c] percent of the core average is typical of current and future low leakage loading patterns. Variations in the power of this region affect the overall core radial power distribution.

[

][a,c]

[ ]a,c

Figure 3.3.3-1 [ ]a,c

[ ]a,c

Figure 3.3.3-2 [ ]a,c

[**a,c**

Figure 3.3.3-3 [**]**[a,c]**

[**a,c**

]

Figure 3.3.3-4 [

]a,c

[**a,c**

Figure 3.3.3-5 [

]a,c

[a,c

]

Figure 3.3.3-6 [

]a,c

[ ]a,c

Figure 3.3.3-7 [ ]a,c

3.4 SMALL BREAK SCOPING STUDY RESULTS

By simulating the SBLOCA events using the Ginna plant input model, this section studies the plant configuration assumptions and modeling parameters known to significantly affect the SBLOCA transients of 2-loop UPI plants.

During any LBLOCA transient, UPI and cold leg LHSI, for 2-loop and 3- (or 4-loop) plants respectively, are important for recovering the reactor core and terminating periods of cladding temperature increase. However, SBLOCAs are mainly mitigated by the performance of HHSI and accumulator injection with little contribution from the low pressure UPI, which can only be activated at sufficiently low RCS pressure after the transient has otherwise been mitigated. Since 2-loop UPI plants have similar HHSI and accumulator configurations with injection into each cold leg as the 3- and 4-loop plants, the SBLOCAs of the 2-, 3- and 4-loop plants are dominated by similar key phenomena, as reflected in their PIRTs in the approved FSLOCA EM (Kobelak et al., 2016).

The assumptions on plant conditions and modeling parameters critical to SBLOCA in PWR plants are identified in the approved FSLOCA method, including:

- Assumptions on offsite power availability and the timing of the operator action on reactor coolant pump trip
- [
-
-
-]^{a,c}

To extend the approved SBLOCA method to 2-loop UPI applications, the effects of the modeling options listed above on UPI plant SBLOCA response were evaluated in scoping studies discussed in Sections 3.4.1 through 3.4.3.

In addition, the Limitations and Conditions of the approved method need to be addressed in the extension 2-loop method. Specifically, Limitations and Conditions #9 and #10 are discussed in Section 3.4.3 relating to Region I SBLOCA analysis.

3.4.1 Offsite Power Availability and Reactor Coolant Pump Trip

The assumptions on pump operation have significant effects on the transient system responses in SBLOCAs within a certain range of break sizes. The break spectrum sensitivity studies of Ginna are discussed in this section to understand the effects of different pump trip delay times assuming offsite power is available (OPA), in comparison with those of pump trip coincident with the reactor trip due to loss of offsite power (LOOP). The results of these OPA and LOOP studies will support the associated modeling approach of Region I SBLOCA analysis using the FSLOCA EM for 2-loop plants, and will demonstrate adherence to the relevant FSLOCA EM limitation and condition, as discussed later in Section 3.4.3.2.

Figure 3.4.1-1 presents the PCT as a function of break diameter for LOOP and OPA with [

]^{a,c}

[

][a,c]

The thermal hydraulic phenomena leading to the **[** **]**[a,c] in LOOP and OPA scenarios are significantly different. **[**

][a,c]

[

]^{a,c}

[ ]a,c

[

]a,c

In summary, the sensitivity break spectrum results of the 2-loop Ginna plant lead to the observation that [

]a,c

[a,c

]

Figure 3.4.1-1 [

]a,c

[a,c

Figure 3.4.1-2a [ ]a,c

[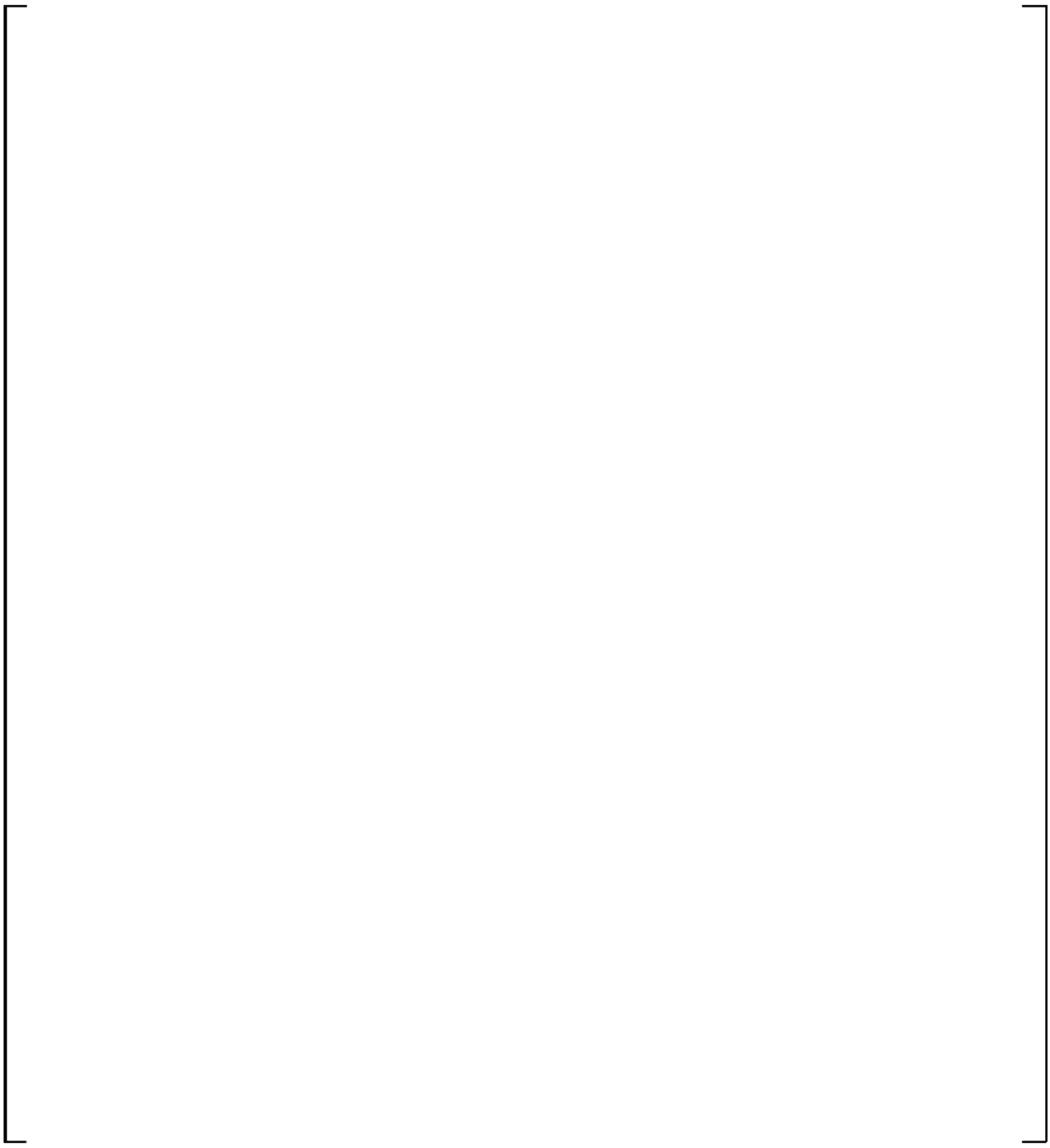]a,c

Figure 3.4.1-2b [ ]a,c

[a,c

]

Figure 3.4.1-3 [

]a,c

[a,c

]

Figure 3.4.1-4 [

]^{a,c}

[a,c

]

Figure 3.4.1-5 [

]a,c

[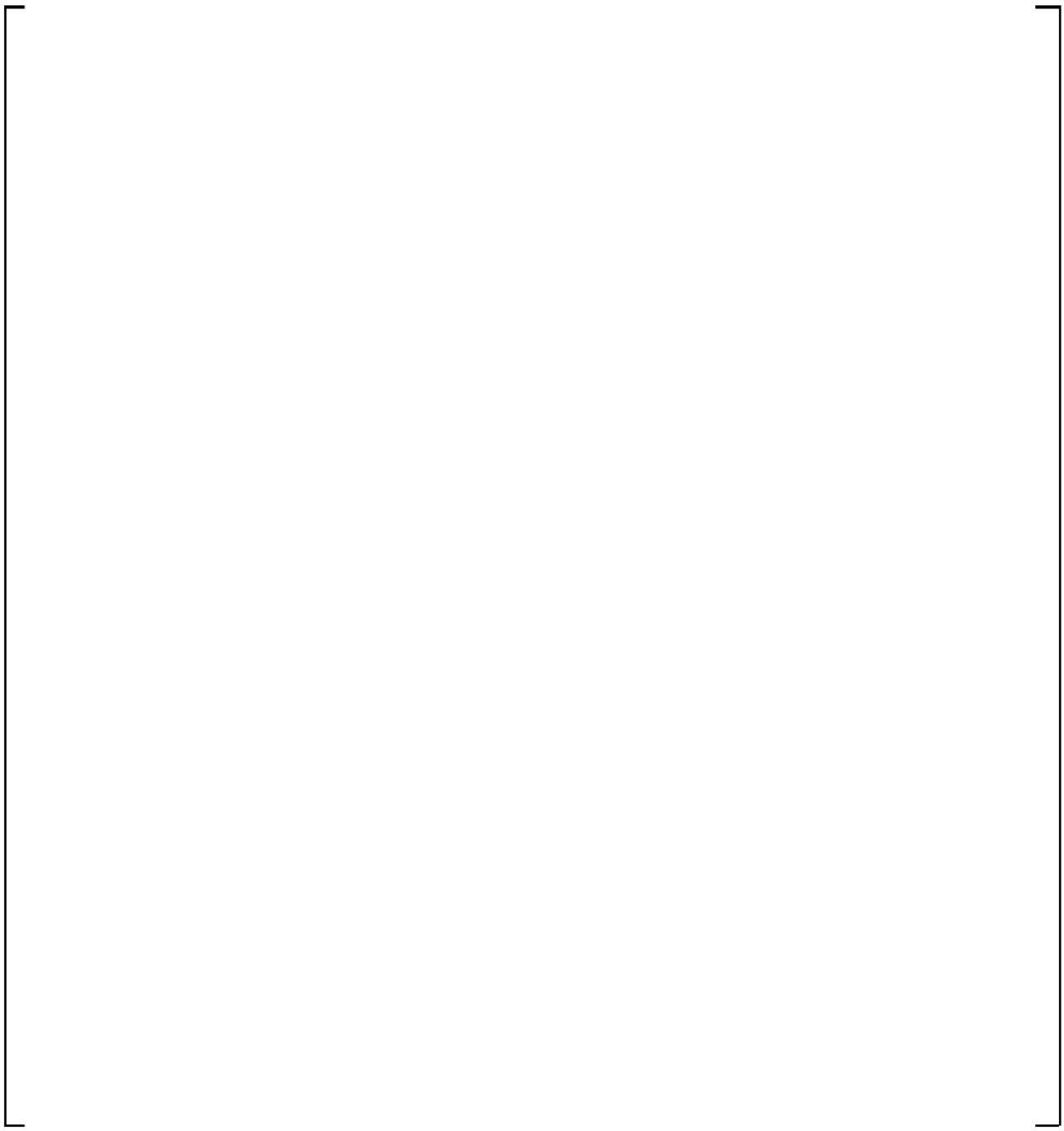]a,c

Figure 3.4.1-6 [

]a,c

[a,c

]

Figure 3.4.1-7 [

]a,c

[a,c

]

Figure 3.4.1-8 [

]

[a,c

]

Figure 3.4.1-9 [

]a,c

[ ]a,c

Figure 3.4.1-10 [ ]a,c

[a,c

]

Figure 3.4.1-11 [

]a,c

[a,c

]

Figure 3.4.1-12 [

]a,c

[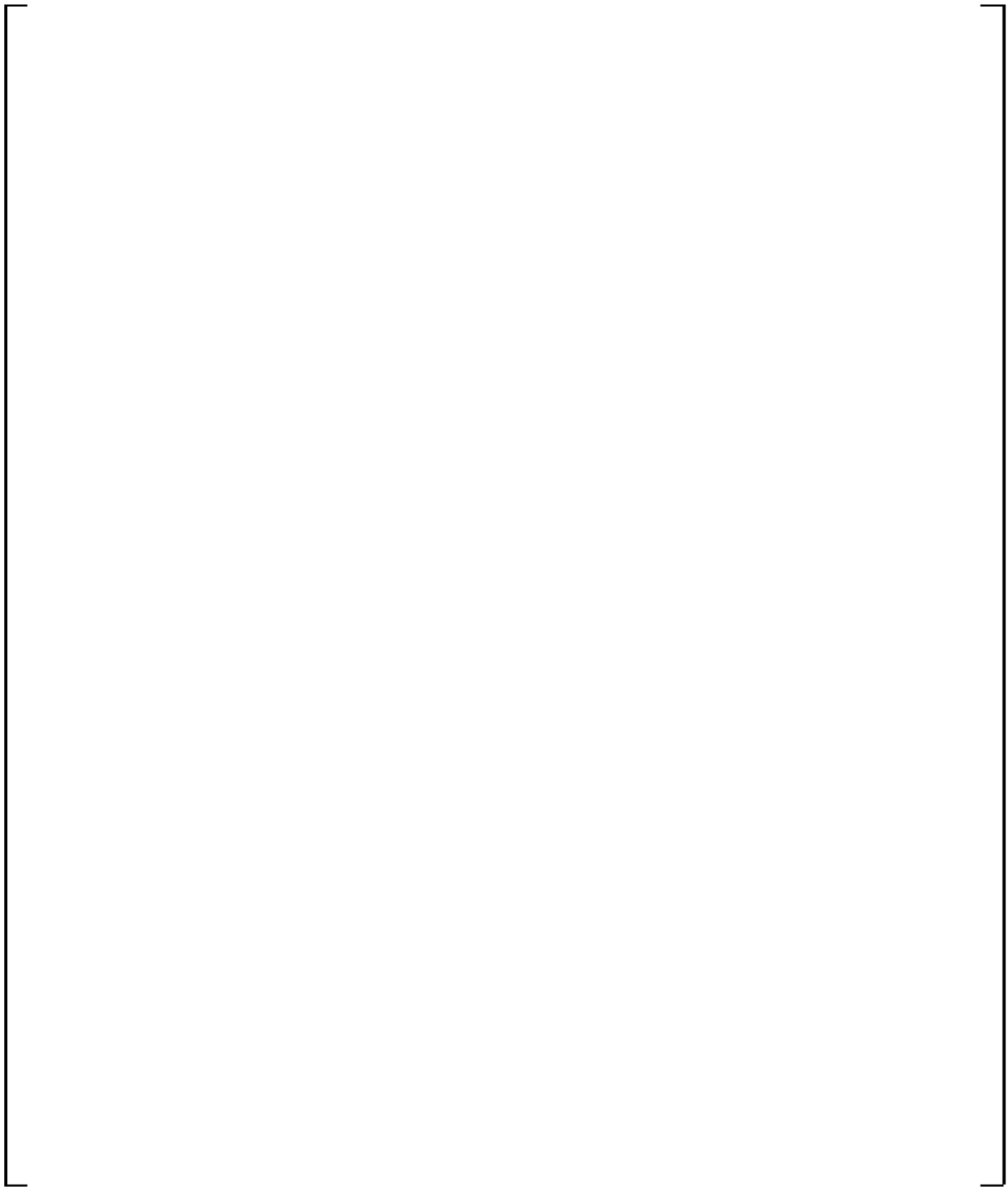]a,c

Figure 3.4.1-13 [ ]a,c

[a,c

] a,c

Figure 3.4.1-14 [

]a,c

[a,c

]

Figure 3.4.1-15 [

]a,c

[a,c

]

Figure 3.4.1-16 [

]a,c

[a,c

]

Figure 3.4.1-17 [

]a,c

[a,c

]

Figure 3.4.1-18 [

]a,c

[a,c

]

Figure 3.4.1-19 [ ]a,c

3.4.2 [ ]a,c

The [ ]a,c is known to affect important thermal-hydraulic aspects of the SBLOCA transient such as break flow, capability of steam venting, depressurization, and liquid inventories throughout the RCS.

[ ]a,c in both physical tests and numeric simulations. In the approved FSLOCA method the [

]a,c

[

]a,c

[

]a,c

In conclusion, the sensitivity studies of [

]a,c

[a,c

]

Figure 3.4.2-1 [ ]a,c

[a,c

]

Figure 3.4.2-2 [

]a,c

[a,c

]

Figure 3.4.2-3 [ ]a,c

[

a,c

]

Figure 3.4.2-4 [

]a,c

[a,c

]

Figure 3.4.2-5 [

]a,c

[a,c

]

Figure 3.4.2-6 [

]a,c

[a,c

]

Figure 3.4.2-7 [

]a,c

[a,c

]

Figure 3.4.2-8 [

]a,c

[a,c

]

Figure 3.4.2-9 [

]a,c

[a,c

]

Figure 3.4.2-10 [

]a,c

[a,c

]

Figure 3.4.2-11 [

]a,c

[a,c

]

Figure 3.4.2-12 [

]a,c

[a,c

]

Figure 3.4.2-13 [

]a,c

[a,c

]

Figure 3.4.2-14 [

]a,c

[a,c

]

Figure 3.4.2-15 [

]a,c

[a,c

]

Figure 3.4.2-16 [

]a,c

[a,c

]

Figure 3.4.2-17 [

]a,c

[a,c

]

Figure 3.4.2-18 [ ]a,c

[a,c

]

Figure 3.4.2-19 [

]a,c

[a,c

]

Figure 3.4.2-20 [

]a,c

[a,c

]

Figure 3.4.2-21 [

]a,c

3.4.3 Assessment of Limitations and Conditions

3.4.3.1 Limitation and Condition 9

The FSLOCA EM limitation and condition number 9 is as follows:

> In PWR plant type-specific applications of the FSLOCA EM for designs which are not Westinghouse 3-loop PWRs, a confirmatory evaluation will be performed for Region I analyses to assess the effect associated with the **[**
>
> **]**[a,c] This confirmatory evaluation will be performed once for each PWR plant type (e.g., Westinghouse design four-loop PWR plant) analyzed with the FSLOCA EM and referenced in subsequent plant-specific FSLOCA analyses of the same PWR plant type.

Individual 3-loop plant type sensitivity studies on **[**

][a,c]

The effect of the Region I uncertainty biasing on peak cladding temperature (PCT) as a function of break size is shown in Figure 3.4.3-1 for LOOP. The core uncovery and cladding heatup in the 1.0-to-3.0 inch break diameter range is **[**

][a,c]

[

]a,c

[a,c

]

Figure 3.4.3-1 [

]a,c

[a,c

]

Figure 3.4.3-2 [

]a,c

[a,c

]

Figure 3.4.3-3 [

]a,c

[a,c

]

Figure 3.4.3-4 [

]a,c

[a,c

]

Figure 3.4.3-5 [

]a,c

[a,c

]

Figure 3.4.3-6 [

]^{a,c}

3.4.3.2 Limitation and Condition 10

The FSLOCA EM limitation and condition number 10 is as follows:

> In PWR plant type-specific application of the FSLOCA EM for designs which are not Westinghouse 3-loop PWRs, a confirmatory evaluation will be performed to demonstrate that the applied break size boundary between Region I and Region II serves the intended goal of **[**
>
> **]**[a,c] As of part this evaluation, it will be demonstrated that no unexplained behavior in the predicted safety criteria, including PCT, occurs across the boundary between Region I and Region II. In addition, it will be confirmed that **[**
>
> **]**[a,c] In addition, it is important to also assure that the limiting small break between about 2- and 4-inch in an equivalent break diameter is properly captured by the robust Region I analysis approach. Plants with larger RCS fluid volumes than the Beaver Valley plant test example in (Kobelak et al., 2016), should cover the same 2- to 4-inch range using break area to RCS volume scaling to assure that the 2- to 4-inch break range is preserved and not artificially truncated. This confirmatory evaluation will be performed once for each PWR plant type (e.g., Westinghouse design four-loop PWR plant) analyzed with the FSLOCA EM and referenced in subsequent plant-specific FSLOCA analyses of the same PWR plant type. The WCOBRA/TRAC-TF2 code is applicable for analysis over the entire break spectrum of LOCA transients. However, for the purpose of the Region II analysis, the minimum of the break area sampling should extend only to 1.0 ft^2 consistent with the ASTRUM LBLOCA EM (WCAP-16009-P-A, "Realistic Large-Break LOCA Evaluation Methodology Using the Automated Statistical Treatment of Uncertainty Method (ASTRUM)," Revision 0) in lieu of the Region I/II boundary.

The FSLOCA EM analysis approach was demonstrated for a Westinghouse 3-loop PWR as described in Section 31.2 of (Kobelak et al., 2016). **[**

][a,c] A similar approach was demonstrated to be applicable to a Westinghouse 4-loop PWR as described in (Bowman, 2018). Specifically, the same approach is used with the **[**

][a,c]

The general ECCS layout is different for 2-loop plants than for 3-loop and 4-loop plants. The typical 2-loop plant layout is such that the LHSI line connects to the upper plenum of the reactor vessel. The HHSI line may connect to the accumulator line, which then connects to the cold leg, or it may connect directly to the cold leg. Typical 2-loop plant high head SI cold leg connecting lines are about 5.1-inches (similar to 3-loop PWRs) and typical accumulator connecting lines are 8.75 inches (inner diameter). For 3-loop plants, **[**

][a,c]

[**]**[a,c] This is illustrated by Figures 4-1 and 4-2 in LTR-NRC-14-29 of the Appendix of (Kobelak et al., 2016).

The FSLOCA EM limitation and condition 10 states that the intended goal of the Region I/II boundary **[** **]**[a,c] should be demonstrated for PWR plant type-specific application of the FSLOCA EM. As part of this demonstration, no unexplained behavior in the predicted safety criteria, including PCT, across the boundary between Region I and Region II should occur. In addition, the limitation and condition **[** **]**[a,c] The limitation and condition does clarify that plants with smaller RCS fluid volumes than the Beaver Valley plant test example in (Kobelak et al., 2016) should cover the same 2-to-4 inch range using break area to RCS volume scaling to assure that the 2-to-4 inch break range is preserved and not artificially truncated. Applying **[**

][a,c]

The applicability of the FSLOCA EM analysis approach described in Section 31.2 of (Kobelak et al., 2016) and adherence to limitation and condition 10 is investigated based on the break spectrum studies performed for R. E. Ginna assuming LOOP and OPA configurations. The PCT results from the LOOP break size sensitivity study (with full ECCS flow) are shown in Figure 3.4.3-7. **[** **]**[a,c] It is also observed that smooth, explainable PCT predictions occur in the 1.0 to 8.0 inch break diameter range, which includes potential 2-loop PWR boundaries between Region I and Region II and satisfies part of the limitation and condition 10. It is noted that PCT is used as a surrogate for all safety criteria as no significant oxidation accrues at the predicted temperatures.

To examine the potential for heatup in **[**

][a,c]

Based on these studies, it is evident that **[**

][a,c]

In summary, LOOP and OPA break spectrum study results from **[**

][a,c]

[

]^{a,c}

It is noted that the Region II analysis considers a minimum break area of 1.0 ft^2 consistent with the ASTRUM LBLOCA EM and the FSLOCA EM limitation and condition 10.

[a,c]

Figure 3.4.3-7 PCT vs Break Diameter – LOOP Configuration with 100% SI Capacity

[a,c

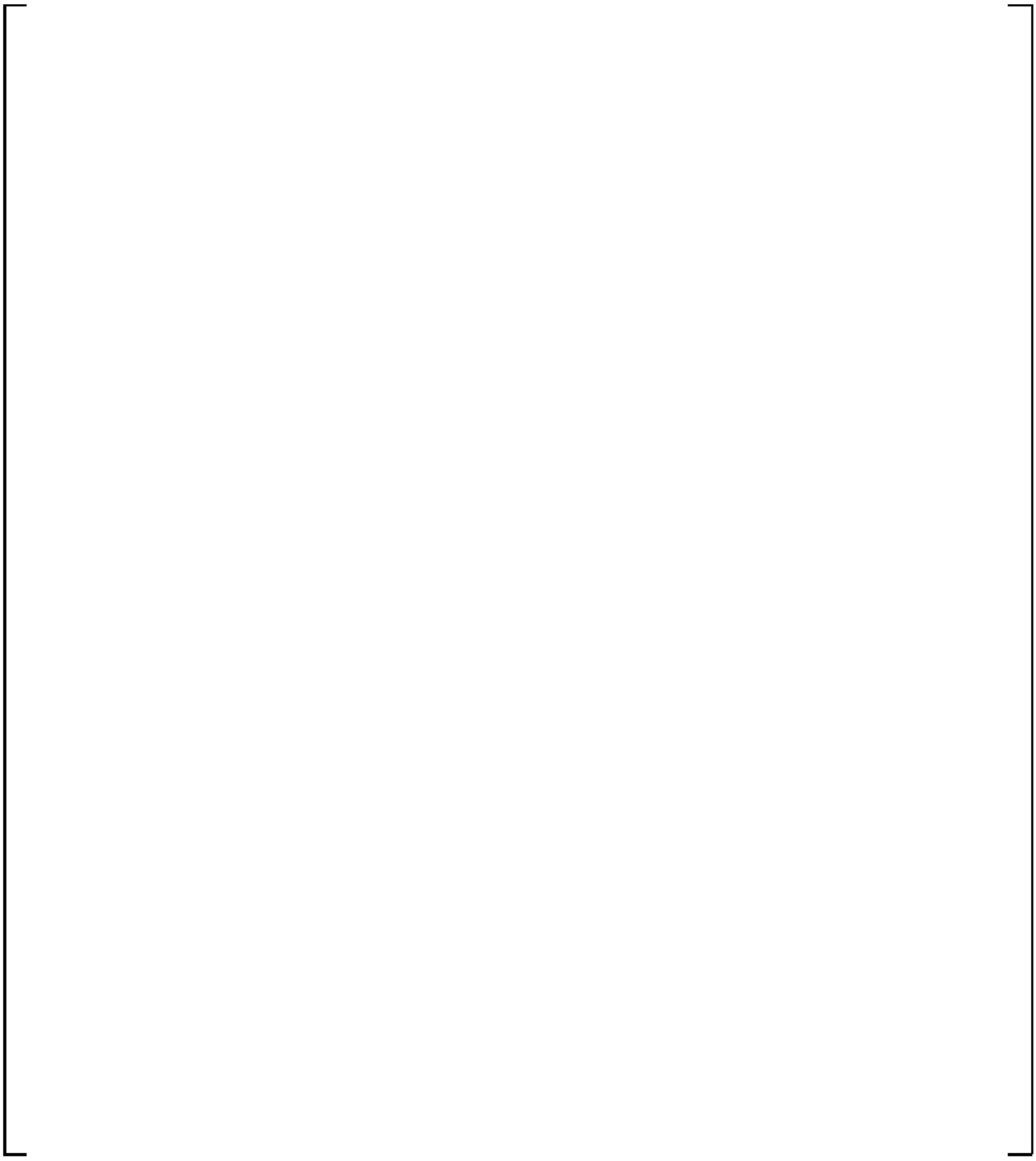

]

Figure 3.4.3-8 PCT vs Break Diameter – LOOP Configuration with 100% and 50% SI Capacity

[a,c

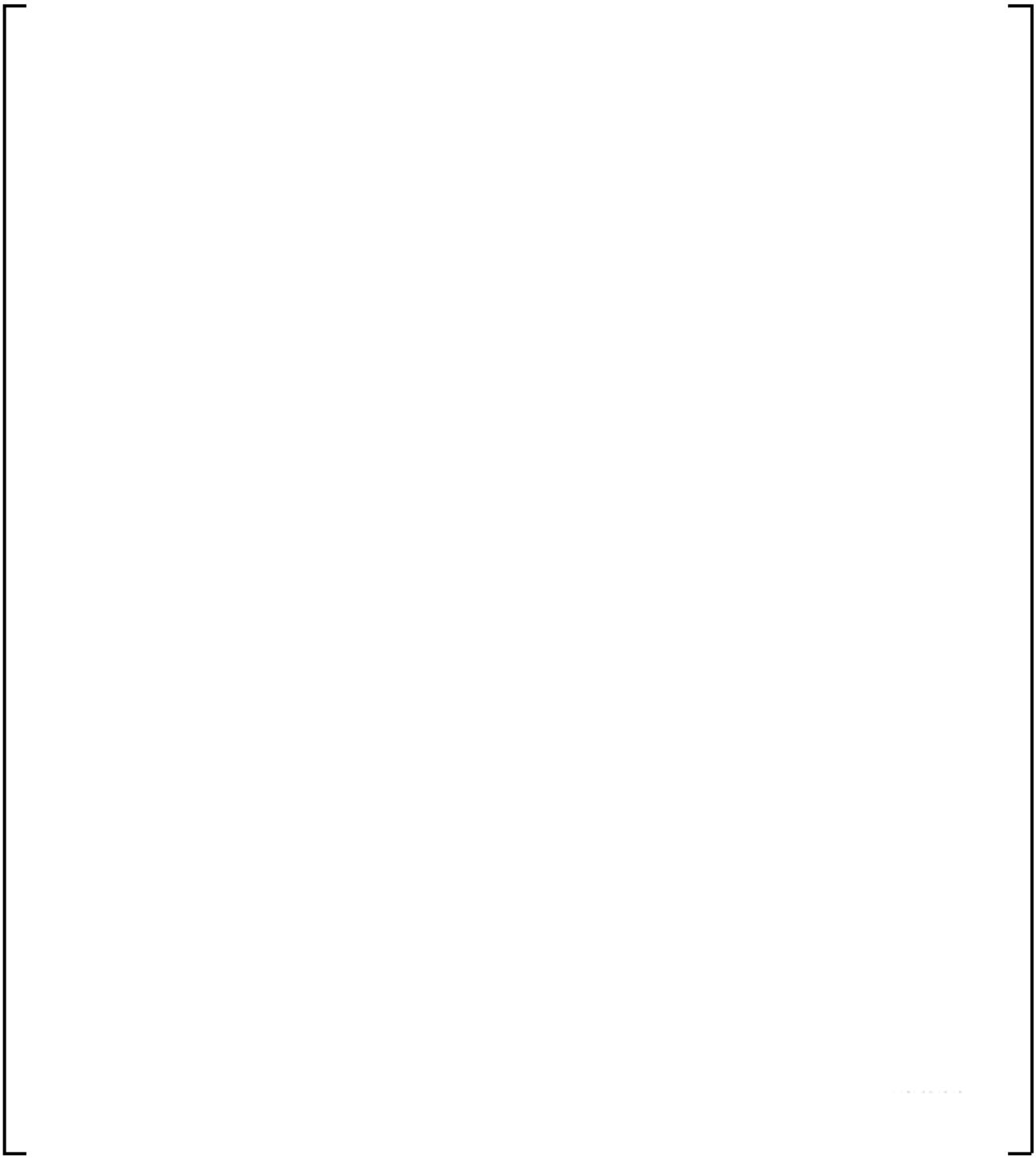

]

Figure 3.4.3-9 PCT vs Break Diameter – LOOP Configuration with 100% and 50% SI Capacity

[a,c

Figure 3.4.3-10 PCT vs Break Diameter – OPA Configuration with 100% and 50% SI Capacity

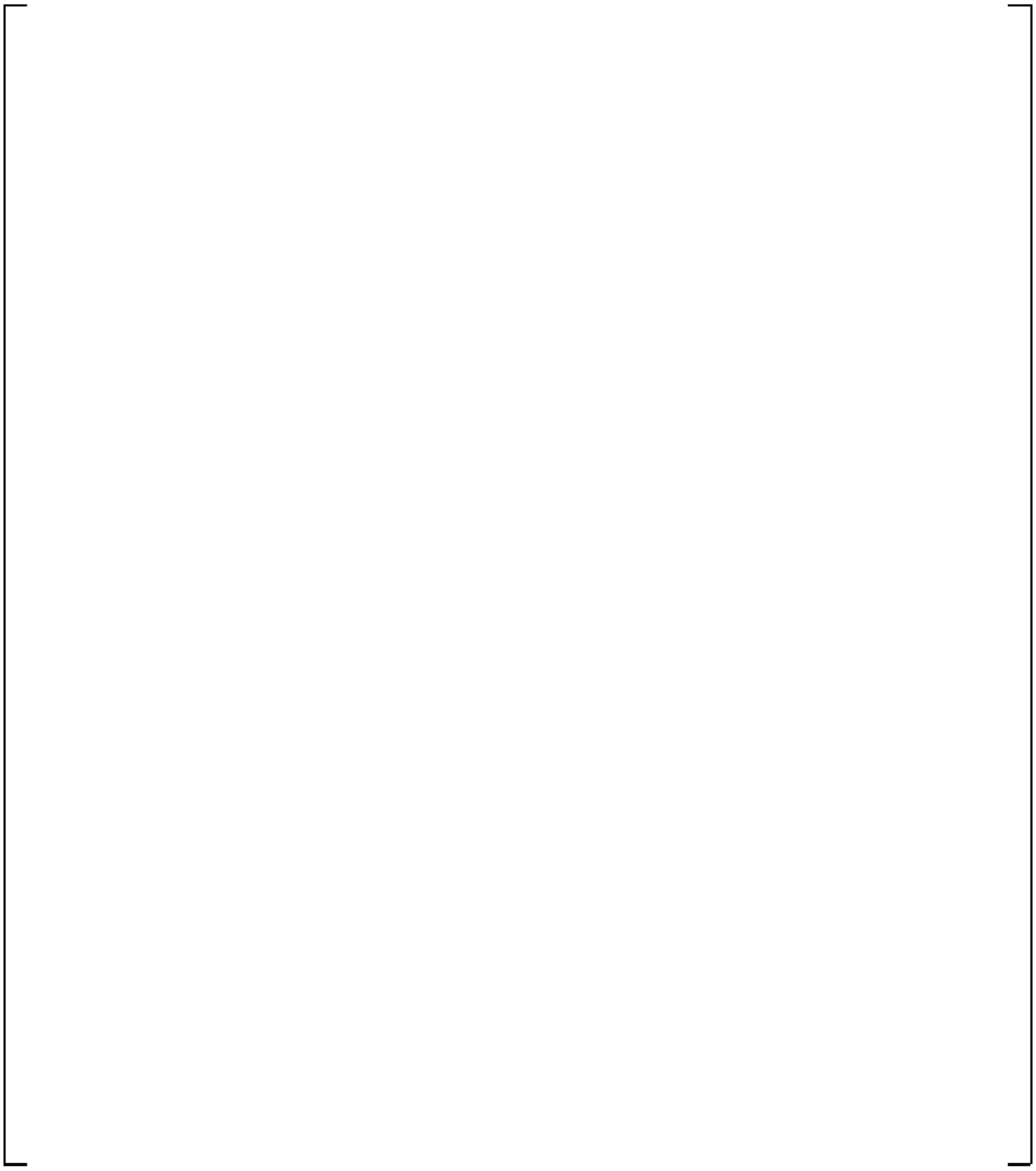

a,c

Figure 3.4.3-11 PCT vs Break Diameter – OPA Configuration with 100% and 50% SI Capacity

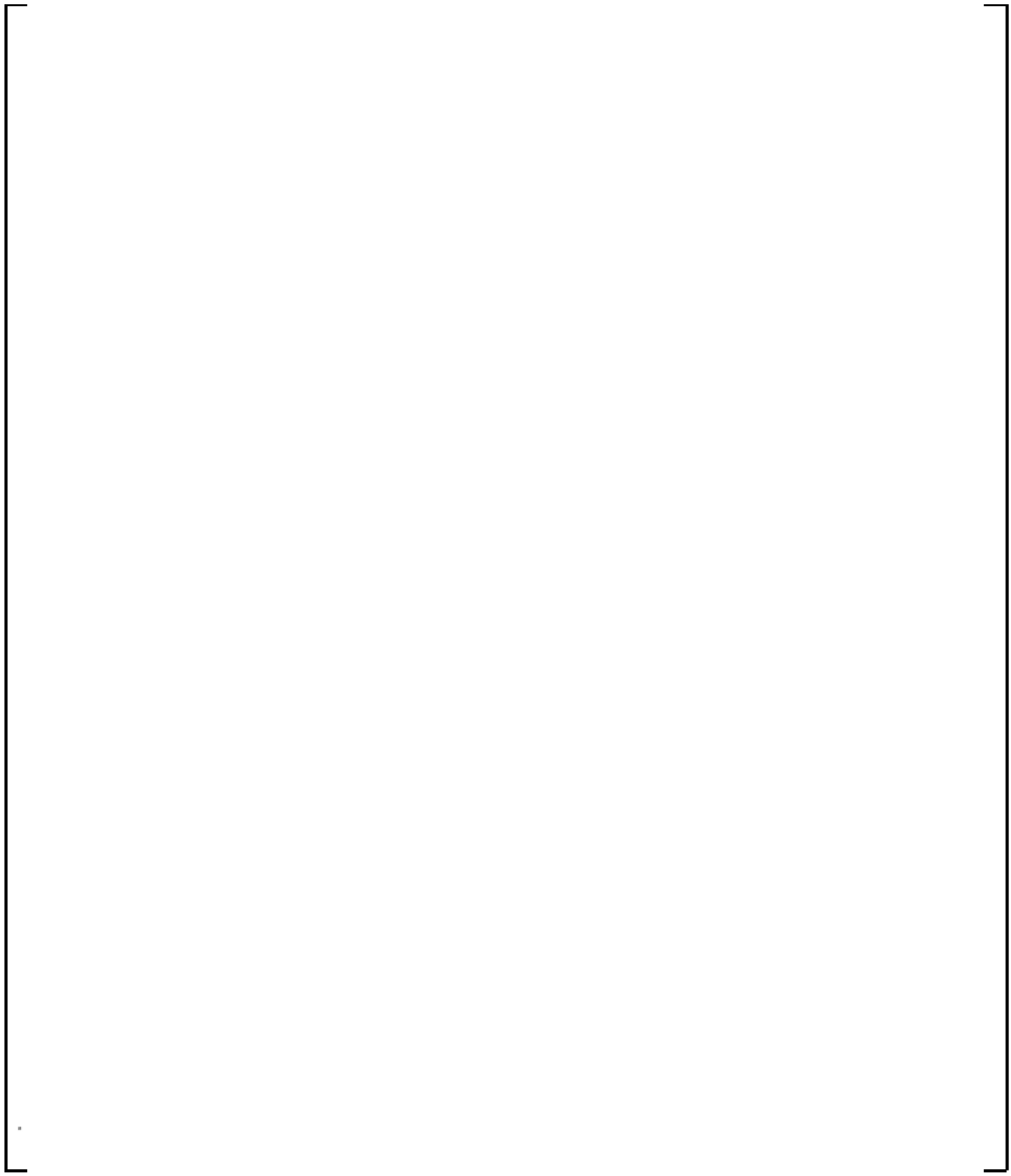

a,c

Figure 3.4.3-12 Illustrative Example of PCT Behavior of SBLOCA, IBLOCA, and LBLOCA Cases

3.5 References

1. Bowman, A. B., et al., 2017, “Westinghouse Performance Analysis and Design Model (PAD5),” WCAP-17642-P-A, Revision 1.

2. Bowman, A. B., 2018, “Information to Satisfy the FULL SPECTRUM LOCA (FSLOCA) Evaluation Methodology Plant Type Limitations and Conditions for 4-loop Westinghouse Pressurized Water Reactors (PWRs) (Proprietary/Non-Proprietary),” LTR-NRC-18-50, Revision 0.

3. Bordelon, F. M. and Murphy, E. T., 1974, “Containment Pressure Analysis Code (COCO),” WCAP-8327.

4. Bordelon, F. M., et al., 1974, “Westinghouse Emergency Core Cooling System Evaluation Model – Summary,” WCAP-8339.

5. Dederer, S. I., et al., 1999, “Application of Best Estimate Large Break LOCA Methodology to Westinghouse PWRs with Upper Plenum Injection,” WCAP-14449-P-A, Revision 1.

6. Kobelak, J. R., et al., 2016, “Realistic LOCA Evaluation Methodology Applied to the Full Spectrum of Break Sizes (FULL SPECTRUM LOCA Methodology),” WCAP-16996-P-A, Revision 1.

4 SUMMARY AND CONCLUSIONS

The extension of the Westinghouse FULL SPECTRUM LOCA (FSLOCA) best-estimate loss-of-coolant accident (BELOCA) analysis methodology (Kobelak et al., 2016) for a pressurized water reactor (PWR) equipped with upper plenum injection (UPI) is presented in this report. The FSLOCA Evaluation Model (EM) using the WCOBRA/TRAC-TF2 code was reviewed and the applicability of the approved methodology to UPI plants was discussed. It was identified in the phenomena identification and ranking table (PIRT) included in (Kobelak et al., 2016) that UPI plants have several uniquely important thermal hydraulic phenomena in the upper plenum of the reactor vessel. The availability of the UPI flow for core cooling during a LBLOCA transient is affected by the upper plenum entrainment and de-entrainment, upper plenum condensation, and counter-current flow limitation (CCFL) at the top of core plate or the top of fuel nozzle under both saturated and subcooled conditions.

The WCOBRA/TRAC-TF2 code, which was approved for application of the FSLOCA EM to 3- and 4-loop Westinghouse-designed plants, was used for this extension of the methodology to UPI plants. Since this application uses the WCOBRA/TRAC-TF2 code with no modifications specific to capturing UPI behavior, the requirement of complete and adequate code documentation is satisfied via Volume I of (Kobelak et al., 2016).

The assessment matrix for the 3- and 4-loop plants documented in (Kobelak et al., 2016) was reviewed for applicability to the UPI plant scenario. The review determined that a supplemental set of tests was needed to validate the capability of WCOBRA/TRAC-TF2 to analyze a UPI LBLOCA. Additional validation tests from the cylindrical core test facility (CCTF), upper plenum test facility (UPTF), and General Electric (GE) counter-current flow limitation (CCFL) test facility were added to the assessment matrix to investigate phenomena unique to the UPI plant calculations, as indicated in the PIRT from (Kobelak et al., 2016).

Test and plant nodalization was established to capture the phenomena particular to the UPI plants. This required **[**

][a,c] A consistent approach was used in the nodalization of the test facilities for the simulation of experiments from CCTF, UPTF, and GE CCFL. The results of the test simulations were examined and show that the code is well suited for UPI analysis applications. The results also indicated that the upper plenum drain behavior is **[**

][a,c] The CCTF and UPTF test results support the conclusion from (Kobelak et al., 2016) that the WCOBRA/TRAC-TF2 code will accurately represent the effects of scale, and no additional scaling uncertainty is required.

The quantification of the uncertainties from the FSLOCA EM was then reviewed. It was concluded that the uncertainty methodology is fully applicable to UPI plants, and **[**

][a,c]

Demonstrative UPI 2-loop plant transients were performed and a detailed discussion of the transient results is presented in this report. Additional PWR runs to illustrate various sensitivities were also performed with the results included in this report. Based on the results of these various sensitivity studies, **[**

][a,c]

With the results of the additional code model assessment for UPI, and the limited changes to the input model development, it is concluded that the methodology presented in this report satisfies the requirements of 10 CFR 50.46 for a best-estimate LOCA analysis model. Therefore, plant-specific FSLOCA EM licensing applications for PWRs equipped with UPI can be performed given the methodology extension presented in this report.

4.1 SATISFACTION OF LIMITATIONS AND CONDITIONS ON THE FSLOCA EM

There are fifteen limitations and conditions (L&Cs) imposed on the approved FSLOCA EM as described in Table 22 of the enclosure to (Morey, 2017) and captured in (Kobelak et al., 2016). The applicability of these limitations and conditions with respect to the extension of the FSLOCA EM to 2-loop PWRs equipped with UPI is as follows:

L&C #1, FSLOCA EM Applicability with Regard to LOCA Transient Phases: This L&C is equally applicable to the analysis of 2-loop PWRs equipped with UPI.

L&C #2, FSLOCA EM Applicability with Regard to Type of PWR Plants: L&C #2 indicates that the FSLOCA EM is applicable to Westinghouse-designed 3-loop and 4-loop PWRs with cold side emergency core cooling injection. This report extends the applicability of the FSLOCA EM to 2-loop Westinghouse-designed PWRs with UPI. The remainder of this L&C remains applicable to the analysis of 2-loop PWRs equipped with UPI.

L&C #3, FSLOCA EM Applicability for Containment Pressure Modeling: This L&C is equally applicable to the analysis of 2-loop PWRs equipped with UPI.

L&C #4, Decay Heat Modeling in FSLOCA EM Applications: This L&C is equally applicable to the analysis of 2-loop PWRs equipped with UPI.

L&C #5, Fuel Burnup Limits in FSLOCA EM Applications: This L&C is equally applicable to the analysis of 2-loop PWRs equipped with UPI.

L&C #6, WCOBRA/TRAC-TF2 Interface with PAD5 in the FSLOCA EM: This L&C is equally applicable to the analysis of 2-loop PWRs equipped with UPI.

L&C #7, Interfacial Drag Uncertainty in FSLOCA EM Region I Analyses: This L&C is equally applicable to the analysis of 2-loop PWRs equipped with UPI.

L&C #8, Biased Uncertainty Contributors in FSLOCA EM Region I Analyses: This L&C is equally applicable to the analysis of 2-loop PWRs equipped with UPI.

L&C #9, Effect of Bias in FSLOCA EM Applications for Region I: This L&C is equally applicable to the analysis of 2-loop PWRs equipped with UPI. This L&C is satisfied for 2-loop PWRs in Section 3.4.3.1 of this report.

L&C #10, Boundary Between FSLOCA EM Region I and Region II Breaks: This L&C is equally applicable to the analysis of 2-loop PWRs equipped with UPI. This L&C is satisfied for 2-loop PWRs in Section 3.4.3.2 of this report. It is noted that the **[**

][a,c]

L&C #11, [ ][a,c] **in FSLOCA EM Uncertainty Analyses for Region II and Documentation of Reanalysis Results for Region I and Region II**: This L&C is equally applicable to the analysis of 2-loop PWRs equipped with UPI.

L&C #12, Steam Generator Heat Removal During SBLOCAs: This L&C is equally applicable to the analysis of 2-loop PWRs equipped with UPI.

L&C #13, Upper Head Spray Nozzle Loss Coefficient: This L&C is equally applicable to the analysis of 2-loop PWRs equipped with UPI.

L&C #14, Correlation for Oxidation: This L&C is equally applicable to the analysis of 2-loop PWRs equipped with UPI.

L&C #15, LOOP versus OPA Treatment in FSLOCA EM Uncertainty Analyses for Region II: This L&C is equally applicable to the analysis of 2-loop PWRs equipped with UPI.

In summary, the L&Cs from the Nuclear Regulatory Commission (NRC) approved FSLOCA EM generally remain applicable to the analysis of 2-loop PWRs equipped with UPI, with the exceptions and additional information noted previously in this section.

4.2 ADDITIONAL METHODOLOGY LIMITATIONS FOR 2-LOOP PWRS EQUIPPED WITH UPI

The Advisory Committee on Reactor Safeguards (ACRS) recommended that the Safety Evaluation Report for the application of the Westinghouse Code Qualification Document (CQD) best-estimate LOCA methodology (Bajorek et al., 1998) to 2-loop PWRs equipped with UPI should caution that applications of the code be limited to conditions representative of those tested, such as the rates of steam flow in UPTF (Powers, 1999). Westinghouse reviewed the test conditions in the validation matrix which was part of that methodology, and committed to limit the application to the conditions discussed in (Dederer et al., 1999). Those limitations were carried forward in the Automated Statistical Treatment of Uncertainty Method (ASTRUM) methodology (Nissley et al., 2005). The same limitations are considered relative to the extension of the FSLOCA EM to 2-loop PWRs equipped with UPI in the following sub-sections.

4.2.1 Core Power Level Addressed by UPTF Tests

Basis for Limitation as described in (Dederer et al., 1999)

Page 11 of the UPTF test report (Siemens, 1988) provides the basis for the UPTF core simulator flow rates. It is stated that **[**

][a,b,c]

FSLOCA EM Assessment

This limitation remains applicable for the extension of the FSLOCA EM to 2-loop PWRs equipped with UPI. Westinghouse will limit the application of the FSLOCA EM to 2-loop PWRs with **[**

][a,c]

4.2.2 Low Power Region Average Linear Heat Rate Addressed by UPTF Tests

Basis for Limitation as described in (Dederer et al., 1999)

[

][a,b,c]

[

]a,b,c

FSLOCA EM Assessment

This limitation remains applicable for the extension of the FSLOCA EM to 2-loop PWRs equipped with UPI. Westinghouse will limit the application of the FSLOCA EM to 2-loop PWRs with [

]a,c

4.2.3 Peak Linear Heat Rate Addressed by CCTF Tests

Basis for Limitation as described in (Dederer et al., 1999)

Page 13 of the CCTF test report (Iguchi, 1985) states that the CCTF power decay was obtained by
[

]a,b,c

FSLOCA EM Assessment

This limitation remains applicable for the extension of the FSLOCA EM to 2-loop PWRs equipped with UPI. Westinghouse will limit the application of the FSLOCA EM to 2-loop PWRs where [

]a,c

4.3 REFERENCES

1. Bajorek, S. M., et al., 1998, “Code Qualification Document for Best Estimate LOCA Analysis,” WCAP-12945-P-A, Volume 1 Revision 2, and Volumes 2 through 5 Revision 1 (Proprietary), and WCAP-14747 (Non-Proprietary).

2. Dederer, S. I., et al., October 1999, “Application of Best Estimate Large Break LOCA Methodology to Westinghouse PWRs with Upper Plenum Injection,” WCAP-14449-P-A, Revision 1.

3. Iguchi, T., et al., July 1985, “Data Report on Large Scale Reflood Test-96, CCTF Core-II Test C2-13 (Run 072),” JAERI-memo 60-157.

4. Kobelak, J. R., et al., November 2016, “Realistic LOCA Evaluation Methodology Applied to the Full Spectrum of Break Sizes (FULL SPECTRUM LOCA Methodology),” WCAP-16996-P-A, Revision 1.

5. Letter, D. A. Powers (ACRS) to W. D. Travers (US NRC), “Application of Westinghouse Best-Estimate Loss-of-Coolant Accident Analysis Methodology to Upper Plenum Injection Plants,” March 1999.

6. Morey, D. C., September 2017, “Revised Final Safety Evaluation for Westinghouse Electric Company Topical Report WCAP-16996-P/WCAP-16996-NP, Volumes I, II, and III, Revision 1, ‘Realistic Loss-of-Coolant Accident Evaluation Methodology Applied to the Full Spectrum of Break Sizes’ (TAC No. ME5244).”

7. Nissley, M. E., et al., 2005, “Realistic Large-Break LOCA Evaluation Methodology Using the Automated Statistical Treatment Of Uncertainty Method (ASTRUM),” WCAP-16009-P-A and WCAP-16009-NP-A.

8. Siemens, 1988, “2D/3D Program UPTF Quick Look Report, Test Number 20, Upper Plenum Injection Simulation Test,” Siemens Report U9 316/88/07.